

**COMPUTATIONAL ANALYSIS OF G-PROTEIN COUPLED RECEPTOR
SCREENING, DIMERIZATION, AND DESENSITIZATION**

by

Peter J. Woolf

A dissertation submitted in partial fulfillment
of the requirements for the degree of
Doctor of Philosophy
(Chemical Engineering)
in The University of Michigan
2002

Doctoral Committee:

Associate Professor Jennifer J. Linderman, Chairperson
Associate Professor David J. Mooney
Professor Richard R. Neubig
Professor Michael A. Savageau
Professor Robert Ziff

Peter J. Woolf

All Rights Reserved

2002

To my sister, Cloe Woolf,
who knew far too little about G-proteins

TABLE OF CONTENTS

DEDICATION.....	ii
LIST OF FIGURES	vi
LIST OF TABLES	x
LIST OF APPENDICES.....	xi
CHAPTER	
I. INTRODUCTION.....	1
1.1 Signal Transduction	1
1.2 G—Protein Coupled Receptors (GPCRs).....	4
1.3 Receptor Dimerization	8
1.4 Receptor Desensitization.....	9
1.5 Drug Screening.....	11
1.6 Overview of Thesis.....	13
II. MATHEMATICAL MODELS OF SIGNAL TRANSDUCTION	16
2.1 Introduction	16
2.2 Models that Change with Time	17
2.2.1 Species Conservation	21
2.2.2 Equilibrium Models	23
2.2.3 Steady State Models.....	27
2.2.4 Unsteady State Models.....	31
2.3 Modeling Spatial Effects.....	36
2.4 Conclusion.....	39
III. AGONIST INVERSION.....	41
3.1 Introduction	41
3.2 Methods.....	42
3.3 Results.....	44
3.4 Discussion	45
3.5 Conclusion.....	49

IV. UNCOVERING BIASES IN HIGH THROUGHPUT SCREENS OF G-PROTEIN COUPLED RECEPTORS.....	50
4.1 Introduction	50
4.2 Methods.....	56
4.2.1 Whole cell model	57
4.2.2 Membrane binding assay model	59
4.2.3 Parameters	62
4.3 Results and Discussion.....	64
4.3.1 Equilibrium analyses: Observed affinity differs between membrane binding assay and whole cell conditions	65
4.3.2 Equilibrium analyses: Membrane binding assay can be refocused to detect inverse agonists	71
4.3.3 Equilibrium analyses: Tracer ligand efficacy does not bias the membrane binding assay.....	73
4.3.4 Kinetic analyses: Binding kinetics give information about ligand efficacy	74
4.3.5 Kinetic analyses: Tracer ligand efficacy can affect binding kinetics	78
4.4 Conclusions	79
V. SELF ORGANIZATION OF MEMBRANE BOUND PROTEINS VIA DIMERIZATION	81
5.1 Introduction	81
5.2 Methods.....	83
5.2.1 Monte Carlo simulations	83
5.2.2 Scaling to GPCRs.....	84
5.3 Results and Discussion.....	85
5.3.1 Dimerization can cause clustering <i>in vivo</i>	85
5.3.2 Dimerization influences receptor cross-talk	90
5.3.3 Dimerization rules describe a spatial grammar.....	92
VI. ACTIVATION, SELF—ORGANIZATION, AND CO—REGULATION OF RECEPTOR DIMERS.....	95
6.1 Introduction	95
6.2 Methods.....	98
6.3 Results.....	101
6.3.1 Dimerization rules affect global organization	101
6.3.2 Dimerization as a route to control cross—talk.....	105
6.3.3 Receptor number co—regulation via dimerization.....	107
6.4 Discussion	109
6.4.1 Dimerization networks exhibit physiologically relevant emergent properties.....	110
6.4.2 Dimerization as a tool for drug development	114

6.4.3 Biological systems affected by receptor organization	117
6.4.3.1 Localization and Signal Regulation of Dopamine and Somatostatin Receptors	117
6.4.3.2 Dimerization Limited Cross—Talk among α_{2b} —Adrenergic, M μ Muscarinic, and δ —Opioid Receptors.....	121
6.4.3.3 Co—Regulation of κ —, δ —, and μ —Opioid Receptors via Dimerization.....	122
6.5 Conclusion.....	123

VII. UNTANGLING LIGAND INDUCED RECEPTOR ACTIVATION AND DESENSITIZATION 125

7.1 Introduction	125
7.2 Methods.....	131
7.3 Results.....	135
7.3.1 Effects of Ligand Properties k_{on} , k_{off} and α	135
7.3.2 Effects of Cell Properties k_i , D , and k_{f-RK}	138
7.4 Discussion	140
7.4.1 Effect of α on the Relative Phosphorylation Rate	140
7.4.2 Minimum Receptor Phosphorylation Rate	142
7.4.3 Cell specific effects on desensitization	143
7.4.4 μ —Opioid Receptor Activation and Desensitization....	145
7.5 Conclusions	148

VIII. CONCLUSIONS AND FUTURE DIRECTIONS 150

8.1 Receptor dimerization.....	150
8.2 Desensitization	154
8.3 Drug Screening	156
8.4 Future Pharmacological Models.....	157

APPENDICES 164

BIBLIOGRAPHY 179

LIST OF FIGURES

Figure

1.1	A drug s view of a receptor	2
1.2	Two views of receptor activation	3
1.3	Physiological roles of GPCRs	5
1.4	GPCR signal transduction cascade	6
1.5	Cross-talk between receptors.....	7
1.6	Impact of location on cross-talk	7
1.7	Receptor dimerization	8
1.8	Mechanism of GPCR desensitization	10
1.9	High throughput screening assay	12
2.1	Pendulum analogy.....	18
2.2	Three representative models of receptor-ligand binding	23
2.3	Three models of signal transduction via GPCRs.....	26
2.4	A steady state G-protein activation reaction	29
2.5	Responses predicted with the equilibrium and steady state CTC model	30
2.6	Desensitization in GPCRs	32
2.7	Relationship between equilibrium, steady state, and unsteady state models	33
2.8	Simultaneous effects of changing the conformational selectivity and desensitization rate constant.....	35
2.9	Monte Carlo simulation environment	38
3.1	Two signal response models.....	43

3.2	An example of agonist inversion	46
3.3	A possible example of an experimental system that exhibits agonist inversion.....	48
4.1	General schematic for GPCR ligand screening assays	52
4.2	Three classes of ligand efficacy in GPCRs	54
4.3	Whole cell model for GPCR signal transduction	58
4.4	Model of the membrane binding assay	60
4.5	Comparison of ligand binding to a membrane assay and a whole cell.....	66
4.6	A qualitative sketch of the energies associated with a system with low constitutive activity.....	68
4.7	Alternate parameter set that exhibits a smaller shift from the whole cell model to the assay model	71
4.8	Predicted signal as a function of time in the membrane binding assay	76
4.9	Steps for binding of positive and inverse agonists in the membrane binding assay	77
5.1	Dimerization can lead to the formation of trimers via diffusion-limited partner switching	82
5.2	Dimerization phase behavior.....	87
5.3	Effects of increasing active and inert particle density on the average cluster size	89
5.4	Snapshots of the positions of two dimerizing protein species.....	91
6.1	Representative receptor organizations under different dimerization rules.....	102
6.2	The effects of changing dimerization rules on the signaling capability of each receptor type.....	107
6.3	Internalization rates of two receptor species under different dimerization rules	108
6.4	Drug induced signals under different dimerization networks	113

6.5	Example of how dimerization can be used to infer properties of a signaling system	114
7.1	Three processes that affect GPCR desensitization	126
7.2	Comparison of activation and desensitization profiles for a variety of drugs on two different receptor systems	128
7.3	Three receptors binding with a single ligand molecule under two limiting kinetic cases.....	129
7.4	Interaction network of the GPCR signaling and desensitization pathways.....	132
7.5	Effects of ligand dissociation rate constant and α on G-protein activation and receptor phosphorylation rates.....	136
7.6	Effects of cell properties on G-protein activation and receptor phosphorylation rates	139
7.7	Activation versus desensitization simulation results for drugs with a variety of different dissociation rate constants and α values	141
7.8	Schematic of the source of receptor kinase near a receptor as a function of the ligand dissociation rate constant	143
7.9	Comparison of the simulation results to the relative activation and desensitization profiles of five drugs	147
7.10	Treatment with morphine and a neutral antagonist results in a longer effect	148
8.1	Protein-protein interaction map	152
8.2	Dimerization induced localization could organize a large number of species together.....	153
8.3	A hypothetical composite screening assay	158
8.4	Extension of the cubic ternary model	160
8.5	A surface of possible conformations a receptor may occupy.....	161
8.6	Cross-reactivity of ligands, receptors, and G-proteins.....	162
B1	Cell membrane surface that smoothly changes from a 2D surface to a 1D line.....	169
B2	Traffic analogy	170

B3	A two dimensional surface model of a four sided pyramid	171
B4	Possible transitions for a two-particle system on a five-site grid	175

LIST OF TABLES

Table

6.1	Average shortest separation radius	105
6.2	Separation distance from simulations compared to FRET efficiency	119
6.3	Predicted activation level of secondary messenger as compared to an experimentally observed increase.....	120
6.4	Predicted internalization rates for each receptor species under different receptor activation conditions.....	121
7.1	Identities of species used in the desensitization model.....	132
7.2	Parameters used in the model	133
7.3	Activation and desensitization profiles of four common ligands to the μ -opioid receptor	146
B1	Probability distribution of a single particle on a 5-point grid	173

LIST OF APPENDICES

Appendix

- A. Model Equations from Chapter 4 164
- B. Effects of Topology on Dimerization Induced Clustering..... 168

ABSTRACT

COMPUTATIONAL ANALYSIS OF G-PROTEIN COUPLED RECEPTOR SCREENING, DIMERIZATION, AND DESENSITIZATION

By

Peter J. Woolf

Chairperson: Jennifer J. Linderman

Mechanistic models of G-protein coupled receptor (GPCR) signaling are used to gain insight into how changes in drug properties affect cellular response. Broadly, this work is divided into three areas focusing on drug screening, desensitization, and receptor dimerization.

First, ordinary differential equation models are used to examine biases in drug screening assays such as those used in drug discovery. It is shown that some screens should be innately biased against detecting inverse agonists and as such may miss pharmaceutically valuable drug leads. However, the results also suggest ways in which the screening assay can be modified to correct this bias.

Second, Monte Carlo simulations of protein diffusion and reaction are used to determine the effects of drug properties on GPCR activation and desensitization. For most GPCRs, drugs cause an initial burst of activity (activation) followed by an attenuation of the signal over long times (desensitization). Simulations of this activation and desensitization process show that the mean drug-receptor lifetime can affect

desensitization in a way that allows receptor activation and desensitization to be partially decoupled.

Third, Monte Carlo simulations of receptor dimerization and diffusion are used to show how dimerization can affect membrane organization. Many membrane bound proteins, including GPCRs, form transient dimers, but the physiological reason for dimerization is not clear. The simulations show that dimerization under diffusion limited conditions can lead to the formation of extended clusters. These clusters, in turn, can alter the receptor internalization rate and the degree of cross-talk among receptors, in agreement with experimental findings.

Overall, this work has a variety of implications. Pharmacologically, this work presents a new way of making drug discovery a more rational process by focusing assays toward drugs with desirable efficacies and improved desensitization profiles. Similarly, receptor dimerization could also provide a novel mechanism for affecting drug signaling. For basic biology, the modeling work presented here suggests that dimerization could provide a new way to control protein organization within the cell membrane. Together this work helps us to provide us with a more mechanistic understanding of how cells communicate via GPCRs.

CHAPTER I

INTRODUCTION

In this thesis I explore spatial and kinetic aspects of drug—receptor binding using computer modeling. This work has provided new insights into drug discovery and provided a more complete understanding of drug action. A common thread through this work is the application of models to the G—protein coupled receptor (GPCR) signal transduction pathway. This receptor system was chosen because of its wide applicability to pharmacology and because years of experimental research on this receptor family has provided a wealth of literature data.

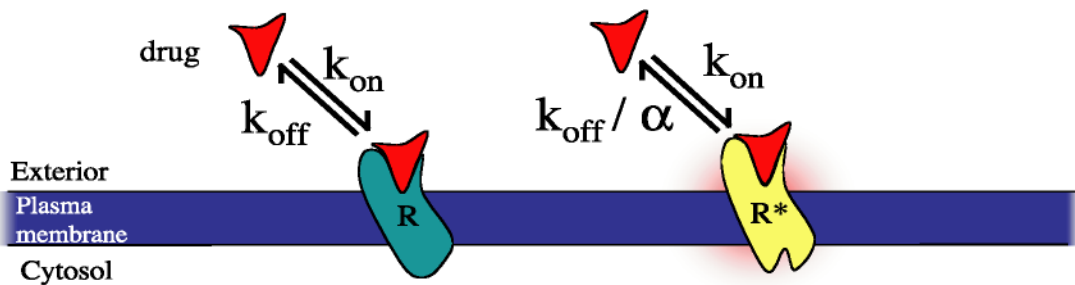
1.1 Signal Transduction

Ligand or drug binding to cell surface receptors initiates a series of events known as signal transduction. In this process, receptors alter the states of other proteins, which in turn leads to an avalanche of changes inside the cell. The cell uses this avalanche of information to describe what is occurring in the cellular environment and then to alter its behavior accordingly. Without signal transduction, the cell would be blind to many environmental changes, making the cellular cooperation we see in most organisms impossible. Therefore the long-term goal of this work is to understand how signal transduction takes place and what factors influence this process.

In this thesis, I assume that the action of a drug on a receptor can be described by three ligand specific parameters, k_{on} , k_{off} , and α as shown in Figure 1.1a. The parameters k_{on} and k_{off} describe the kinetic association and dissociation rate constants for ligand

binding to receptor. The ratio of these two parameters gives the equilibrium binding affinity of the ligand for the receptor. The third parameter, α , also known as the conformational selectivity factor, describes the relative affinity of the ligand for active and inactive receptor conformation as shown in Figure 1.1b. Roughly, α describes the ability of a ligand to hold a receptor in an active conformation. This conformation might activate secondary messengers, or could induce dimerization for example.

a)



b)

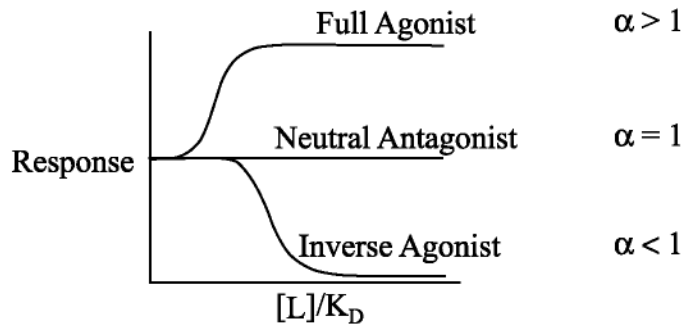


Figure 1.1 a) A drug's view of a receptor. Using a simplified view of drug–receptor interactions, the drug can only bind to (k_{on}) and dissociate from (k_{off}) the receptor, selecting for a specific conformation (α). b) Cell response as a function of ligand conformational selectivity, α . By changing α , one can obtain all three experimentally observed drug behaviors.

These three parameters describe ligand–receptor interactions if the receptor has only two states, active and inactive. The reason is that the cell's signal transduction machinery can only detect the identity and presence of a ligand through the conformation of the receptor.

Therefore if the receptor only exists in an active or inactive state, then the cell can only base its response on the frequency of receptor activation. The assumption of two states can be somewhat relaxed to include a one dimensional continuum of states between active and inactive states without changing this argument as shown in Figure 1.2.

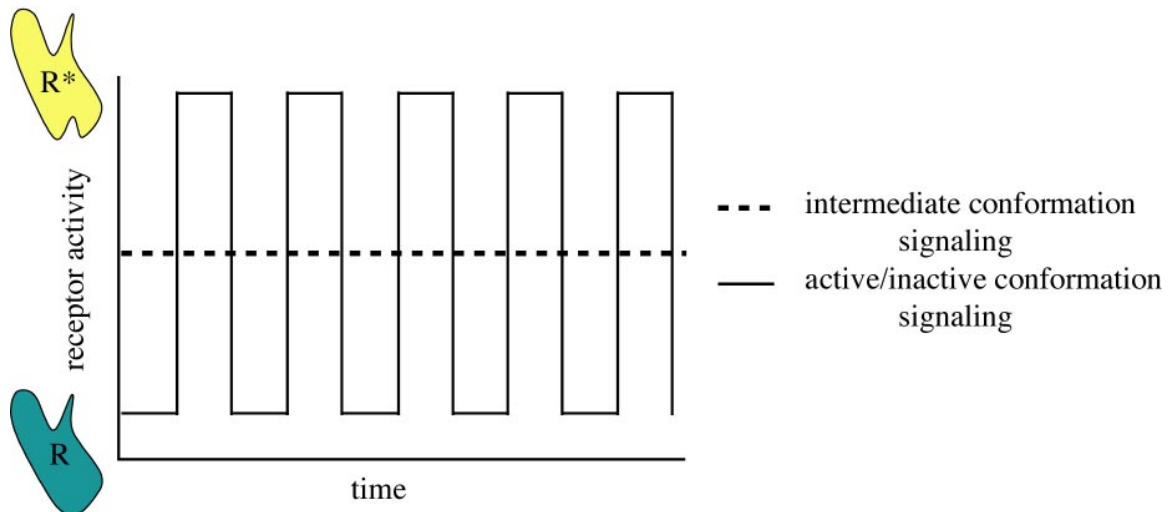


Figure 1.2 Two views of receptor activation. Receptor activity can be viewed either as rapidly switching from an active to inactive conformation (solid line) or as existing as continuum of receptor conformations ranging from an inactive to active conformations (dotted). Assuming the switching frequency from the active to inactive conformation is sufficiently rapid, then both views produce practically identical results.

Other ligand specific parameters have been suggested in the literature, but these parameters are generally not mechanistically realistic or are redundant if we assume the receptor exists in only an active or inactive conformation. For example, a number of models of receptor action include an additional equilibrium term β , which describes the ability of a ligand bound receptor to bind to G-proteins (Samama et al. 1993; Weiss et al. 1996). If we assume that the receptor can only exist between two states, active and inactive, then β must be set equal to one. A non-unity value of β indicates that the G-protein can distinguish between ligand bound and unbound receptor independent of

the activity of the receptor, implying that the receptor has an additional conformation beyond the active and inactive states. If future experimental evidence supports the existence of additional physiologically relevant receptor conformations, then additional terms describing drug–receptor interactions must be included.

The work in this thesis describes how drugs can influence drug screening, receptor organization and signaling via dimerization, and receptor desensitization. By describing the ligand with three established parameters, k_{on} , k_{off} , and α , I can probe how changes in the drug should affect each of these processes. These results demonstrate how this simplified view of drug action can yield pharmacologically useful predictions that are able to direct future research.

1.2 G—Protein Coupled Receptors (GPCRs)

In this work I focus on a pharmacologically important class of receptors known as GPCRs. As their name implies, GPCRs transmit their signal by coupling with guanine nucleotide binding proteins (G—proteins). Approximately 80% of all known hormones, neurotransmitters, and neuromodulators are believed to transmit their signal through these G—protein coupled receptors (GPCRs) (Lesch and Manji 1992), and pharmacologists estimate that 60% of all medicines used today act through G—protein signaling pathways (Roush 1996). Examples of such GPCR systems include the β —adrenergic receptor (involved in regulating heart contractility), theopioid and dopamine receptors (involved in brain function), and the N—formyl peptide receptor (involved in the immune response). Figure 1.3 illustrates a number of other important physiological uses of GPCRs in the human body. Abnormalities in GPCR signaling are involved in numerous diseases and disorders and are therefore a major target for

therapeutic intervention (Arvanitakis et al. 1998). By working to understand GPCR signaling, I hope to foster the development of better, more effective drugs to improve human health.

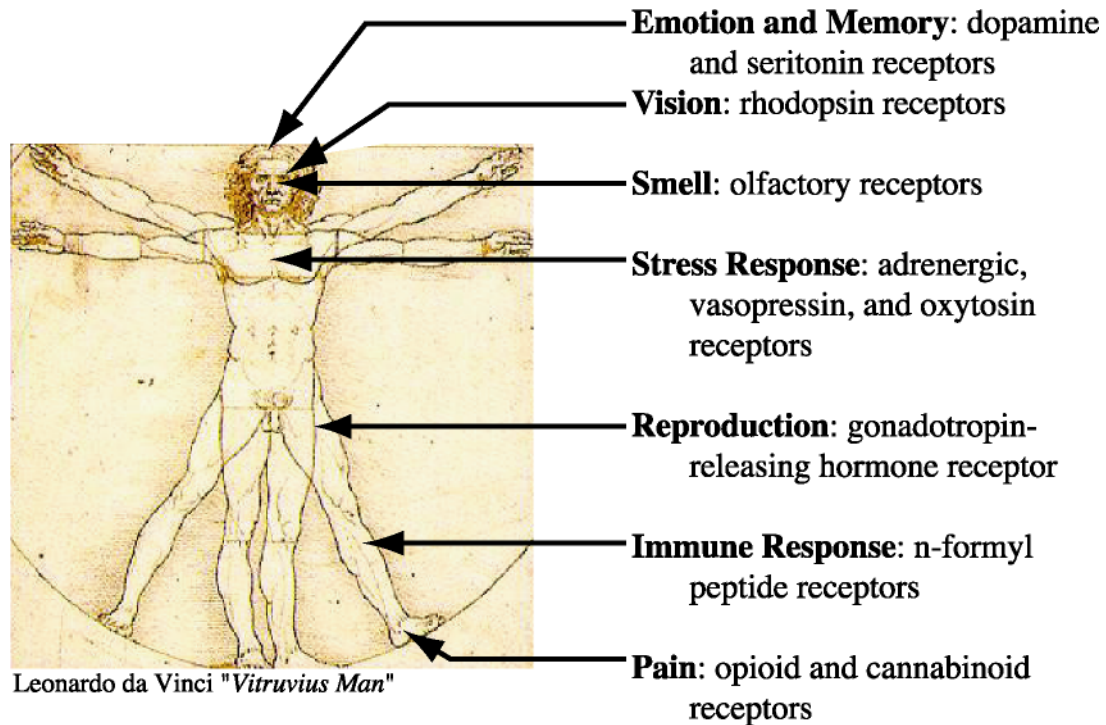


Figure 1.3 Physiological roles of GPCRs throughout the human body.

Receptor mediated G—protein activation has been well characterized both experimentally and theoretically (Neer 1995; Berman and Gilman 1998) and is shown schematically in Figure 1.4. With no ligand present, GPCRs generally favor the inactive conformation with only a small fraction of the total receptors in the active conformation, leading to a low level of constitutive signaling (Lefkowitz et al. 1993). However, in the presence of a strong agonist, receptors will change to the active conformation. While in the active conformation, the receptor can bind to inactive G—proteins, the heterotrimer $\alpha\beta\gamma$ —GDP. In the presence of GTP, the G—protein can then exchange GTP for GDP on its

α subunit, causing the dissociation of the G—protein into two subunits α —GTP and $\beta\gamma$. Both α —GTP and $\beta\gamma$ are believed to propagate the signal inside the cell, thereby initiating the changes that lead to a response within seconds to minutes of receptor activation (Kenakin 1996). The α subunit possesses intrinsic GTPase activity that deactivates the α subunit, allowing the α —GDP and $\beta\gamma$ subunits to reform the inactive G—protein. Thus G—protein activation serves as a timed molecular switch.

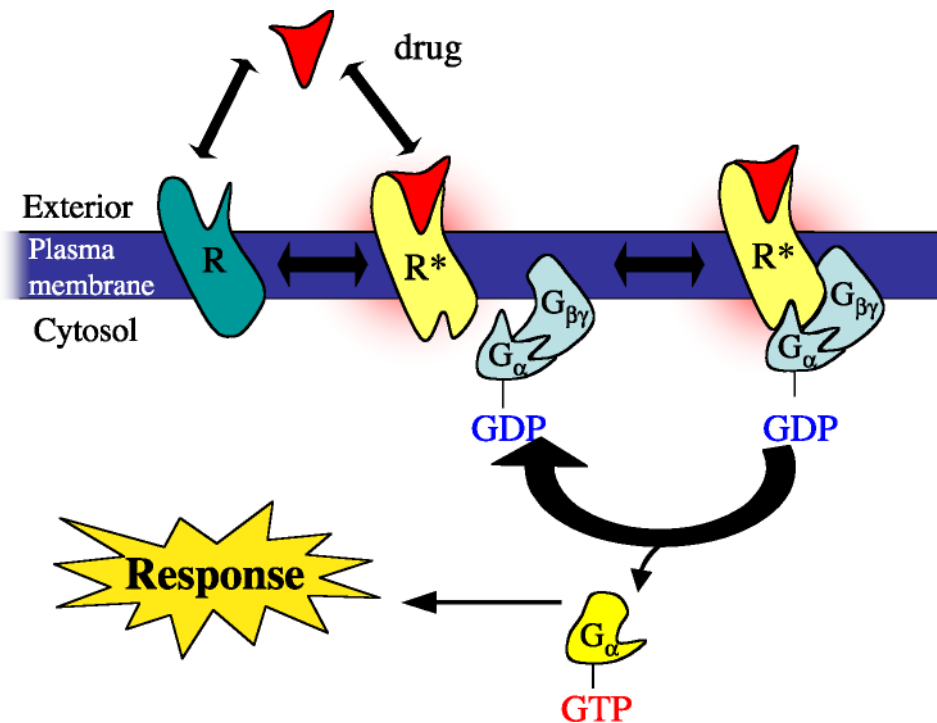


Figure 1.4 GPCR signal transduction cascade. First, ligand binds to the receptor and alters its conformation. The active conformation can then bind with the G-protein and catalyze the exchange of GDP for GTP. In the active GTP bound state, the G-protein dissociates into two subunits, G_α and $G_{\beta\gamma}$, both of which can propagate a signal. With time the active G_α subunit reverts to the inactive GDP form and rebinds the $G_{\beta\gamma}$ subunit to recover an inactive G-protein.

When multiple species of G-protein and receptor are present, then there is the possibility of receptor cross—talk. Receptor cross—talk describes the process in which activation of one receptor species co—activates the signal transduction pathway of a

second, inactive receptor species (Tomura et al. 1997). For example, ligand binding to the D_2 dopamine receptor has been shown to affect the signaling ability of the somatostatin receptor SSTR5 (Rocheville et al. 2000). In this thesis I will only focus on cross-talk at the level of receptors and G-proteins. In this case, we assume that each receptor species primarily acts on a single species of G-protein, but weakly cross-reacts with a second species of G-protein as shown in Figure 1.5. In this case, the degree of receptor cross-talk between any two receptor species could be influenced by the spatial organization of receptors on the cell membrane as shown in Figure 1.6. In Figure 1.6a, each species of receptor is spatially isolated resulting in low levels of cross-talk, while in Figure 1.6b, the receptors are well mixed resulting in increased cross-talk.

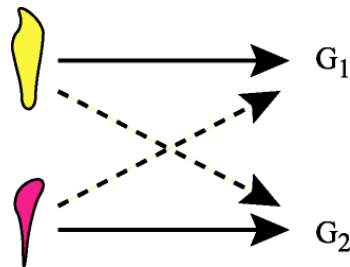


Figure 1.5 Cross-talk between receptors. In this scheme each receptor activates its primary G-protein (heavy line), but can also cross-react with a secondary G-protein (dotted line).

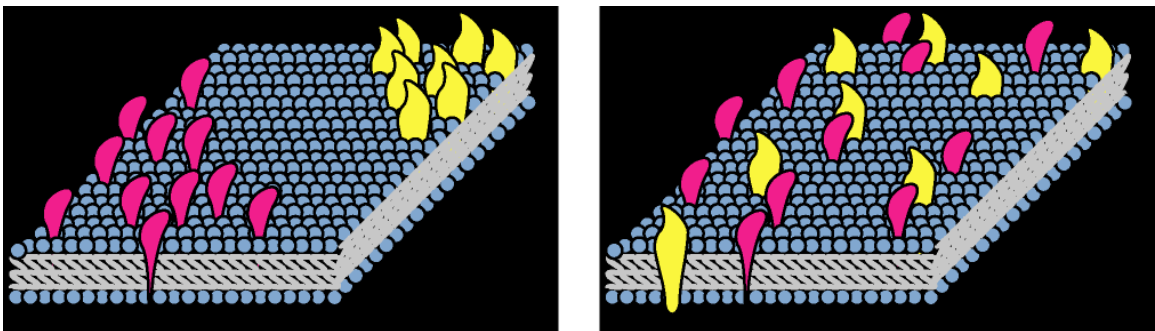


Figure 1.6 Impact of location on cross-talk between two distinct receptors species (pink and yellow). a) Receptors that cluster into homogeneous islands are expected to exhibit little cross-talk. b) Well mixed pools of receptors may have increased cross-talk.

1.3 Receptor Dimerization

Dimerization of membrane bound proteins is ubiquitous although its impact on cell function has not been well characterized. A simplified view of protein dimerization is shown in Figure 1.7, whereby dimerization of two monomers is described by the rate constant k_{dimer} , and breakup of a dimer into two monomers is described by the rate constant k_{mono} . Ligands might influence this process by changing the conformation of the receptor. Therefore, if we assume that only active or inactive receptors form dimers, then the ligand specific parameters α should also describe the degree of receptor dimerization at any given time.

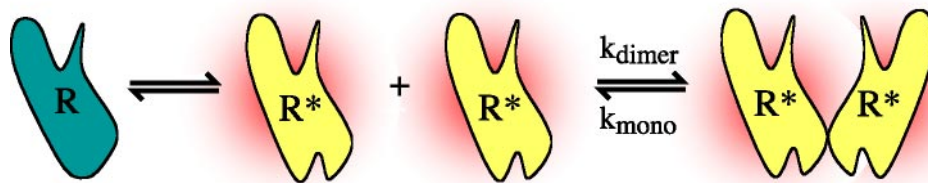


Figure 1.7. Receptor dimerization. Dimerization and monomerization rates depend on the activity of the receptor.

The role of dimerization is not clear for many receptor systems. For receptor tyrosine kinase proteins, dimerization is thought to bring reactive species together to transduce a signal (Weiss and Schlessinger 1998), although dimerization alone may not be sufficient to transduce a signal (Burke and Stern 1998). In other systems the physiological role of dimerization is less clear. For example, it has been recently revealed that a large number of G-protein coupled receptors (GPCRs) are able to form homo- and heterodimers (Nimchinsky et al. 1997; Hebert and Bouvier 1998; Gines et al. 2000; Overton and Blumer 2000). In most cases, dimerization of GPCRs does not correlate with signaling, but instead is thought to affect signal cross talk among receptor types or desensitization of the receptor via an unknown mechanism (George et al. 2000; Jordan et al. 2001). Similarly, the bacterial receptor Tar (Gardina and Manson 1996), human nerve growth factor receptor (Schlessinger and Ullrich 1992), and the bacterial

and plant Photosystem II proteins (Jahns and Trissl 1997) are all able to form transient dimers in the membrane, but the reasons for these interactions are unknown.

Although the role of dimerization is not well characterized, dimerization appears to be an evolutionarily conserved property of many signaling proteins and as such is likely to play a critical role. In chapter 5 we discuss how dimerization could provide a means to localize GPCRs on the cell membrane. In chapter 6 we show how this organization could influence receptor physiology.

1.4 Receptor Desensitization

After sustained receptor activation, the number of receptors in the cell membrane drops in a process termed long term desensitization (January et al. 1997; Krupnick and Benovic 1998). This process serves two related roles in that it maintains the sensitivity of the cell's downstream signaling machinery while regulating receptor number. The result is that the cell's downstream signaling machinery, such as G-proteins and adenylyl cyclase, cannot remain saturated by activating a single receptor species and therefore will always be available for other receptors to use. In addition, receptor desensitization provides a convenient and distributed method for dynamically regulating receptor expression levels on the cell surface. For example, when no ligand is present then constitutive receptor signaling will maintain a larger number of receptors on the cell surface, thereby making the cell sensitive to ligands. Upon ligand addition, the cell will reduce the number of receptors on the cell surface (Ciruela et al. 1997; Aragay et al. 1998). Because long term desensitization alters the number of receptors expressed on the cell surface, it is thought to play a key role in processes such as drug addiction, drug tolerance, and cellular development (Chuang et al. 1996; Nestler and Aghajanian 1997).

One mechanism of GPCR desensitization is shown in Figure 1.8. According to this mechanism, the $\beta\gamma$ subunit of the active G-protein is able to recruit a receptor kinase to the cell membrane. This receptor kinase in turn is able to phosphorylate the active receptor, thereby initiating a cascade of events that eventually leads to receptor internalization (Lefkowitz et al. 1992; Aragay et al. 1998; Elorza et al. 2000) on a time scale of hours. This form of desensitization is elegantly distributed in that it relied on G-protein activation as the signal for desensitization, thereby requiring no central controller to automatically self-regulate. The spatial implications of the desensitization pathway will be modeled in chapter 7 of this thesis.

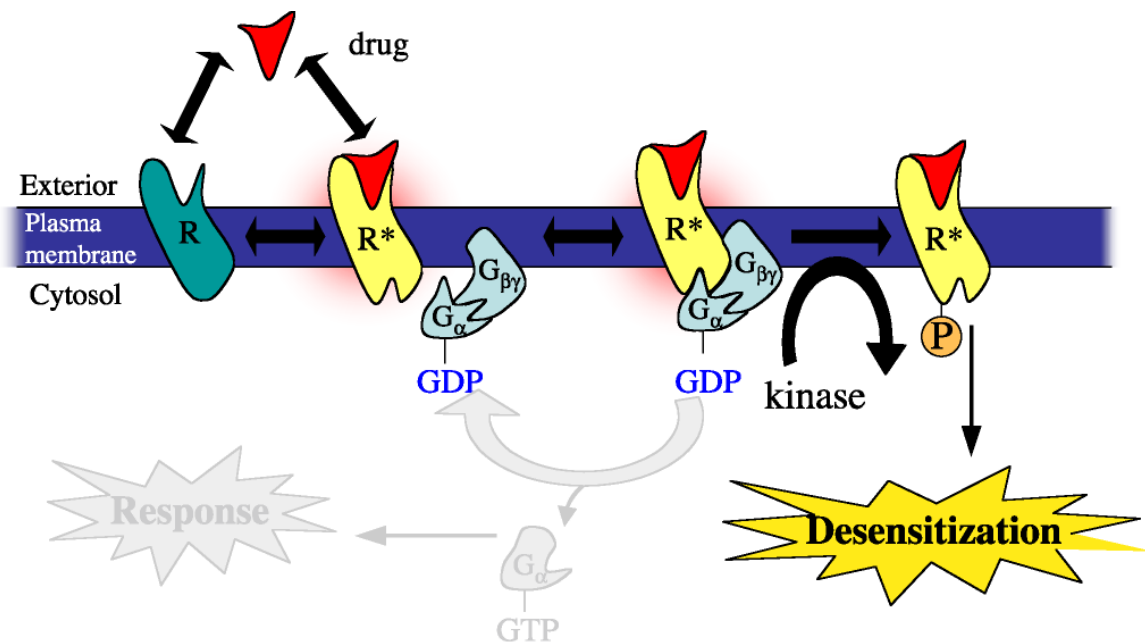


Figure 1.8 Mechanism of GPCR desensitization. The active G $\beta\gamma$ is able to recruit receptor kinase from the cytosol. This membrane bound receptor kinase can then phosphorylate receptors in the active conformation. With time these phosphorylated receptors will be removed from the cell surface, resulting in long term desensitization.

Other forms of rapid signal desensitization also take place, but will not be considered in this work because they are insufficiently characterized. For example, it has been shown that receptor desensitization is affected by protein kinase A (PKA) and

protein kinase C (PKC) (Fonseca et al. 1995; Penn et al. 1998; Seibold et al. 2000). However, the mechanism by which PKC and PKA act and become activated themselves is currently poorly understood and likely more complicated than the receptor kinase pathway. Similarly, desensitization also takes place at the level of adenylyl cyclase or further down the signal transduction pathway (Parent et al. 1998), but the mechanism of this downstream form of desensitization is not clear at this time and as such can not be included in a mechanistic model.

1.5 Drug Screening

New drugs are generally found using random screens of large chemical libraries. At this time it is not uncommon to screen more than one million small molecules in a high throughput screen to detect a handful of lead compounds. Later in the drug development process, this list will be further shortened due to drug toxicity, low solubility, and side effects (Drews 2000). Therefore it is important to have as large and accurate of a high throughput screen as possible to generate viable lead compounds.

One common approach to high throughput screens is to use a binding assay such as the scintillation proximity assay shown schematically in Figure 1.9 (Bosworth and Towers 1989). This assay uses a radio labeled tracer ligand that is known to bind to the receptor. Upon binding the labeled tracer ligand, the radioactive decay activates a fluor that causes an optical signal. Drug binding is detected by measuring the signal drop caused by an unlabeled test ligand competing with the labeled tracer. If the signal drops sufficiently, then the test drug is categorized as a hit and is passed on for further analysis.

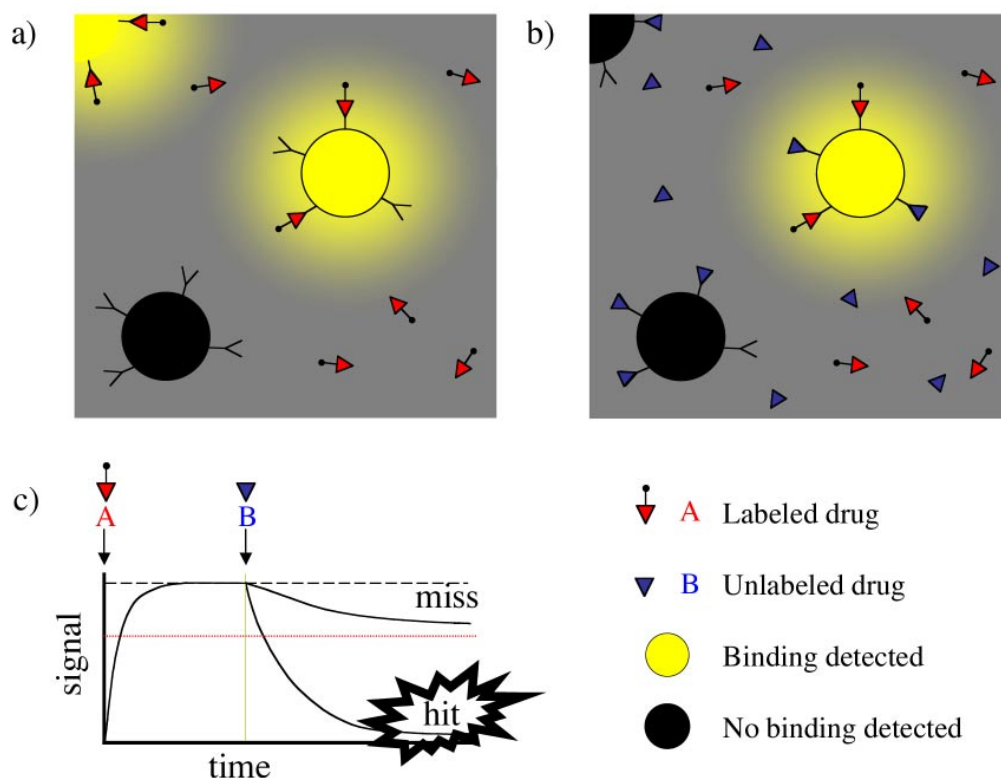


Figure 1.9 A high throughput screening assay based on the scintillation proximity assay. a) Assay with only radio labeled tracer to produce a base signal. b) Assay after the addition of a test molecule to compete with the tracer. c) The affinity of the test ligand for the receptor can be measured by following the drop in signal.

Most drug screens are designed on the premise that we first must find a drug that binds to the receptor, and then optimize that drug to achieve the desired effect.

Admittedly, drug—receptor binding is the first step in drug action, but not only does this binding depend on the drug but also the receptor conformation that binds the drug. Using a lock and key analogy, we need a key that not only fits but also opens doors. Elmer's glue and toothpicks both bind tightly to locks, but neither opens doors! Therefore, in chapter 3 of this work we show how drug screens are biased against certain classes of drugs, but can be tailored to screen for drug that not only bind tightly but also produce the desired response.

1.6 Overview of Thesis

While a great deal of theoretical and experimental research has been directed toward understanding GPCR signal transduction, much remains to be done. Historically GPCR research has focused on identifying the individual parts of the signal transduction pathway at a single time in isolation. Although this reductionist approach has proven invaluable in describing the system, it provides little information as to how the parts work together as a complete system.

The work in this thesis uses computer models to bring the pieces of GPCR signal transduction pathway together to gain a better understanding of signaling in general, with a specific focus on how this new knowledge can be used to aid drug development. In particular I have examined how the drug's dissociation rate, conformational selectivity, and ability to induce dimerization affect how the cell responds to the drug. Computer models are used because they allow us to integrate a wide variety of findings from the literature into our model while still maintaining tight control on the physics of the system. This approach allows us to make general predictions that should be true for many receptor types and therefore provide useful insight into drug discovery and development.

This thesis employs two distinct modeling approaches that are reviewed in Chapter 2. The first approach, used in Chapters 3 and 4, examines how a system varies with time and species concentrations. This approach has the advantage that it is fairly easy to include many species and is fast to simulate. The second approach, used in Chapters 5, 6, and 7, includes spatial effects to show how diffusion can influence receptor signaling. Both approaches are valid, but provide different information under specific conditions.

Chapter 3 uses a steady state solution of a thermodynamically complete model of GPCR signaling to show a phenomenon I have termed agonist inversion . Normally a drug can be classified as an agonist, antagonist, or inverse agonist independent of the stoichiometry of signaling components in the cell. However, under certain conditions, a drug can change from an agonist to an inverse agonist (hence agonist inversion) by changing the number of G—proteins in the system. This finding could have implications for the development of novel drugs that are selective for subpopulations of cells.

Chapter 4 demonstrates how some high throughput screening techniques could bias against the detection of inverse agonists. This finding is made using ordinary differential equation models of whole cells and a membrane bound screening assay. These models are then used to show that inverse agonists bind more weakly and more slowly than positive agonists in the screening assay, and as such could be missed. However, these findings also indicate that manipulating the total number of G—proteins in the system should focus the assay toward detecting drugs with any efficacy, thereby better utilizing the screening assay as a tool for drug discovery.

In chapter 5 receptor dimerization is shown to cause self—organization of the cell membrane. The effects of dimerization are shown using Monte Carlo simulations of receptors diffusing and interacting on a two-dimensional model of the cell membrane. Depending on the rates of receptor monomerization, dimerization, and diffusion, an ensemble of receptors can exist in either a monomer state, dimer state, or intermediate gel type state where extended clusters form. Our simulations of dimerization demonstrate a new mechanism for understanding how receptors are trafficked on the cell membrane.

Chapter 6 discusses the physiological implications of dimerization induced receptor localization with implications for drug design. Ligands to GPCRs influence dimerization, but it is not clear why. Using Monte Carlo simulations we show that dimerization induced localization of multiple receptor species should influence receptor cross-talk, internalization, and signal amplification. We further demonstrate that this organization is in principle measurable and can be manipulated by ligands. Therefore ligand-induced dimerization could provide a new tool with which pharmacologists can manipulate cell response.

Chapter 7 includes a desensitization mechanism into the Monte Carlo model and shows that ligand induced signaling and desensitization can be decoupled. The model shows that by varying the ligand dissociation rate receptor desensitization can be controlled via a receptor switching mechanism. This result explains why in some cases receptor signaling and desensitization are not correlated, and provides a novel route for controlling drug desensitization.

CHAPTER II

MATHEMATICAL MODELS OF SIGNAL TRANSDUCTION

Within the next half—century, with all genes identified and all possible cellular interactions and reactions charted, pharmacologists developing a drug or toxicologists trying to predict whether a substance is poisonous may well turn to computer models of cells to answer their questions.

(Collins and Jegalian 1999)

2.1 Introduction

Models of signal transduction have enhanced our understanding of cellular communication, and in doing so may someday help us to produce better pharmaceutical agents. For example, the two state receptor model has helped us to understand how the receptor is able to transmit a signal from the outside of the cell to the inside. This knowledge in turn has helped pharmacologists to understand why certain drugs are more effective, or efficacious, than others, leading to advances in drug discovery and development. Therefore, models of signal transduction play a key role in modern biotechnology and will most likely play an increasingly large role in the future.

Models of signal transduction can be most easily distinguished by how they handle time and space. The real signal transduction system changes with time and exists in a finite space, however modeling this complete system is not practical due to lack of computing time and realistic parameters. For example, a receptor diffusing on a cell membrane is able to explore a large amount of space as time progresses, however to understand ligand binding to this receptor, the absolute position of the receptor in the membrane is not important and could, in some cases, be difficult to calculate. To avoid

modeling all of the dynamics of the system, modelers have developed techniques to simplify time and space, thereby making the problem tractable and intuitive.

In the next section I first examine three approaches to handle time varying systems and then discuss how spatial effects can be included. All of these approaches are used throughout the research in this thesis, therefore this overview is meant to give a general understanding of how each approach can be used in a simpler, more approachable context.

2.2 Models that Change with Time

To illustrate how time is modeled in this thesis, I will discuss three simple mechanistic models of GPCR activation and show how each model can yield useful insights. With regard to time, mechanistic models can be categorized as equilibrium, steady state, or unsteady state models. Equilibrium models deal with systems that do not change with time and require no energy inputs to sustain a particular state. Steady state systems also do not change with time, but do require an energy input to maintain a state. Unsteady state models describe systems that do change with time.

As an analogy to these three types of models, consider the physical example of a pendulum shown in Figure 2.1. The equilibrium solution of a pendulum places the pendulum hanging straight down. This is the state that the pendulum is “trying” to get to, but keeps swinging past. If the pendulum were instead driven in one direction by a motor or a constant breeze, then we would use a steady state model, which would place the pendulum at an angle. This new state is similar to the equilibrium state except that it includes the effects of some external energy input (drag from the wind or electricity for the motor). Finally, to look at the time varying swinging of the pendulum we can use an unsteady state model. The unsteady state model will show us how high the pendulum

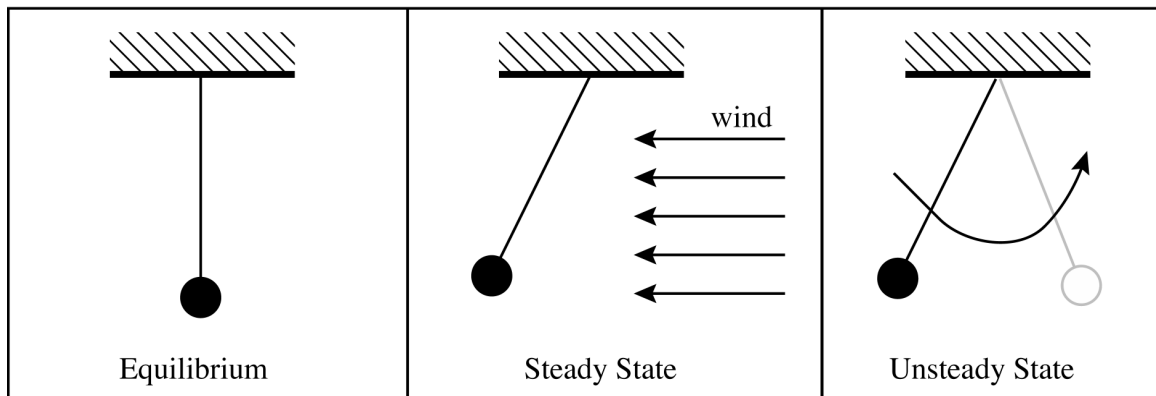


Figure 2.1 A pendulum analogy to describe the three types of models discussed in this thesis. At equilibrium the pendulum hangs straight down. When the pendulum is driven by an energy source (i.e. wind) then the pendulum hangs at an angle in a steady state. The unsteady state model describes how the pendulum moves with time.

swings, how fast the pendulum moves, and how long it will take the pendulum to stop moving. Thus our choice of which model to use depends on the type of behavior we want to describe.

Equilibrium models are the most commonly used type of model in pharmacology. One of the main reasons for this model's popularity is that this class of models tends to have parameters that are easily measured and the mathematics is generally simple. By definition, these models assume that the system is at thermodynamic equilibrium – a state that requires no energy to maintain and does not change with time.

In biology, the equilibrium state corresponds to death; however, equilibrium models can still be useful for modeling certain pharmacological systems. For example, some experimental systems such as membrane preparations can be used to obtain equilibrium data. Although these *in vitro* measurements may not correspond exactly to the *in vivo* situation, in many cases the agreement is sufficiently good to warrant using this simpler system. In other cases, equilibrium models can be used to describe an

"apparent" equilibrium between species in the cell, even though the system might in truth be an energy-requiring steady state system. For example, consider the "equilibrium" number of receptors on the cell surface. In truth, receptors are constantly being shuttled to and from the cell surface. However, at any given time there appears to be fixed number of receptors on the surface. In this way, equilibrium models are often used as a first approximation to fit the mechanics of the system.

Steady state models describe a system that is not in equilibrium, but the apparent concentrations of each species do not change. For example, consider a metabolic cycle like the Krebs cycle, which converts acetyl CoA to energy and CO_2 . The concentrations of intermediates in the cycle do not change with time; however, there is a constant flux of acetyl CoA into the system. To maintain such a state of stable dis-equilibrium, the system requires a constant input of energy in some form, in this case the bond energy of acetyl CoA.

Steady state models are generally more realistic models of biological systems than equilibrium models. Nearly every biological system requires energy to maintain its state, and as such nearly every biological reaction is in a constant state of flux. For models of drug action, ongoing and energy-requiring processes such as G-protein activation and receptor phosphorylation can have profound effects on the behavior of a drug and are important to include.

Unsteady state models provide an even more general description of a system because they include the effects of time. Steady state and equilibrium models assume that the system has had an infinite amount of time to stabilize, and as such remove all dependence on time and initial conditions. In contrast, unsteady state models describe

how the system evolves with time and can be used to describe systems that have no steady state, such as periodic or chaotic systems.

Unfortunately, unsteady state models are also some of the most complicated to solve. Often, these models are formulated as coupled sets of differential equations and in many cases there is no analytical solution. Even a numerical solution may be difficult to obtain. In spite of these problems, unsteady state models are probably the best choice if sufficient data are available to motivate their development.

One disadvantage to using the more detailed models, e.g. unsteady state models, is the need for more parameters to describe the system. For example, for the equilibrium solution to the pendulum problem we don't need any information because the pendulum is always down no matter how much it weighs or how long it is. In contrast, for the unsteady state solution, we must know all about the pendulum plus we must know where the pendulum was started and how fast it was moving when it started. In complicated biological systems such as a signal transduction pathway or metabolic cycle, a large number of parameters are also needed to describe the unsteady state behavior. However, by using many parameters to describe a complex biological system we are not "fitting an elephant." This is because the parameters in the unsteady state model describe specific physical phenomena related to the mechanics of the process, not empirical correction factors used to simply *fit* the data. The parameters used in describing these biological systems are (at least in principle) measurable physical quantities just like mass and length used to describe the pendulum. Fortunately, in many cases the exact parameter values are not needed because we are only interested in the qualitative behavior of the system. For example, we may be interested in determining whether a ligand is a positive or inverse

agonist, and whether it is possible for a ligand to be both but under different circumstances. Thus even crude experimental measurements can be helpful in predicting the behavior of the response, even though they may not give the exact magnitude or duration of the response.

2.2.1 Species Conservation

Along with the type of model we choose, we must also determine which simplifying assumptions are reasonable to make. One major simplifying assumption that is often made in pharmacological models is that the concentration of some species is constant. For example, during a binding experiment, the free ligand concentration may not change significantly. In this case, we can approximate the system by modeling the free ligand concentration as a constant, thereby ignoring any dynamics that might come about due to ligand depletion. The concentration of a species can be approximated as a constant if (1) the species is in great stoichiometric excess or (2) the system has access to a near infinite reservoir of the species at a fixed concentration.

When these conditions are not met, however, depletion effects must be included through the use of species conservation equations. For example, receptors are known to saturate (depletion of free receptors) when enough ligand is added, implying that we need to include a receptor conservation equation in our model. This conservation equation can be stated as:

$$R_{\text{bound}} + R_{\text{free}} = R_{\text{total}} \quad (2.1)$$

This species conservation equation enforces that the model has access to only R_{tot} receptors, making the maximum number of receptors that can bind ligand equal to the total number of receptors.

Why isn't species conservation always included? We know that no species *really* comes from an infinite source, so we are always safe to include species conservation equations even if they have little effect on the predictions of the model. However, including species conservation also makes the model equations more difficult to solve, as the model often changes from linear to nonlinear. Linear models are generally easy to solve both analytically and numerically, and the results they generate are easy to interpret. In a linear model, doubling the value of an input will always double the output. In contrast, nonlinear models often have no analytical solution and can be more difficult to solve numerically. Interpretation of nonlinear models can also be more challenging because, for example, doubling the value of an input may or may not double the output. Thus many researchers choose not to include species conservation even if it is known to play an important role so as to simplify their models enough to tease out some, but perhaps not all, relevant behaviors.

Without explicit spatial considerations, unsteady state models that include species conservation will ultimately provide the best insight into GPCR signal transduction. Signal transduction via GPCRs is an inherently unsteady state process because it is designed to detect *changes* in the environment—time varying information. Thus GPCR pharmacology is essentially the study of how to manipulate this information given to cells to change their states, making unsteady state models an invaluable tool in this field. For an unsteady state model to function properly we must also allow the concentration of each species (e.g. free receptors, inactive G proteins) to vary and if need be deplete, and thus species conservation must be included. However, this is not to say that equilibrium models or models without species conservation are useless. On the contrary, equilibrium

models describe where the system “wants” to go given enough time, and as such can be used as a landmark when analyzing the more complicated unsteady state systems. Models without species conservation describe a system under a limited set of conditions, but in a much more simple way. Therefore it is instructive to begin by looking at simple equilibrium models and then see how these models can help us understand more complicated unsteady state models. Through the use of simpler models to understand more complex and realistic models, we can begin to explain and predict the complex events of GPCR signaling, giving us insight into the mechanisms of drug action on this receptor.

2.2.2 Equilibrium Models

In this model section and in the two that follow, I begin first with a simple didactic model before moving on to the case of GPCRs. A simple example of an equilibrium process is receptor–ligand binding (Figure 2.2a). In this model, ligands bind to receptors at a rate proportional to k_1 ($M^{-1} \text{ sec}^{-1}$) and dissociate with rate constant k_{-1}

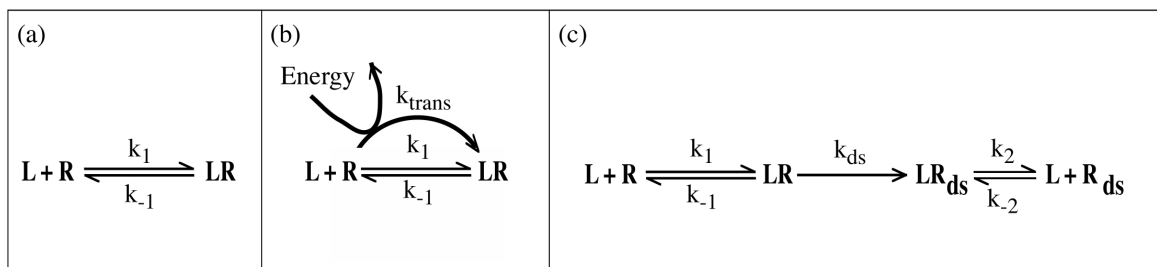


Figure 2.2 Three representative models of receptor–ligand binding: (a) equilibrium; (b) steady state; and (c) unsteady state. These are simple models used to illustrate the principles behind each technique.

(sec^{-1}). At equilibrium, the forward reaction is exactly balanced by the reverse reaction, resulting in the equilibrium relationship:

$$K_{eq} = \frac{k_{-1}}{k_1} = \frac{[R][L]}{[RL]} \quad (2.2)$$

Here $[R]$ represents the concentration of free receptors on the cell surface, $[RL]$ is the number of ligand-bound receptors, $[L]$ is the free ligand concentration, and K_{eq} is the equilibrium dissociation constant. In the equilibrium state there is no net binding or dissociation of the ligand from the receptor, so the system is at thermodynamic equilibrium – the state that receptors and ligands "want" to go if left to themselves. To include receptor conservation, the term $[R]$ can be replaced with $R_{tot} - [RL]$ to give the familiar expression for receptor–ligand binding:

$$K_{eq} = \frac{k_{-1}}{k_1} = \frac{(R_{tot} - [RL])[L]}{[RL]} \quad (2.3)$$

By knowing the free ligand concentration (generally assumed equal to the ligand concentration added, a reasonable assumption if the number of ligand molecules is significantly greater than the number of receptor molecules (Lauffenburger and Linderman 1993)), the number of ligand-bound receptors, and total number of receptors, we can calculate the equilibrium constant between the bound and free receptors.

Although signal transduction via GPCRs begins with receptor–ligand binding, binding alone is insufficient to describe the ligand's effects on the cell. For example, receptor–ligand binding alone can not predict inverse agonism because this would require the receptors to be bound with a *negative* number of ligands. Clearly other signaling phenomena must be included. In the case of GPCRs the natural next step is to include

more of the signal transduction pathway, such as the G-proteins which receive the signal inside the cell.

What happens to the predicted cellular response when G-proteins are added? G-protein reactions, such as receptor-G-protein binding, allow us to simulate the first signaling events inside the cell, thereby generating a more accurate picture of the signal transduction events caused by a particular ligand. Experimental evidence suggests that GPCR exist in at least two signaling-capable states on the cell surface, an “active” or R* conformation and an “inactive” or R conformation (Lefkowitz et al. 1993; Samama et al. 1993). The R* state is able to interact with G-proteins to produce G-protein activation; the R state is not. These active and inactive states presumably represent sets of conformations of the receptor (Kenakin 1996), and the receptors are likely to move between these states fairly rapidly.

GPCRs are typically modeled using what are termed ternary (for ligand/receptor/G-protein) complex models, or TCMs (reviewed in (Kenakin 1996)). Recent models which include the R* and R states are the extended ternary complex model (Samama et al. 1993) and the more thermodynamically complete cubic ternary complex (CTC) model (Weiss et al. 1996; Weiss et al. 1996). The CTC model is shown in Figure 2.3a. These models (and other related TCMs) are equilibrium models and have found some use in describing unique drug properties.

In the CTC model shown in Figure 2.3a, ligands influence the distribution of R* and R states (and thus potentially efficacy) via the *conformational selectivity parameter* α . At high α values ($\alpha > 1$) the ligand induces or selects the active receptor state (positive agonism), whereas when α is low ($\alpha < 1$) the ligand induces or selects the inactive receptor

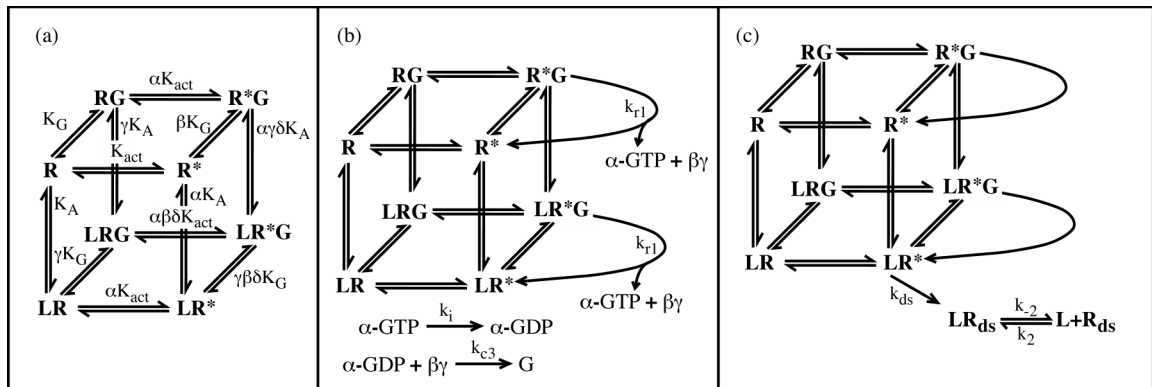


Figure 2.3 Three models of signal transduction via GPCRs. (a) The Cubic Ternary Complex (CTC) model (Weiss et al. 1996) that describes the equilibrium between receptor, G–protein, and ligand. (b) A steady state variant of the CTC model that includes an explicit G–protein activation step (Linderman 2000; Shea et al. 2000). (c) An unsteady state version of the CTC model that includes a desensitization step for ligand–bound active receptors.

state (inverse agonism). When α is exactly equal to 1, the ligand has no effect on the receptor conformation and does nothing but block the effects of other drugs (neutral antagonism). In the CTC model, α is just one of many ligand–specific parameters that determines how the cell will respond to a drug (Weiss et al. 1996).

Equilibrium models are used in Chapters 3–6 of this thesis. In chapter 3, equilibrium models are used to show how a ligand can change from a positive agonist to an inverse agonist by changing the stoichiometry of the system alone. In chapters 4–6 it is shown how diffusion and dimerization at equilibrium can induce receptors to self–organize and thereby affect receptor signaling. Although these later models also have a spatial component, the system is at equilibrium and as such is similar to the models presented in this section.

2.2.3 Steady State Models

To illustrate how a steady state model could evolve before examining such a model for GPCRs, consider the receptor–ligand binding as described in Figure 2.2b. In this scenario, imagine that the ligand is actively transported toward the receptor, thereby introducing an energy–requiring step that would disrupt the equilibrium. In our model, this active transport could be included by adding an additional binding step governed by the rate constant k_{trans} ($\text{M}^{-1} \text{sec}^{-1}$). The overall rates of formation of R and LR can be written as:

$$\begin{aligned} r_{\text{R}} &= k_{-1}[\text{LR}] - k_1[\text{L}][\text{R}] - k_{\text{trans}}[\text{L}][\text{R}] \\ r_{\text{LR}} &= k_1[\text{L}][\text{R}] + k_{\text{trans}}[\text{L}][\text{R}] - k_{-1}[\text{LR}] \end{aligned} \quad (2.4)$$

By setting the rates of formation equal to zero, we can obtain an expression for the steady state values of [R], [L], and [LR]:

$$K_{\text{eq}}^* = \frac{k_{-1}}{k_1 + k_{\text{trans}}} = \frac{[\text{R}][\text{L}]}{[\text{LR}]} \quad (2.5)$$

Note the similarity to the equilibrium model solution (Eqn. 2.2). Here the apparent equilibrium constant, K_{eq}^* , can be related to the true equilibrium constant by adding k_{trans} to the denominator. Another way to interpret this steady state result is that the form of the steady state solution is identical to the equilibrium solution except that the value of the equilibrium constant is different. This relationship between equilibrium and steady–state models is true as long as all steps are reversible. When irreversible steps are included, the structure of the solutions may also change. The implication of this finding is that experimental data taken from true equilibrium systems (such as membrane extracts) can not easily be applied to living steady state systems. In the example given here, the equilibrium dissociation constant K_{eq} could be much greater than the

equilibrium dissociation constant K_{eq}^* in the steady state system, causing a significant error in the interpretation of *in vivo* data based on data from membrane systems. Adams et al. (Adams et al. 1998) describe a similar example in which the amount of receptor/G-protein precoupling (association prior to ligand binding) measured in membrane assays may overestimate that present *in vivo*.

A steady state analysis can be done on more complicated systems such as GPCR activation of G-proteins. As discussed earlier, G-proteins cycle from an active GTP-bound state to an inactive GDP-bound state. In modeling terms, this cycling from an active to an inactive state indicates that this process cannot be modeled as an equilibrium process because it requires energy to maintain. By adding an explicit G-protein activation step to the CTC model, we create a steady state model that follows the signal transduction pathway farther into the cell. This model and is shown in Figure 2.3b (Linderman 2000; Shea et al. 2000).

This new model of GPCR activation has many of the same properties of the equilibrium CTC model. However, as described above, the values of many of the parameters can be expected to differ. For example, consider the reversible reaction between R^* and R^*G shown in Figure 2.4. The analysis of this step is identical to that done earlier for receptor-ligand binding shown in Figure 2.2b, resulting in the following apparent equilibrium constant:

$$K_G^* = \frac{k_2}{k_{-2} + k_{r1}} = \frac{[R^*G]}{[R^*G][G]} \quad (2.6)$$

Thus if k_{r1} is set to zero then we recover the original equilibrium model.

Note that in this steady state model, we must explicitly keep track of the number of inactive and active G-proteins by using a species conservation relationship for the

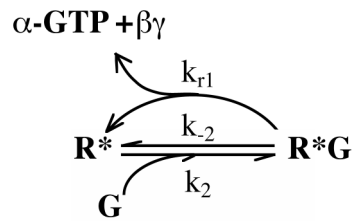


Figure 2.4 A steady state G–protein activation reaction. This reaction is just one step in the steady state CTC model of Figure 2.3b.

model to be realistic. Before receptor activation, very few of the G–proteins should be in the active state (in a system with low constitutive activity) and therefore a majority of the G–proteins will be in the free, inactive state ($\alpha\beta\gamma$ –GTP, denoted as simply G in the model schematic and equations). However, upon agonist binding the receptor should activate many of the accessible G–proteins in order to propagate the signal inside the cell. Therefore the free G–protein concentration [G] must change as a key step in the dynamics of signal transduction.

A striking example of the difference between the equilibrium and steady state models is shown in Figure 2.5 for one set of reasonable parameter values. Here the equilibrium model predicts the ligand will behave as a positive agonist, while the steady state model predicts inverse agonism. Why are the predictions so different? There are two contributing factors. First, as noted before, many steady state models are similar to equilibrium models but with different parameter values. In fact, any steady state model should give the equilibrium solution when no energy is put into the system (no GTP present in the case of GPCR activation). In other words, steady state models are more

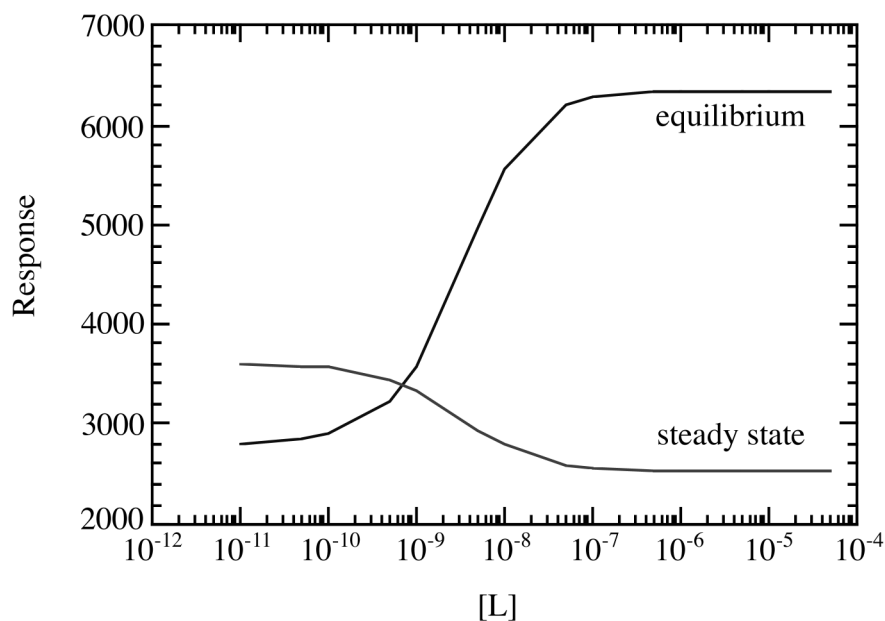


Figure 2.5 Responses predicted with the equilibrium and steady state version of the Cubic Ternary Complex model. For a particular set of realistic parameter values, the equilibrium model predicts that the drug will behave as a positive agonist, while the steady state model predicts that the drug will be an inverse agonist.

general forms of equilibrium models. A related and similar phenomenon will be discussed in Chapter 3 when describing the topic of agonist inversion.

One possible explanation for the different predictions in Figure 2.5 is that the response in the equilibrium model is assumed to be proportional to $[R^*G] + [LR^*G]$, while in the steady state model the response is assumed to be proportional to $[\alpha\text{-GTP}]$. The reason for this difference is that the steady state model follows the signal transduction pathway farther into the cell, thus one would expect the $[\alpha\text{-GTP}]$ concentration to better represent the cell's response than $[R^*G] + [LR^*G]$. Although $[\alpha\text{-GTP}]$ is clearly related to $[R^*G] + [LR^*G]$, the two measures of response are coupled nonlinearly because $[\alpha\text{-GTP}]$ can also be irreversibly depleted to $[\alpha\text{-GDP}]$. The result of this nonlinear

coupling is that $[\alpha\text{-GTP}]$ should not identically track $[\text{R}^*\text{G}]+[\text{LR}^*\text{G}]$; or said more generally, downstream responses generally will not be proportional to the concentration of upstream signaling molecules.

Thus the development of a simple steady state model for G-protein activation (Fig. 2.3b) allows us to demonstrate the limitations of the equilibrium model as well as improve our ability to model the process. The simplified equilibrium criterion of Eqn. 2.2 was used to qualitatively explain some of the behavior in the steady state model. The ability to use a simpler model as a guide in the analysis of more complex behavior is a common theme in modeling and represents a very powerful tool for both the theorist and experimentalist.

In Chapter 4 of this work, a more complete steady state model of GPCR activation is used to uncover a systematic bias in drug screening assays. Although the model presented later in this work includes more species, the steady state modeling approach is the same as that presented in this section.

2.2.4 Unsteady State Models

In reality, most biological systems are constantly changing with time, and as such never reach a true steady state. The cells in our body are constantly being bombarded with new information, which causes the cell to change its behavior dynamically. The process of signal transduction is an excellent example of this, as it includes both activation and desensitization dynamics (Figure 2.6) as will be discussed in Chapter 7 of this thesis. Assuming complete desensitization can occur, the steady state solution would be simply that of no cellular response. Thus analyzing a system with desensitization requires that an unsteady state model be used.

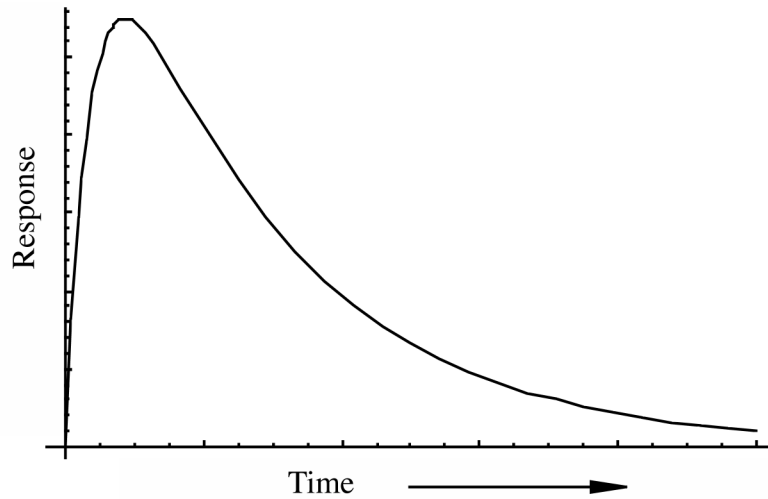


Figure 2.6 Desensitization in GPCRs. Persistent agonist stimulation initially causes the response (proportional to the concentration of ligand-bound active receptor [LR] in this case) to increase, however with time proteins inside the cell deactivate the signaling receptors causing the signal to drop, thereby desensitizing the receptor.

Returning first to our simple model of receptor–ligand binding, we can now add in the simple desensitization step shown in Figure 2.2c. The dynamics of this process are described by the two coupled ordinary differential equations:

$$\begin{aligned}\frac{d[R]}{dt} &= k_{-1}[LR] - k_1[L][R] \\ \frac{d[LR]}{dt} &= k_1[L][R] - k_{-1}[LR] - k_{ds}[LR]\end{aligned}\tag{2.7}$$

with initial (time = 0) conditions $[R]=R_{tot}$ and $[LR]=0$. Because receptor desensitization is essentially the depletion of free receptors, $[R]$ must be allowed to change with time—therefore species conservation on the receptor must be included. Fortunately, the form of the differential equations in Eqn. 2.7 automatically accounts for this, so no further terms must be added. Assuming no significant ligand depletion ($[L]$ is constant),

these differential equations are linear and as such are amenable to an analytical solution for $[R](t)$ and $[LR](t)$. The latter is plotted in Figure 2.6.

Note that the unsteady state model becomes the equilibrium model if k_{ds} is assumed to be zero and time is taken to be infinity. Similarly, if k_{ds} is set to 0 and k_1 to k_1+k_{trans} , we can recover the steady state model in the limit of infinite time. Thus the unsteady state model is a more general view of the system, and the steady state and equilibrium models are simply subsets of the unsteady state model (see Figure 2.7).

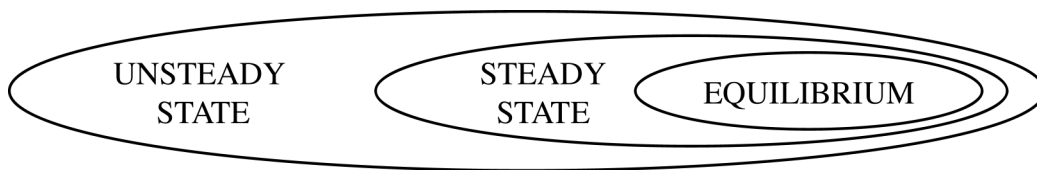


Figure 2.7 The relationship between equilibrium, steady state, and unsteady state models.

To find the parameters for an unsteady state model, we need to gather time varying (kinetic) data. For example, experimental groups have gathered high quality kinetic data for the binding of ligands to the N-formyl peptide receptor on human neutrophils (Fay et al. 1991; Neubig and Sklar 1993; Hoffman et al. 1996; Hoffman et al. 1996). An advantage to this system is the ability to use fluorescently labeled ligands and to monitor binding with flow cytometry.

Earlier work in our group modeled desensitization and activation in GPCRs using a simplified version of the model shown in Figure 2.3c (Riccobene et al. 1999). This

model is unique in that it includes a desensitization step⁼ and as such represents an inherently unsteady state process. From a pharmacological point of view, we are likely most interested in the transient response that occurs prior to significant desensitization, and this can only be simulated using an unsteady state model.

This model was constructed in an attempt to understand the mechanistic basis for ligand efficacy. It has been hypothesized that ligands may differ in efficacy because they have different values of the conformational selectivity α and/or different values of the desensitization rate constant k_{ds} (Linderman 2000). The ligand-specific parameter α was discussed earlier. The desensitization rate constant may also be influenced by the identity of the ligand bound to the receptor. For example, the receptor may be held in slightly different conformations by different ligands, or the differing dissociation rate constants of ligands may allow for different spatial organization of membrane species relevant to desensitization (Shea and Linderman 1997; Shea et al. 1997; Shea and Linderman 1998). Ligands with high values of α or small values of k_{ds} are predicted to have greater efficacy than ligands with small values of α or large values of k_{ds} . However, because only active (R^*) receptors are believed to desensitize, the effects of k_{ds} can not be analyzed independently of α . A model can be used to understand the synergy between these two parameters in determining the activation/desensitization profile of a given drug.

The predictions of the GPCR unsteady state model are shown in Figure 2.8. As expected, both α and k_{ds} effect receptor activation and desensitization. In all cases,

⁼ Only desensitization of the LR^* form of the receptor is shown. For constitutively active systems, desensitization via R^* should also be included, but was omitted here for simplicity.

increasing α causes both more activation and more desensitization, whereas increasing k_{ds} causes less activation and more desensitization.

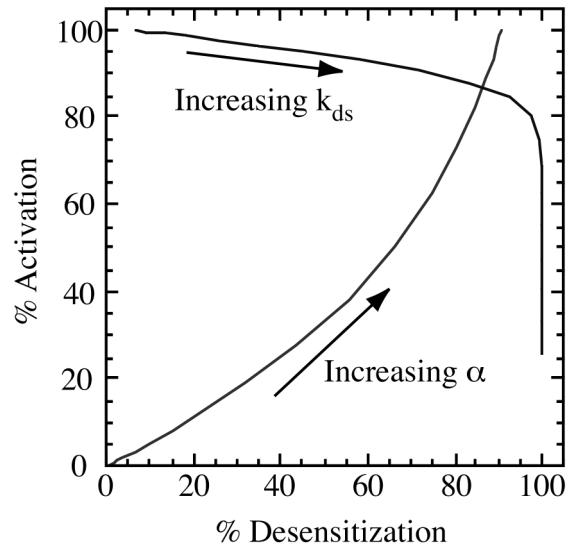


Figure 2.8 The simultaneous effects of changing the conformational selectivity factor α and the desensitization rate constant, k_{ds} , on receptor activation and desensitization (taken from (Riccobene et al. 1999)).

In order to use these predictions to understand ligand efficacy, the results of Figure 2.8 were compared with data from GPCR systems in which both activation and desensitization have been measured. Literature data on the β_2 -adrenergic receptor (Benovic et al. 1988), μ -opioid receptor (Yu et al. 1997), and the dopamine D_1 receptor (Balmforth et al. 1990; Barton and Sibley 1990) all show the trend of activation and desensitization increasing in parallel, suggesting that the primary differences between ligands in these particular systems is the value of the conformational selectivity α of the ligand. Previous data from our lab using the N-formyl peptide receptor system also support this conclusion (Riccobene et al. 1999). Thus the interpretation of data with this unsteady state model has suggested a mechanism behind ligand efficacy in these systems.

2.3 Modeling Spatial Effects

It is often assumed that membrane—associated proteins (e.g. receptors and G—proteins) are evenly distributed over the membrane. However, this is unlikely to be true. Most proteins throughout the cell are trafficked to specific locations on the membrane, where they often cluster into groups. By clustering proteins, the cell gains the ability to accelerate reactions well beyond what could be achieved in under well mixed conditions and to control which reactions take place (Allison et al. 1986; Bray 1998).

For GPCRs, spatial organization is thought to play a key roles in both receptor number regulation and receptor cross talk. GPCRs are removed from the cell surface after clustering into clathrin coated pits, followed by internalization via endocytosis. In this case, the spatial organization of the receptors on the cell determines whether the receptor stays on the surface or is internalized. There is also evidence that clustered receptors may be able to co—localize with and activate some tyrosine kinase receptors (Hall et al. 1999; Lin et al. 1999; Luttrell et al. 1999) in a form of receptor cross talk. This cross talk between different receptor types may be essential to transducing some signals, and as such is pharmacologically important.

A subtle spatial effect is a phenomenon that has been termed switching (Stickle and Barber 1989; Mahama and Linderman 1994; Mahama and Linderman 1995; Shea and Linderman 1997; Shea et al. 1997; Shea and Linderman 1998). When a GPCR is activated by a ligand, then the receptor acts to activate all nearby G—proteins. If the ligand remains bound to the receptor, then eventually all of the local G—proteins will be activated, leaving the ligand—bound receptor with nothing more to activate. In contrast, if the ligand quickly dissociates from first receptor and that ligand or another one binds to a second receptor, then the activate-able G—proteins around any particular receptor are

less likely to be depleted and the signal can continue to be propagated efficiently. Thus a highly active ligand that dissociates slowly may have less of an effect than a less active ligand that dissociates quickly. Only by including spatial effects — actually monitoring the distance between bound receptors and G-proteins - in our models can we simulate these phenomena.

Spatial effects are commonly modeled using two different methods: Monte Carlo (MC) simulations or partial differential equations (PDEs). MC methods employ a stochastic algorithm to mimic molecular motion. In contrast, PDE methods use a deterministic algorithm that tracks the density of particles to model molecular motion. Both methods can be used to track equilibrium and kinetic phenomena, but they differ in that MC methods function at the level of individual particles while PDE methods follow particle densities.

As an example consider diffusion of an inert particle on a membrane. Using an MC approach, the particle would be placed on a grid as shown in Figure 2.9. At each time step, the particle would move one grid spacing in a random direction with a probability proportional to the diffusion coefficient. After repeating this cycle many times, one could gather statistics describing the position of the particle as a function of time and thereby describe the diffusion motion of the particle. The advantage to using MC methods is that the individual histories of each particle can be tracked, often making the simulations more intuitive and easier to construct. However, these simulations generally require large amounts of computer time in order to make accurate predictions, and as such are not feasible for all systems.

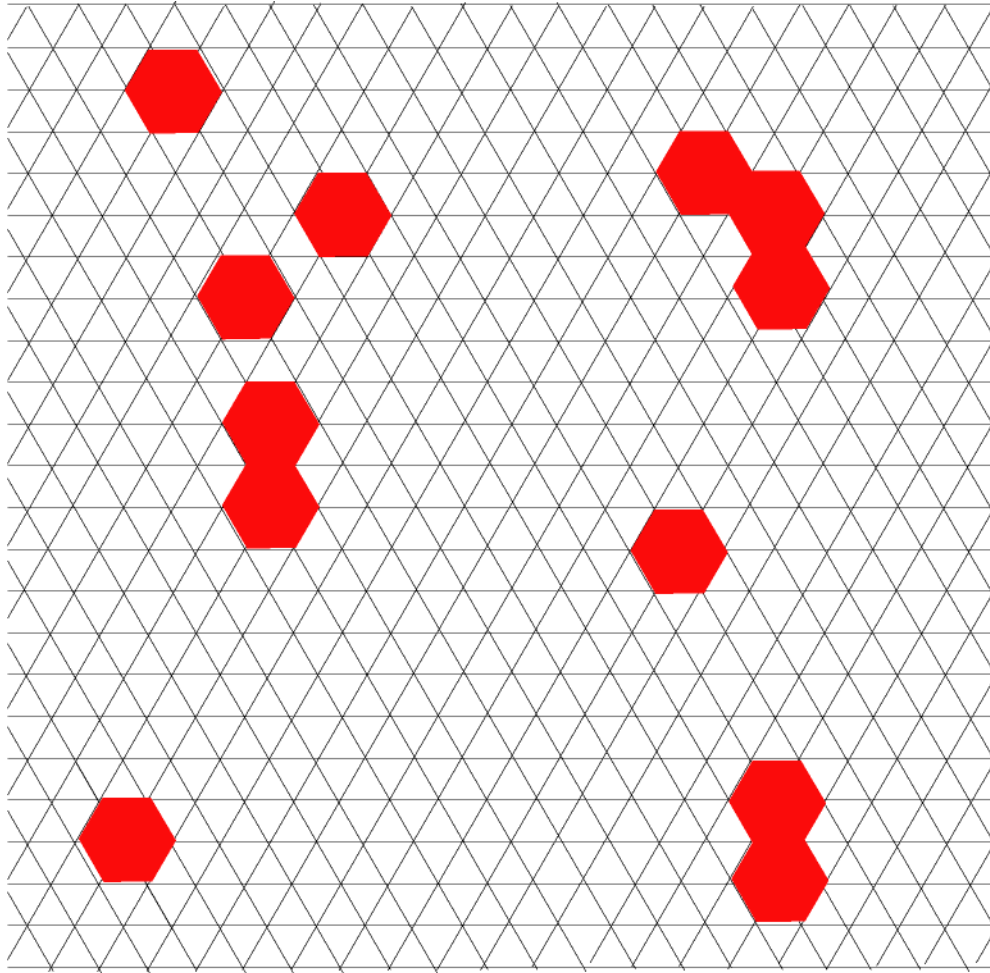


Figure 2.9 Monte Carlo simulation environment on a two dimensional triangular lattice. Proteins (colored) occupy 7 sites on the lattice. If proteins can react, then they are allowed to react if they are within a specified interaction radius.

Using a PDE approach, diffusion can be described using Fick's law for unsteady state diffusion in two dimensions:

$$\frac{\partial C}{\partial t} = D \left(\frac{\partial^2 C}{\partial x^2} + \frac{\partial^2 C}{\partial y^2} \right) \quad (2.8)$$

where C is the concentration of the particle, t is time, D is the diffusion coefficient, and x and y are spatial dimensions. Using appropriate boundary conditions, this equation can be solved numerically or in some cases analytically to yield information about the particle concentration as a function of time and space. Because PDE models only track the density of particles, they are generally more computationally efficient than MC approaches. However, PDE models are continuum models, and as such implicitly assume that the volume or area of a particle is very small such that discrete events can be smeared together.

In Chapters 5 and 6 of this thesis, I use an MC modeling approach to determine how spatial effects influence drug signaling. Chapter 7 uses an MC approach to explore how drug properties influence desensitization. Finally, Appendix B describes some preliminary work using MC and PDE approaches to model diffusion on a non—flat surface.

2.4 Conclusion

The mathematical models presented in this chapter allow us to describe receptor/ligand binding and the early stages of signaling at a number of levels of resolution and complexity. At the simplest level are the equilibrium and steady state models that can be used to rapidly assess where the system tends to move. The effects of time can next be included in an unsteady state model to predict the kinetics of the system. Finally, spatial effects can also be included to explore how the location of receptors in the cell membrane affects the signaling properties.

Our choice of which model to use depends both on the suitability of the model to the system and the practicality of the model. For example, when modeling kinetic

phenomena, it is key to use an unsteady state model so that we can simulate the system dynamics. If the process in question involves a spatial component, then a Monte Carlo approach may provide the best alternative. For example, the models of receptor dimerization in Chapters 5 and 6 of this thesis are fundamentally modeling a spatial effect and as such must account for motion in space. Monte Carlo simulations are ideally suited for such applications.

Therefore the modeling approaches presented in this chapter provide us with the framework required to model most pharmacological systems, assuming the system is sufficiently well characterized. Our choice of model depends on the assumptions we make about the importance of time and space, and the availability of resources to carry out the model.

CHAPTER III

AGONIST INVERSION

3.1 Introduction

Does a drug that is categorized as an agonist in one system always remain an agonist in all systems? Following the simplified picture in Figure 1.1, it would seem that any ligand with an α value greater than 1 would always be a positive agonist. However, in more complicated models this assumption breaks down as other ligand specific parameters are included. For example, in the cubic ternary complex model (Figure 2.3a) the ligand specific parameters β and δ also affect the signal.

Using ordinary differential equation-based pharmacological models I have found that sometimes a ligand can change from a positive agonist to a negative agonist (or vice versa) – something that might be termed *agonist inversion*. In agonist inversion, the efficacy of the ligand can be modulated simply by changing a parameter in the model, such as the conformational selectivity α (a ligand-specific parameter) or the G-protein concentration (reflecting a state inside the cell). This phenomena of agonist inversion is similar to "protean agonism" introduced by Kenakin (Kenakin 1995; Kenakin 1997); however, protean agonism only focuses on changing K_{act} , while agonist inversion describes a more general phenomenon that could be caused by changes in other parameters.

3.2 Methods

Using a steady state or equilibrium model, one can determine the apparent efficacy of a drug by comparing the signal activity caused by the drug to the activity when no drug is present. If the model is sufficiently simple, then this comparison can be made analytically to produce a general expression of the equilibrium signal ratio:

$$\frac{\text{Limit [Signal Response]}_{L \rightarrow L_0}}{\text{Limit [Signal Response]}_{L \rightarrow 0}} = \begin{cases} > 1 & \text{positive agonist} \\ = 1 & \text{neutral antagonist} \\ < 1 & \text{inverse agonist} \end{cases} \quad (3.1)$$

Depending on the value of this ratio, the drug can be categorized as a positive agonist, neutral antagonist, or inverse agonist. Note that the denominator of Eqn. 3.5 can theoretically go to zero, yielding an infinite signal ratio corresponding to a perfect positive agonist. However, in practice nearly all receptors have some level of constitutive activity, resulting in a finite equilibrium signal ratio.

The signal response varies for each model, but is generally the species farthest down the signal transduction pathway that is described for the model. For example, in the ternary complex models for GPCR activation, the signal response is generally assumed to be the sum of all of the active receptor species bound to G—proteins. Thus for the cubic ternary complex model, the signal response is proportional to $[R^*G + LR^*G]$.

First the equilibrium signal $[R^*G + LR^*G]$ for the simpler extended ternary complex (ETC) model (Samama et al. 1993) shown in Figure 3.1a was derived using the following system of mass balance equations:

$$\begin{aligned} [R^*G] &= K_G [R^*][G] \\ [R^*] &= K_{act} [R] \\ [LR] &= K_a [L][R] \\ [LR^*] &= \alpha K_{act} [LR] \\ [LR^*G] &= \beta K_G [G][LR^*] \\ R_{total} &= [R] + [R^*] + [R^*G] + [LR] + [LR^*] + [LR^*G] \end{aligned} \quad (3.3)$$

These values were used to derive the signal response with and without drug to calculate the equilibrium signal ratio in Eqn. 3.1. Note that in a strict two state model, the parameter β would have a value of 1 and could be dropped from the calculation.

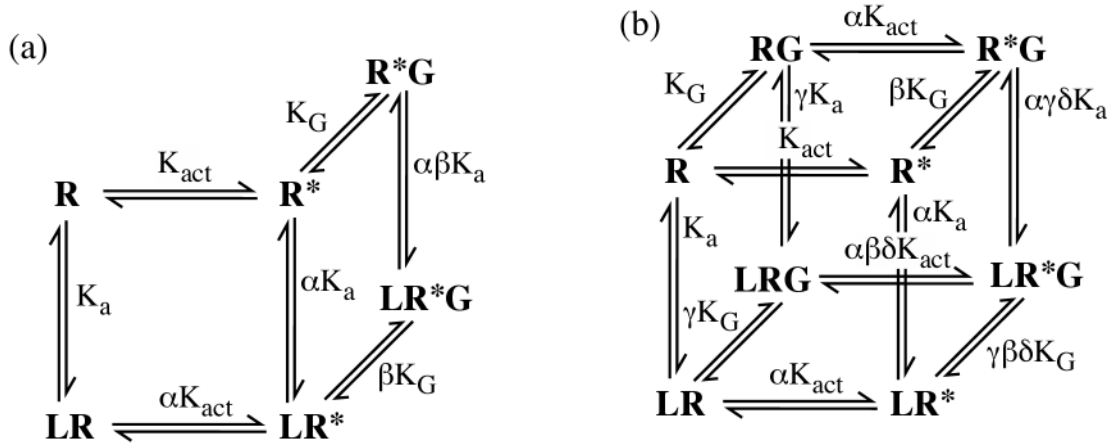


Figure 3.1 Two models used to calculate the equilibrium signal response ratio. (a) The extended ternary complex model (Samama et al. 1993) (b) The cubic ternary complex model (Weiss et al. 1996).

Next the equilibrium signal for the cubic ternary complex model (CTC) (Weiss et al. 1996) shown in Figure 3.1b was derived from the following system of mass balance equations:

$$\begin{aligned} [\mathbf{RG}] &= K_G [\mathbf{G}][\mathbf{R}] \\ [\mathbf{R^*G}] &= \beta K_G K_{act} [\mathbf{G}][\mathbf{R}] \\ [\mathbf{R^*}] &= K_{act} [\mathbf{R}] \\ [\mathbf{LR}] &= K_a [\mathbf{L}][\mathbf{R}] \\ [\mathbf{LR^*}] &= \alpha K_{act} K_a [\mathbf{R}][\mathbf{L}] \\ [\mathbf{LR^*G}] &= \alpha\beta\delta\gamma K_G K_a K_{act} [\mathbf{G}][\mathbf{R}][\mathbf{L}] \\ [\mathbf{LRG}] &= \gamma K_G K_a [\mathbf{G}][\mathbf{R}][\mathbf{L}] \\ R_{total} &= [\mathbf{R}] + [\mathbf{R^*}] + [\mathbf{R^*G}] + [\mathbf{RG}] + [\mathbf{LR}] + [\mathbf{LR^*}] + [\mathbf{LRG}] + [\mathbf{LR^*G}] \end{aligned} \quad (3.2)$$

Although other models for GPCR signaling exist (see examples in Figure 2.3), the ETC and CTC models are two of the most used and best accepted models currently in

use. However, the techniques developed here are general and could be applied to any equilibrium or steady state model.

Analytical calculations were made using the Solve and Simplify functions in the program Mathematica.

3.3 Results

In both model models, I found that agonist inversion could take place and depended on a different set of model parameters. Using the ETC model, the following expression was found:

$$\alpha (\beta + K_{\text{act}} (\beta - 1)) \begin{cases} > 1 & \text{positive agonist} \\ = 1 & \text{neutral antagonist} \\ < 1 & \text{inverse agonist} \end{cases} \quad (3.4)$$

If using a strict two state model, then $\beta=1$ for the ETC model. The result of this change is that drug efficacy can be modeled using only the parameter α .

Using the CTC model, the following equilibrium signal ratio was found:

$$\alpha \delta \gamma + G K_G \gamma (\alpha \delta - 1) + K_{\text{act}} \alpha (\delta \gamma - 1) \begin{cases} > 1 & \text{positive agonist} \\ = 1 & \text{neutral agonist} \\ < 1 & \text{inverse agonist} \end{cases} \quad (3.5)$$

where $\alpha, \delta, \gamma, K_G, K_{\text{act}}$ are equilibrium parameters and G is the number of free G-proteins (in the form $\alpha\beta\gamma\text{-GDP}$, i.e. “activate-able” G-proteins).

The key difference between Eqns. 3.4 and 3.5 is that 3.5 depends on the absolute concentration of G-protein, while 3.4 does not. However the ETC model is less thermodynamically complete than the CTC model, and as such is expected to display a smaller palette of behaviors.

3.4 Discussion

The key finding in this work is that the equilibrium signal ratios in Eqns. 3.4 and 3.5 have both positive and negative terms. By varying the values of the parameters, one can obtain values that range from well below 1 to well above 1 — thereby spanning the range from inverse agonist to positive agonist. For example, by varying K_{act} , we obtain the protean agonism behavior described in the literature (Kenakin 1995; Kenakin 1997).

Interestingly, according to Eqn. 3.5 varying the G-protein number can also cause agonist inversion, implying a novel mechanism for the cell to regulate the information it receives. Cells are thought to regulate the number of G-proteins they express (Lesch and Manji 1992), therefore cells could alter the signals they receive. For example, exposing human neutrophils to N-formyl peptide ligands has been shown to upregulate the number of G-proteins (Yatsui et al. 1992; Durstin et al. 1993), although the magnitude and timing of this increase have not been carefully studied.

According to Eqn. 3.5, this change in G-protein number could have a profound effect on how the cell responds to a ligand. For example, imagine a cell is stimulated by a positive agonist. By definition, a positive agonist means that the ligand-stimulated signal is greater than the unstimulated signal and Eqn. 3.5 has a value greater than 1. However, if the cell reduces the number of G-proteins able to interact with the receptor (by degradation or sequestration for example), then the value of the second term in Eqn. 3.5 would drop. Thus the cell could selectively tune out that particular ligand, changing it from a strong positive agonist to a neutral antagonist or inverse agonist, effectively ignoring that ligand. Note that while the cell may tune out one ligand, it may still be able to detect other ligands that have different parameters (e.g. α).

Agonist inversion caused by changes in G-protein number is demonstrated in the simulation results shown in Figure 3.2. At a low free G-protein concentration the signal without ligand is greater than the signal with ligand, and the ligand behaves as an inverse agonist. However, once the free G-protein concentration reaches a critical value, the ligand begins to behave as a positive agonist. Therefore, under conditions for agonist inversion, a positive agonist does not have to always be a positive agonist, but instead could vary from cell to cell depending on the state of the signal transduction pathway.

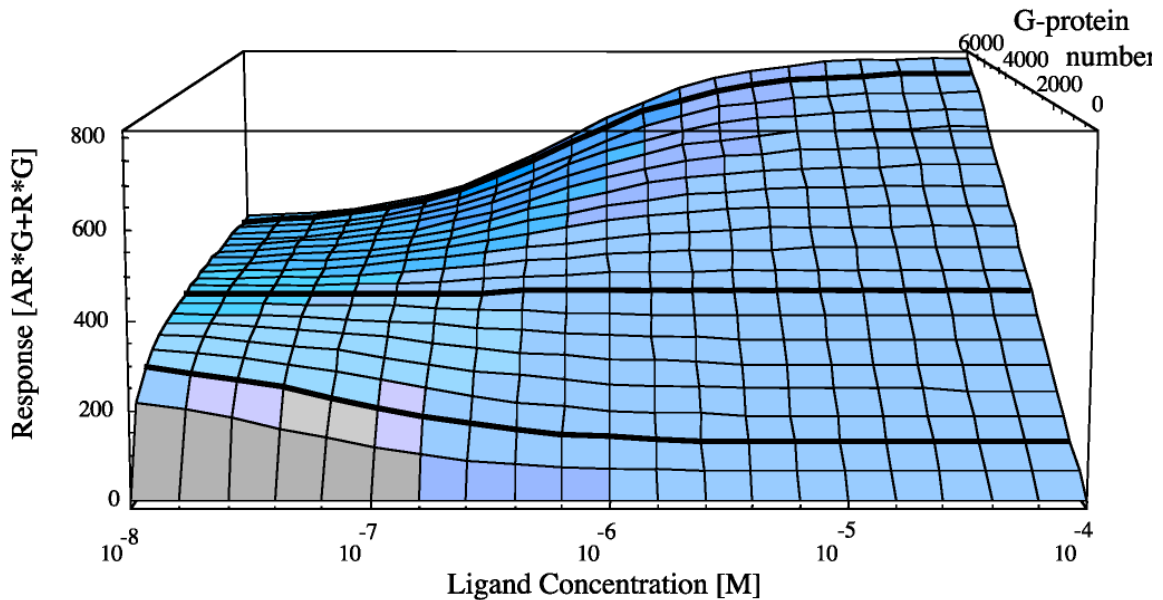


Figure 3.2 An example of agonist inversion in the CTC model as the G-protein number is changed. Dark lines show the response generated by a drug when a constant number of G-proteins are included. Note that at high ligand concentrations, a reduction in G-protein number can cause a drug to shift from a positive agonist to an inverse agonist. Parameter values used in the model include: $K_a=10^7$; $R_{total}=10^5$; $\alpha=0.1$; $\beta=0.01$; $\delta=92.38$; $\gamma=0.01$; $K_G=0.0245$; $K_{act}=10.824$.

Thus we must consider both the drug's impact on the cell as well as the cell's impact on the drug when describing a drug's physiological effect.

Qualitatively, agonist inversion can be thought of as a transition between two qualitatively different states. Take as an analogy the two possible states of a pendulum:

swinging back and forth or spinning around in circles, like the propeller of an airplane. Depending on how the pendulum was pushed, how heavy the weight, and how long the arm, the pendulum will either swing back and forth or will spin. Similarly, depending on the equilibrium constants of the CTC model, most drugs will either be a positive agonist or negative agonist. By changing the values the equilibrium constants, we can then get a qualitatively different behavior, just as in the case of a pendulum we can change a spinning pendulum into a swinging pendulum just by increasing the weight. However, a living cell strongly differs from a pendulum in that the cell can dynamically change its parameters in response to its environment.

It is not known whether agonist inversion occurs in nature. Chidiac et al. (Chidiac et al. 1996) found that dichloroisoproterenol acting on β_2 -adrenergic receptors could show either positive or inverse agonist behavior depending upon the cell preparation used in the experiment, as is shown in Figure 3.3. One possible explanation is that the G-protein number in each cell preparation was different, causing an agonist inversion in some cells as described by Eqn. 3.5. Perhaps the reason that there is relatively little experimental support for agonist inversion is because the right experiment has not been done, or we do not have the sensitivity to detect the small changes involved. Similarly, although agonist inversion is predicted by an equilibrium version of the CTC model, maybe other non-equilibrium effects such as receptor desensitization or G-protein activation also affect inversion.

Based on the analytical results in Eqn. 3.5, agonist inversion due to changes in G-protein number could take place a number of ways depending on the cell system and the drug. For example, if the parameters $\alpha\delta > 1$, then any increase in G-protein

concentration will result in an increased equilibrium response ratio. If at low G-protein concentration the equilibrium response ratio is less than one, then increasing the number of G-proteins under these conditions will change a drug from an inverse agonist (ratio <1) to a positive agonist (ratio >1). Alternatively, if $\alpha\delta < 1$ in Eqn. 3.5, then increases in G-protein number will tend to reduce the equilibrium signal ratio. Therefore if at low G-protein number the signal ratio predicts a positive agonist, increasing the G-protein number will depress the signal ratio and cause the drug to be have as an inverse agonist. Unfortunately, these predictions rely on precise knowledge of the α and δ values of a drug and cell respectively, neither of which are known at this time.

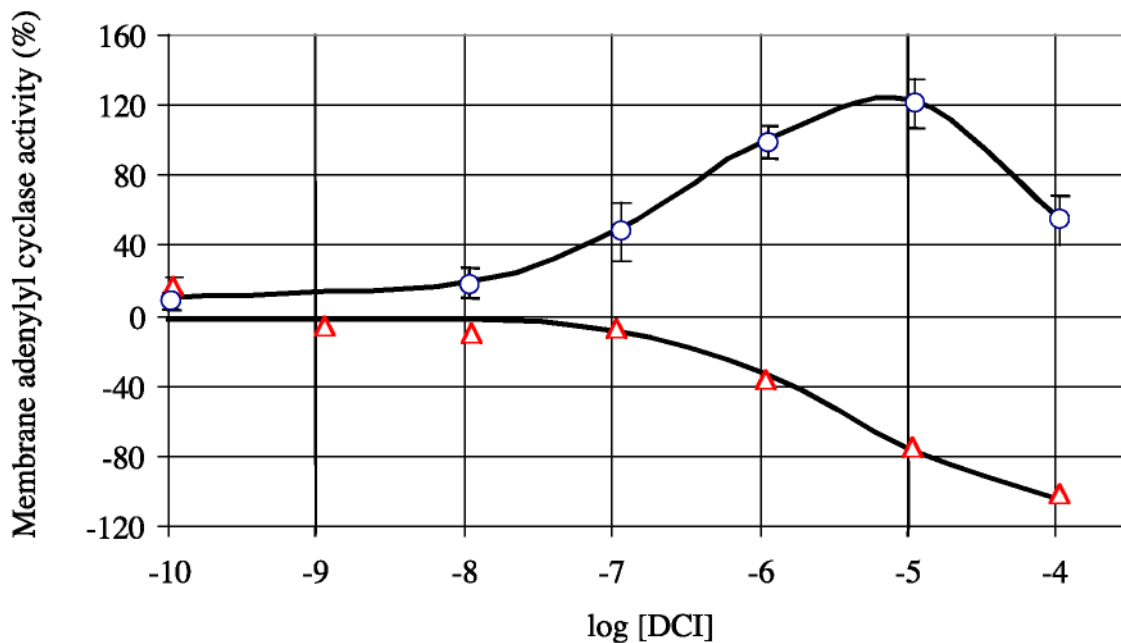


Figure 3.3 A possible example of an experimental system that exhibits agonist inversion. The drug DCI interacting with the same receptor type yields either positive or inverse agonist activity depending on the individual cell. Data taken from (Chidiac et al. 1996).

3.5 Conclusion

The modeling results developed in this chapter bring into question a common pharmacological assumption that a drug that is classified as a positive agonist in one system will be a positive agonist in all systems. Even if the receptor and drug are identical in two systems, the total number of G-proteins could be different, or the receptor could be interacting with a different class of G-protein with a different K_G value. This finding could help to explain the variation generally seen in pharmacological data, and could provide a new research avenue.

CHAPTER IV
UNCOVERING BIASES IN HIGH THROUGHPUT SCREENS OF G-PROTEIN
COUPLED RECEPTORS

4.1 Introduction

High throughput screening involves testing a large number of compounds (currently over 1 million) against a biological target to identify potential drug leads. However, if a drug is missed in the initial screening, then that potentially valuable drug will not be developed and the chemical palate available to pharmacologists will be artificially limited. Therefore an understanding of the factors that allow drug detection in a screening assay is vital to the success of modern drug discovery.

High throughput screens are normally run either using a functional assay or a binding assay. Functional assays measure the signal generated by a biological reporter, *e.g.* (Lerner 1994; Brauner-Osborne and Brann 1996; Jayawickreme et al. 1998), allowing this type of assay to detect drugs that produce a biological response. However, if the biology of the system is poorly characterized or the screen is seeking both antagonists and agonists, functional assays can not be used. In contrast, binding assays measure the competitive binding between a labeled tracer ligand and an unlabeled test ligand. Because this assay only measures binding, it can be used to detect ligands of any type, even if the biology of the system is not understood.

In this work we examine membrane binding assays because of their ease of implementation and ability to detect a wide variety of drugs. Membrane binding assays measure ligand binding to receptors in membrane fragments, not whole cells. Not only are membrane assays more stable over time, but they are also not influenced by cellular processes such as receptor down-regulation, modification, or desensitization. Because membrane assays differ from conditions present when using whole cells, the results of the membrane based screening assay may be biased toward the detection of drugs with certain properties. This bias could be an advantage if it amplifies the signals of a desirable class of drugs or a disadvantage if it reduces those signals. If the reasons for the bias can be understood, then high throughput screens could be designed to search for specific classes of drugs such as inverse agonists,

As a model system, we focus on drug binding to G-protein coupled receptors (GPCRs). Approximately 80% of all known hormones, neurotransmitters, and neuromodulators are believed to transmit their signal through GPCRs (Lesch and Manji 1992), and it is estimated that 45% of all medicines used today act through G-protein signaling pathways (Drews 2000). Examples of such GPCR systems include the β -adrenergic receptor (involved in regulating heart contractility), the opioid and dopamine receptors (involved in brain function), and the N-formyl peptide receptor (involved in the immune response). Because GPCRs are such fruitful targets for drug action, most new ligands for this receptor are detected using high throughput screening.

The most popular membrane binding assays used for detecting drugs to GPCRs are homogeneous—meaning that they do not require a step to separate bound from free ligand before a measurement is taken. Some examples of commonly used homogenous

binding assays include the scintillation proximity assay (SPA), homogeneous time-resolved fluorescence (HTRF) and fluorescence polarization (FP). SPA uses fluomicrospheres that emit light when in close proximity to a radiolabeled compound. By coating the fluomicrosphere with membrane-bound receptors and radiolabeling a tracer ligand, SPA can measure the ability of an unknown ligand to compete with the tracer ligand by the decrease in fluorescence (Bosworth and Towers 1989). The HTRF and FP format give similar results using different techniques (Hemmila et al. 1984; Beisker and Eisert 1985; Mathis 1995; Nasir and Jolley 1999). In each case, these assays measure the change in the binding of a labeled tracer when an unlabeled test ligand is added to the mixture and can compete for receptor sites (see Figure 4.1). If the test

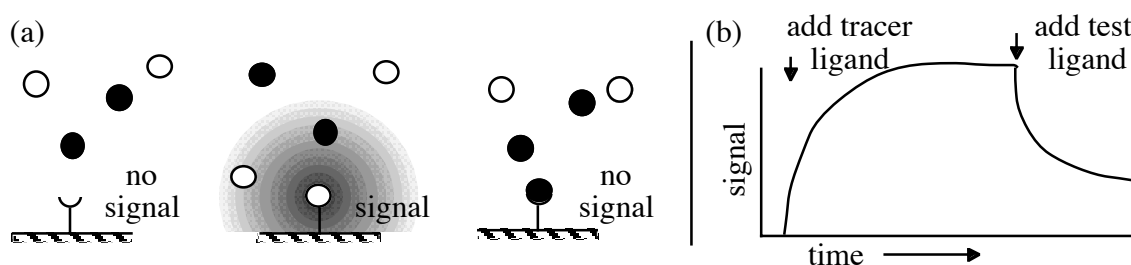


Figure 4.1 General schematic for GPCR ligand screening assays. a) When the receptor is unoccupied or bound to the test ligand B (filled circle) then no signal is detected. However, when the receptor binds the labeled tracer ligand A (open circle) a signal is emitted. By measuring the drop in signal after the test ligand is added, the test ligand’s affinity for the receptor can be calculated. b) The typical screening assay begins with the addition of a tracer ligand to the receptor mixture, causing the signal to rise to a base line signal. After the system has equilibrated, the test ligand is added. By observing the magnitude of the signal drop, the ligand can be scored as either a “hit” or a “miss.”

compound displaces a significant amount of the labeled tracer, then the signal drops and the test compound is registered as a “hit” worthy of future study. Otherwise the tracer

will remain bound and the signal will remain high, registering the test compound as a “miss.”

How can bias in a drug screen be detected? Experimentally, bias can be difficult to assess because of the relatively small number of available ligands for each receptor. Results gleaned from one system may or may not indicate a systematic bias. Similarly, finding drugs that have been overlooked by a screen requires screening a library of compounds multiple times using multiple assays—an effort far too costly for most research groups to undertake. In light of these problems, we chose to look for bias using kinetic models of drug-target interactions. Kinetic models are used in pharmacology to describe the dynamics of known physical interactions between different parts of the signal transduction pathway. By taking a modeling instead of an experimental approach, we are not limited by the number of available compounds and can therefore scan the whole range of possible drug properties with a variety of assay formats.

Although binding is clearly required for any drug to have an effect on the cell, other drug properties – such as its ability to change the receptor’s conformation – determine what the drug does once bound to the receptor and thus contribute to drug efficacy. Experimental data suggest that GPCRs exist in at least two conformations, commonly referred to as the active and inactive states, and that the proportion of receptors in each of these two states can be altered by ligands of different efficacy. The existence of these two states has been shown by agonist-induced affinity changes (Stadel et al. 1980) and mutation studies (Cotecchia et al. 1990; Ren et al. 1993; Samama et al. 1993), both of which show a distinct change from one state to another. Although the receptor presumably has more than two possible conformations (Kenakin 1996), two

receptor states are sufficient to describe most pharmacological observations on a single signaling pathway.

For GPCRs, the efficacy of a drug can be divided into three classes: 1) positive agonists, 2) neutral antagonists and 3) inverse agonists as shown in Figure 4.2. Positive agonists cause an increased response by binding to the active receptor conformation.

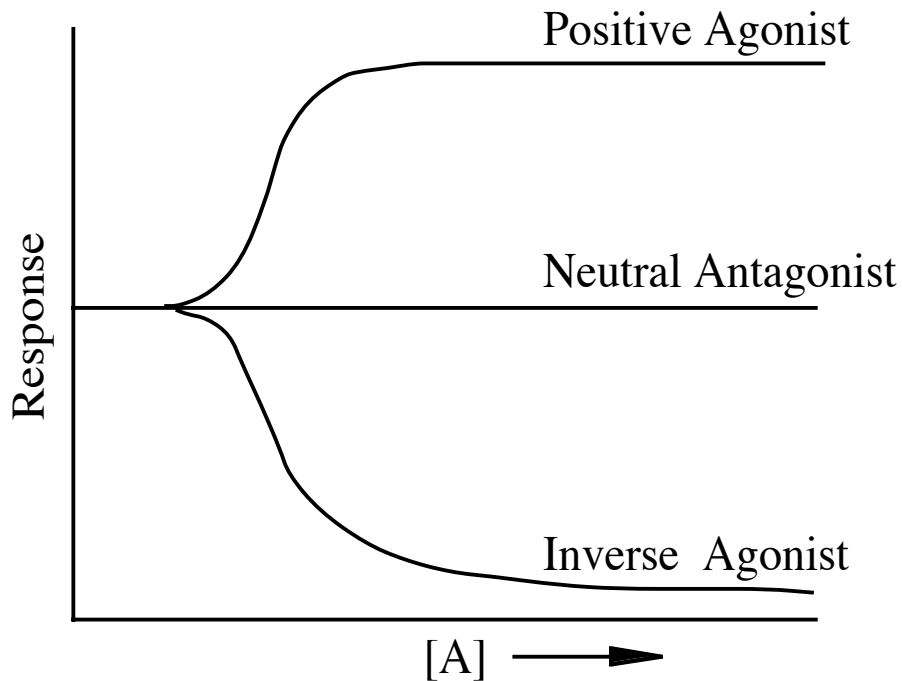


Figure 4.2 Three classes of ligand efficacy in GPCRs. Ligands can increase a response (positive agonist), cause no response but block the effects of other ligands (neutral antagonist), or decrease a response (inverse agonist).

Neutral antagonists cause no response, but do compete with other ligands for binding to the active site on the receptor. Inverse agonists reduce the response below the basal level by binding to the inactive conformation of the receptor. Much is known about positive agonists and neutral antagonists; however, inverse agonists have only recently been

identified. It has been speculated that inverse agonists could help treat diseases such as familial hypoparathyroidism, congenital night blindness, and some forms of cancer (Arvanitakis et al. 1998), and therefore represent a new and important class of drugs.

As just described, the efficacy of a drug is determined at least in part by its relative binding affinity for a specific receptor conformation. Thus binding affinity and efficacy of a drug are related (Colquhoun 1987). Therefore if binding assays measure the affinity between a ligand and a receptor, it is reasonable to hypothesize that these same assays also unintentionally screen for drugs with a particular efficacy. Similarly, the speed with which a ligand binds to a receptor could also affect which drugs are detected and which are not. Drugs that bind quickly would be expected to cause a rapid signal change, while those drugs that bind slowly may cause the signal to drop too slowly to be detected within the time frame of the assay.

In this chapter I examine the effect of ligand efficacy on binding affinity and binding kinetics in both a membrane binding assay and a whole cell. Understanding how drug efficacy affects the observed affinity between ligand and receptor can help to uncover systematic biases in the assay. For example, should membrane binding assays uncover more positive agonists than inverse agonists? Similarly, do the kinetics of ligand binding relate to the efficacy of the drug being bound? By understanding how a screening assay will perform with certain classes of drugs we may be able to design assays to focus on drugs with particular characteristics.

4.2 Methods

Our approach is to develop two simple and related models, one applicable to the membrane binding assay used for high throughput screening and the other describing conditions in the whole cell. The binding of ligands of different efficacies in the two models is then compared to determine when and if the equilibrium binding affinity differs. The kinetics of binding are also examined. A description of the techniques used to analyze equilibrium and kinetic pharmacological models can be found elsewhere (Woolf and Linderman 2000).

Following the convention of most screening assays, each model is run using two competing ligands, A and B. Ligand A is a labeled tracer compound that is known to bind to the receptor. Ligand B is an unlabeled test compound that is being assayed. By predicting the amount of ligand A bound before and after B is added, it is possible to determine which test ligands would qualify for further study as drug candidates.

A simple model that is often used in pharmacological modeling of GPCRs is the extended ternary complex (eTC) model (Lefkowitz et al. 1993; Samama et al. 1993). The eTC model is characterized by having an active (R^*) and inactive (R) receptor conformation, along with the ability to form a complex between ligand, receptor, and G-protein. G-proteins in this model are allowed to bind with the active form of the receptor, which is consistent with experimental findings (De Lean et al. 1982). Traditionally this model has been used primarily to describe systems at equilibrium. A related model, the cubic ternary complex (cTC) model (Weiss et al. 1996), additionally allows G-proteins to bind to inactive receptors. Although this latter model is more thermodynamically complete, it is also more complex. Thus in the present work we have focused on the eTC

model. Because of the similar structures of the models, the trends we discuss here are similar for both models.

I have modified the eTC model to include the kinetics of various receptor state changes as well as the effects of competing ligands. In the whole cell model, subsequent G-protein activation steps are included to better represent drug binding in a living system. We do not expect these models to yield quantitatively exact predictions because these models only represent a small part of a much larger system of the cell and as such can only approximate the behavior. However, the trends predicted by these models are credible and can provide practical insight into how screening assays might be improved.

4.2.1 Whole cell model

In a living cell, receptor activation is followed by G-protein activation, as shown in Figure 4.3. In the first step of G-protein activation, the G-protein exchanges GDP for GTP, and then breaks into two signaling subunits, $G_{\alpha\text{-GTP}}$ and $G_{\beta\gamma}$. This first step is governed by a single reaction rate constant k_{r1} because the dissociation step between $G_{\alpha\text{-GTP}}$ and $G_{\beta\gamma}$ has been shown to be rate limiting compared to GDP removal and GTP addition (Thomsen and Neubig 1989). Next, the intrinsic GTPase activity of the G_{α} subunit reverts $G_{\alpha\text{-GTP}}$ to $G_{\alpha\text{-GDP}}$. This change from $G_{\alpha\text{-GTP}}$ to $G_{\alpha\text{-GDP}}$ acts as a molecular timer that ensures that the signal will be propagated inside the cell, but also that the signal will stop soon after the stimulus is removed. The $G_{\alpha\text{-GDP}}$ subunit then recombines with the $G_{\beta\gamma}$ subunit to reform the inactive G-protein, which can again interact with receptors to repeat the cycle. Other work using this and related whole cell models has demonstrated that the model can be used to successfully model receptor desensitization

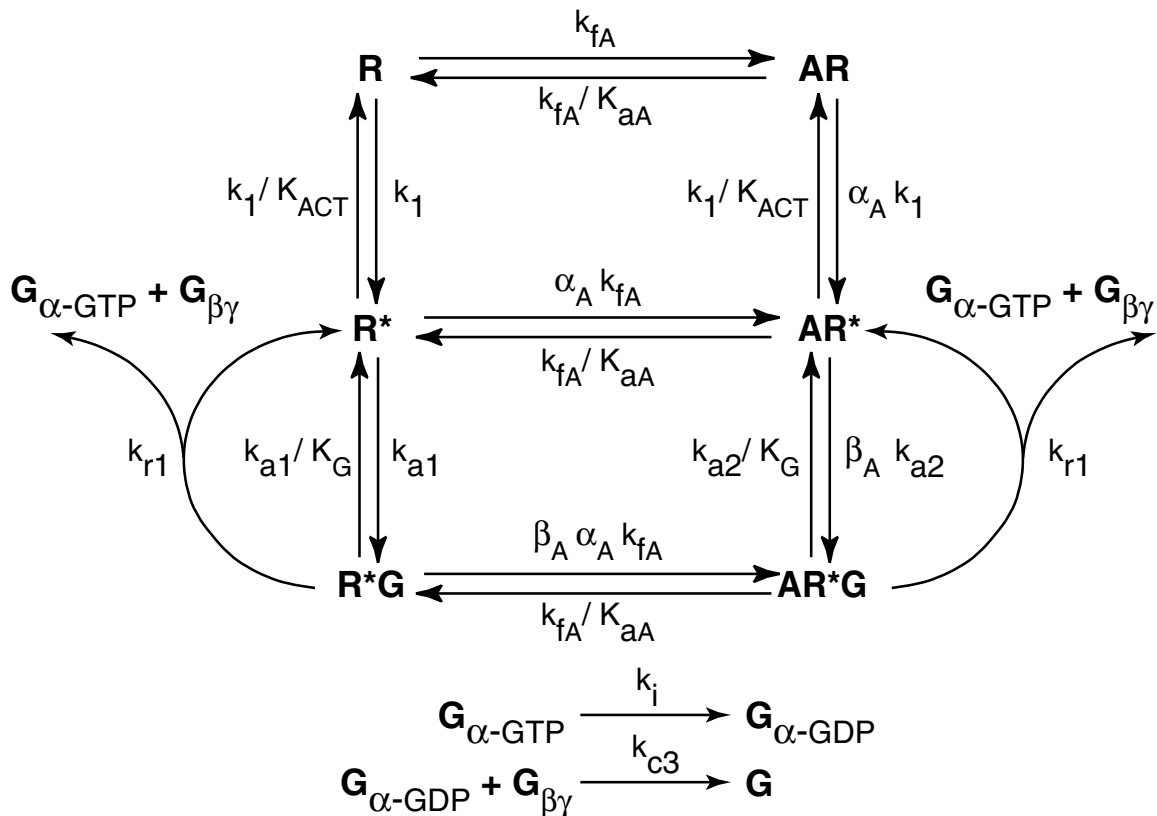


Figure 4.3 Whole cell model for GPCR signal transduction (Shea *et al.*, 2000). G-proteins can be activated by the active receptor conformation, R^* . Note that here the ligand A is the only ligand shown to bind, however in the simulation a second ligand B is also allowed to bind competitively to give BR , BR^* , and BR^*G . Rate constants associated with each step are shown next to the appropriate arrow. As described in the text, ligands of different efficacy are assumed to have different values of the conformational selectivity α .

(Riccobene *et al.* 1999), the activity of constitutively active mutants (Linderman 2000), and the effects of ligand binding kinetics (Shea *et al.* 2000). This model closely approximates what is known about the early events in GPCR signal transduction, and as such will be used to describe how a ligand would bind to a living cell. The detailed mass balance equations are shown in Appendix A.

4.2.2 Membrane binding assay model

High throughput equilibrium binding assays are generally run on membrane preparations, not living cells. The reason for using membrane preparations is they are easier to maintain than living cells, and some assays such as SPA require that the membrane-bound receptor be attached to a detector, thereby precluding the use of whole cells. These membranes contain receptors, G-proteins and other proteins that associate with the membrane, but leave behind the cellular components found in the cytosol.

One important component that is lost when making membrane preparations is the soluble GTP. As described earlier, GTP is required for G-protein activation. When GTP is removed from the system, the first G-protein activation step is removed from the model ($k_{r1}=0$). Running the assay without GTP can also cause the G-protein to adopt the “empty pocket” state, which further stabilizes the bond between the receptor and G-protein (Hamm 1990; Hamm 1998). In modeling terms, the “empty pocket” state could be approximated by an increase in the receptor/G-protein equilibrium binding constant, K_G . By including these changes in the whole cell model, we can simulate GPCR binding in membrane preparations. This binding assay model is shown in Figure 4.4 and the detailed mass balance equations can be found in Appendix A. Membrane binding assays used in high throughput screening measure the binding affinity of a test ligand, B, relative to a tracer ligand, A. The affinity of a test ligand is measured via a signal that is proportional to the amount of tracer ligand bound to the receptor. In the binding model, this signal is proportional to the sum of the concentrations of AR, AR*, and AR*G. By measuring how much the signal changes after the test ligand is added, the affinity of the test ligand for the receptor can be calculated.

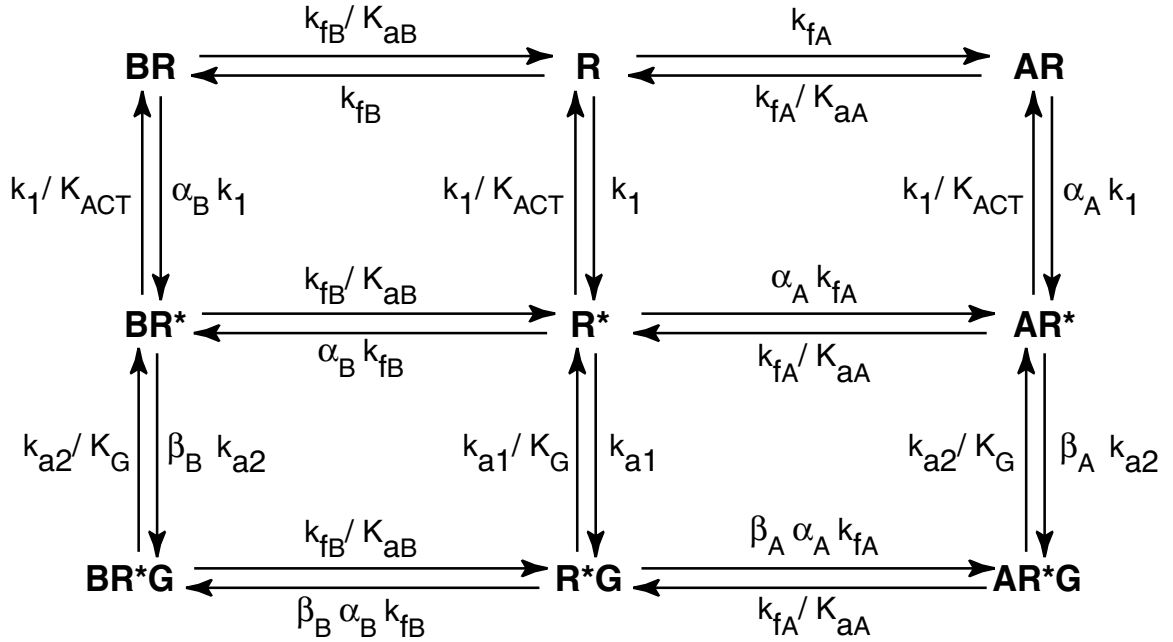


Figure 4.4 Model of the membrane binding assay based on the extended ternary complex model of Samama et al. (Samama, 1993). Here two ligands, the tracer (A) and the test ligand (B), compete for binding sites on the receptor. G proteins are not activated because GTP is absent. Rate constants associated with each step are shown next to the appropriate arrow. As described in the text, ligands of different efficacy are assumed to have different values of the conformational selectivity α .

One can define an equilibrium signal ratio as the amount of tracer ligand bound *after* the test ligand is added divided by the amount of tracer ligand bound *before* adding the test ligand. The equilibrium signal ratio for the limiting case of a constant number of free (“activate-able”, or $G_{\alpha\text{-GDP}\cdot\beta\gamma}$) G-proteins can be given as

$$\text{Equilibrium signal ratio } S = \frac{N + M_A}{N + M_A + M_B} \quad (4.1a)$$

where

$$N = 1 + K_{\text{act}} + G K_g K_{\text{act}} \quad (4.1b)$$

$$M_A = [A] K_{aA} (1 + K_{\text{act}} \alpha_A (1 + G K_g \beta_A)) \quad (4.1c)$$

$$M_B = [B]K_{aB} \left(1 + K_{act} \alpha_B (1 + G K_g \beta_B) \right) \quad (4.1d)$$

An equilibrium signal ratio value approaching 1 indicates that the test ligand did not displace a significant amount of the tracer (a “miss”), while a value approaching 0 indicates that the test ligand markedly displaced the tracer (a “hit”). The equilibrium signal ratio is a useful indicator to predict whether a given ligand will or will not be detected in an assay depending on the tracer ligand concentration and binding parameters ($[A], \alpha_A, \beta_A, K_{aA}$), the test ligand concentration and binding parameters ($[B], \alpha_B, \beta_B, K_{aB}$), and the system properties (G, K_G, K_{act}). N, M_A , and M_B are dimensionless groups that describe the propensity of the system, tracer ligand, and test ligand respectively to activate the G-protein. For example, increasing the value of N increases the level of constitutive signaling in the system. The competition between N, M_A , and M_B determines how the signal is perceived by the assay.

In order to simplify our result, Eqn. 4.1a was derived assuming that the number of free G-proteins is constant. The actual variation in the number of free G-proteins during signaling is not known. Experimental work in neutrophils finds a ratio of G-proteins to receptors of ~10:1 (Bokoch et al. 1988), which suggests that the change in free G-protein number during activation might be a small fraction of the original amount. In other situations, however, one can envision a smaller number of G-proteins or perhaps receptor access to G-protein restricted by microdomain boundaries. For this reason, we use Eqn. 4.1a only to help elucidate general trends in the binding assay model for study of the binding assay. When G-protein activation is included (as in the whole cell model) or when doing numerical simulations on the binding assay model, we use the full nonlinear

model (Appendix A) and allow the G-protein number to change according to the laws of mass action, thereby ensuring that the results are as realistic as possible.

The time course of ligand binding is analyzed numerically using the ordinary differential equation models shown in Appendix A. Models are evaluated using the standard ODE solving package in Mathematica™ which uses a combination of the non-stiff Adams method (order 1-12) and the stiff Gear method (order 1-5). Analytical expressions to large nonlinear algebraic systems are generated using Mathematica's™ Solve function.

4.2.3 Parameters

The parameters for the models describe specific, and in principle measurable, events in GPCR binding and signaling. Of particular interest in this work are the equilibrium association constant K_a , and the conformational selectivity α , both ligand-specific parameters. Ligand binding to inactive receptors is described by the equilibrium constant K_a , while binding to active receptors is described by αK_a . The ratio of ligand affinities for the active to inactive receptors is then simply α . Thus a conformational selectivity of $\alpha=10$ indicates that the ligand binds ten times more tightly to the active receptor conformation than to the inactive receptor conformation—making α essentially a measure of ligand efficacy. Positive agonists prefer to bind to the active conformation and therefore have $\alpha>1$. Neutral antagonists bind equally well to either conformation, represented by $\alpha=1$. Inverse agonists prefer to bind to the inactive receptor and as such have $\alpha<1$. To test drugs of different efficacy this study, simulations were run using α values of 0.01, 0.1, 1, 10, and 100 to span the range from strong positive agonist to strong

inverse agonist. Note that the ligand induced G-protein binding coefficient, β , could also be used as a measure of efficacy. However, in a strict two state model the ligand can only distinguish between active and inactive receptors, forcing $\beta = 1$. Values of β not equal to 1 imply that the ligand can distinguish not only between active and inactive receptors, but also G-protein bound and G-protein unbound receptors, which would require at least three distinct receptor conformations (R, R*, and R*G). Therefore, in an effort to simplify the analysis and maintain a strict two state model, only α was used as a measure of ligand efficacy for this initial study.

To make a fair comparison among ligands of different efficacy, a set of ligands with the same *observed* binding affinity in one system were tested in the other system. For example, we created five ligands with different efficacies that all bound with the same observed affinity in the whole cell and then tested those same ligands in the membrane binding assay. The observed binding affinity, K_{Obs} , is the receptor-ligand affinity that would be measured in an experimental system at equilibrium. This observed affinity is distinct from the ligand's intrinsic equilibrium association constant, K_a , in that K_a is a measure of the ligand's affinity for the inactive form of the receptor in the absence of G-proteins. An analytical expression for K_{Obs} derived from the membrane binding assay model is

$$K_{obs A} = \frac{M_A}{[A] N} \quad (4.2)$$

where N and M_A are given in equations 4.1b and 4.1c, and $[A]$ is ligand concentration. This result assumes a constant free G-protein concentration. This observed affinity is a function of both the conformational selectivity, α , and the intrinsic affinity for the receptor, K_a . To compare ligands with different values of α , equation 4.2 was solved for

a value of K_a that would maintain a constant value of K_{obs} . In this way we were able to decouple efficacy and intrinsic affinity, thereby isolating the effects of efficacy on the screening assay.

The values of the remaining parameters in the models were either taken from the literature or estimated so as to agree as well as possible with experimental data. For each figure, parameter values are given in the legend.

Note that beyond the specific parameter values, the structure of the model defines what behaviors the system may exhibit. When possible, models were analyzed analytically to derive qualitative behaviors that are insensitive to changes in parameter values. In this way it was possible to determine a characteristic response of the system, where specific parameter values only rescale the result but do not change the qualitative behavior. Therefore many of the results presented here are general to the model itself and do not rely on the system being in a specific parameter regime.

4.3 Results and Discussion

Ligand binding is first examined using equilibrium (membrane binding assay) or steady state (whole cell) analyses. These results describe the system at long times, when the concentration of each species is no longer changing. Studying the system at equilibrium or steady state rather than at earlier times has the advantage that it is mathematically simpler, and as such more amenable to analytical solutions. Using an equilibrium analysis, we also explore the behavior of the assay when the G-protein concentration or tracer ligand identity is altered. Some of these results, such as the GTP-shift, are well-known by the pharmacological community and are used to validate the

model. Other predictions such as the effect of different tracer ligands on the assay are new.

We next examine the kinetics of ligand binding, i.e. a description of the system when species concentrations are changing. We explored the possibility that membrane binding assays fail to detect some drugs because measurements are taken too quickly. The use of the assay as a tool for predicting ligand efficacy based only on kinetic binding data is proposed. The effects of the tracer ligand efficacy on the test ligand binding kinetics are also discussed.

4.3.1 Equilibrium analyses: Observed affinity differs between membrane binding assay and whole cell conditions

A key difference between the membrane binding assay and the whole cell is the whole cell's ability to activate G-proteins—an ability that requires the presence of GTP. The effects of G-protein activation on ligand binding were explored by comparing how ligands of different efficacy bind in the membrane binding assay and the whole cell models.

A set of five ligands that range from a strong positive agonist ($\alpha=100$) to a strong inverse agonist ($\alpha=0.01$) is tested for binding in both a membrane binding assay and a whole cell assay. In the example shown in the top of Figure 4.5a, the positive agonists appear to bind tightly in the membrane binding assay, with a half maximal effective concentration, EC_{50} , of approximately 10 nanomolar, while the inverse agonists bind weakly (EC_{50} of ~5000 nanomolar). For many drugs found by high throughput screening, the EC_{50} is the initial criteria used to screen out drugs that do not bind tightly enough and as such would likely require unreasonably high ligand concentrations to have a

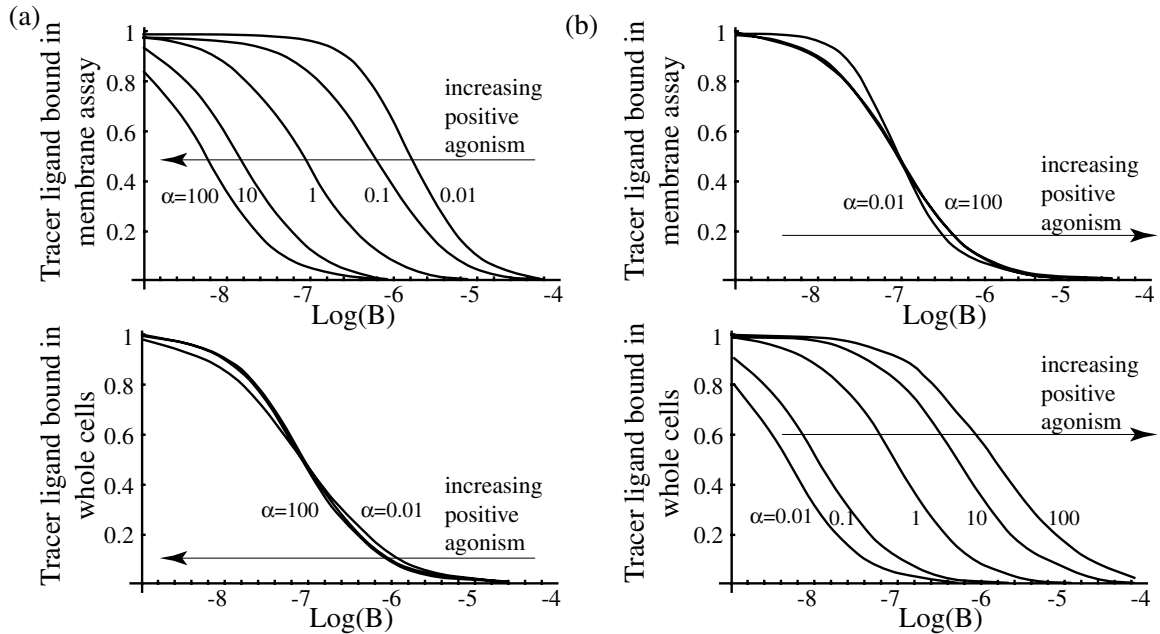


Figure 4.5 Comparison of ligand binding to a membrane assay and whole cell. (a) Five test ligands, ranging from a strong positive agonist ($\alpha_B=100$) to a strong inverse agonist ($\alpha_B=0.01$), that bind with the same observed affinity in the whole cell (bottom) were selected. When these same ligands are examined in the membrane binding assay (top), the positive agonist binds much more tightly than the inverse agonist, making the inverse easy to overlook. (b) A different set of 5 ligands with similar values of K_{obs} in the membrane assay (top) were selected. When these ligands are tested in the whole cell (bottom), the strong inverse agonists bind most tightly, while the positive agonists bind weakly. This result implies that the membrane binding assay only detects those inverse agonists that bind very tightly, but can find positive agonists that bind relatively weakly. Parameters used in the membrane assay model: $R_{tot}=10,000$ #/cell; $G_{tot}=100,000$ #/cell; $K_{act}=0.001$; $K_G=10$ (#/cell) $^{-1}$; $K_{obsA}=K_{obsB}=10^7$ M $^{-1}$; $\alpha_B=0.01, 0.1, 1, 10, 100$; $\alpha_A=1$; $\beta_A=\beta_B=1$; $[A]=10^{-7}$ M. Parameters in the whole cell model are the same as the assay model plus the following kinetic rate constants: $k_1=0.00002$ sec $^{-1}$; $k_{a1}=k_{a2}=0.00001$ sec $^{-1}$; $k_i=10^6$ M $^{-1}$ sec $^{-1}$; $k_{r1}=0.01$ sec $^{-1}$; $k_{c3}=0.001$ M $^{-1}$ sec $^{-1}$; $k_i=0.001$ sec $^{-1}$, $A=10^{-7}$ M.

biological effect. However, if these same five ligands were subjected to a secondary assay using whole cells (Figure 4.5a bottom), then it would be found that all of the ligands bind with the same affinity. The result is that an inverse agonist that would bind appreciably *in vivo* would be overlooked using a membrane binding assay, generating a “false negative” result.

In Figure 4.5b, 5 drugs with similar observed affinity in the membrane binding assay (top) are tested in the whole cell model (bottom). Here, these 5 drugs could all be registered as “hits” in the membrane binding assay because they all have an EC_{50} of 100 nanomolar. However, when these same 5 drugs are examined in the whole cell (Figure 4.5b bottom), it is found that the positive agonists detected by the membrane binding assay bind weakly, while the inverse agonists bind much more tightly. In this situation, the positive agonists found by the membrane binding assay bind too weakly to be useful, but they are still detected. Therefore, weakly binding positive agonists can give “false positive” results in a high throughput screen that uses membrane binding.

These comparisons suggest that the membrane binding assay is biased to preferentially detect positive agonists and overlook some pharmaceutically important inverse agonists. In particular, the stronger the inverse agonist (the smaller the value of α) the more difficult that drug will be to detect in the membrane binding assay, making finding strong inverse agonists that bind with high affinity a difficult task. Experimental work with constitutively active α_1 and α_2 -adrenergic receptors is consistent with this conclusion in identifying many weak but few strong inverse agonists for the receptors (Rossier et al. 1999). The proposed bias in the membrane binding assay might in part account for paucity of known strong inverse agonists for GPCRs.

The magnitude of the observed affinity difference between the membrane binding assay and whole cell models depends on the parameter values chosen for the models, but the qualitative trend is independent of the parameters used. As shown in Figure 4.3, any increase in the G-protein activation rate constant, k_{r1} , will destabilize R^*G and AR^*G . These receptors freed from G-proteins will initially be in the active, R^* , state, which in

turn will drive the formation of more inactive receptors, R —an effect that should be particularly strong in most common systems that have a low level of constitutive activity. A sketch of this phenomena is shown in Figure 4.6, which shows a situation where the receptor is most stable in either the inactive state, R , or the G-protein bound state, R^*G ,

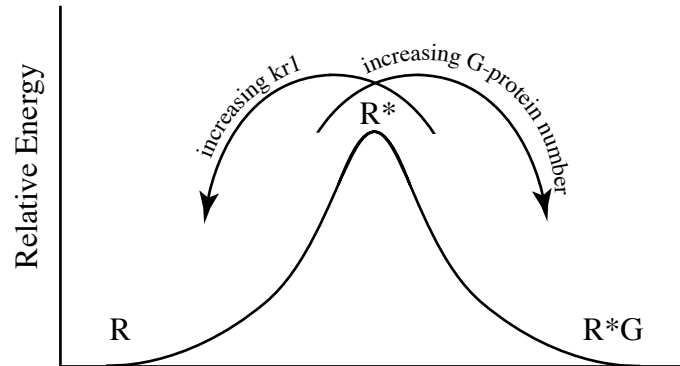


Figure 4.6 A qualitative sketch of the energies associated with inactive receptor, R , active receptor, R^* , and G-protein bound receptor, R^*G , for a system with low constitutive activity. When not stimulated, the receptor tends to stay in the inactive conformation due to the high energy barrier associated with receptor activation. This effect is enhanced by increasing the G-protein activation rate constant, k_{r1} . However, when the receptor does become active (R^*) there is a strong energetic drive to couple with G-proteins (R^*G) and transduce the signal inside the cell. This drive is enhanced when the total number of G-proteins is increased. Were this not the case, active receptors would not cause a biological response and as such could not detect changes in the environment.

with the R^* state as an unstable intermediate. Following this logic, unstimulated receptors will remain in the inactive, non-signaling state, while active receptors will be energetically driven to seek out G-proteins and thereby propagate the signal inside the cell. Therefore, according to the whole cell model, increasing the G-protein activation rate constant k_{r1} will *always* increase the observed binding affinity of inverse agonists (recall that inverse agonists have a higher affinity for R than for R^*) and decrease the observed affinity of positive agonists, regardless of the parameter values are used in the

model. In the limit of the G-protein activation rate constant dropping to zero, we recover the membrane binding assay model, which most strongly favors positive agonists over inverse agonists.

These modeling results are supported by experimental data describing the well-known effects of GTP on ligand binding, or what has been termed the “GTP shift” (Lawson et al. 1994; Krumins and Barber 1997). For known positive agonists, the removal of GTP can cause up to an 800-fold increase in the observed binding affinity (Florio and Sternweis 1989), while for known inverse agonists the observed binding affinity can drop by ~ 3 fold (Costa and Herz 1989). The reason for this change in binding affinity relates to GTP’s ability to activate G-proteins as is illustrated in the whole cell model in Figure 4.3. At high GTP concentrations, the G-protein is easily activated (k_{r1} large) and as such spends more time in the dissociated, signaling state. In this state the G-protein can not interact with the receptor causing the system to behave as if there were *less* G-protein present. At low GTP concentrations, however, the G-protein is not easily activated (k_{r1} small) and as such spends more time with the receptor, mimicking an *increase* in G-protein concentration. An increase in effective G-protein concentration is similar to adding a positive agonist to the system, for both positive agonists and G-proteins stabilize the active receptor conformation. Therefore increasing G-protein number tends to drive the receptor into the active conformation, making positive agonists bind more tightly at the expense of inverse agonist binding.

The reported GTP shifts are mirrored in the modeling results in Figure 4.5. The membrane binding assay represents a situation where GTP is removed from the system and thus G-protein can not be activated, while the whole cell model mimics the system

with GTP present. Following the binding of a strong positive agonist ($\alpha=100$) in Figure 4.5a, the binding affinity shifts from approximately 10 nanomolar in the membrane assay (top) to 100 nanomolar in the whole cell—representing a ~ 10 fold decrease in binding affinity. Similarly, for a weak inverse agonist ($\alpha=0.1$) in Figure 4.5a, the binding affinity shifts from 1000 nanomolar in the membrane assay (top) to 100 nanomolar in the assay—representing a ~ 10 fold increase in binding affinity on the whole cell.

In some experimental systems, the observed effect of GTP is smaller than the change presented in Figure 4.5, in which case the assay bias would still be present but possibly not detectable. For example, it has been shown that the α_{2A} -adrenergic receptor increases its binding affinity for agonist by a factor of 3 to 9 when GTP is removed, while the decreasing its affinity for inverse agonist by only a factor approximately 2 (Wade et al. 2001). In modeling terms this smaller shift could be accounted for by reducing the value of K_G , thereby reducing the influence of G-proteins on the receptor conformation. An example of how binding in the assay and whole cells would behave with an alternate parameter set is shown in Figure 4.7. In these cases, the GTP shift would still bias against detecting inverse agonists, but the magnitude of this shift may be sufficiently small such that the bias does not present a screening problem.

At this time it is not clear when the screening assay would produce a significant bias and when it would not. As I have shown, changes in the receptor-G-protein equilibrium constant (K_G) can alter the magnitude of the bias, but the value of K_G is not known at this time and would likely be different for each receptor-G-protein combination. Additional experimental work is needed to determine when the assay bias is significant.

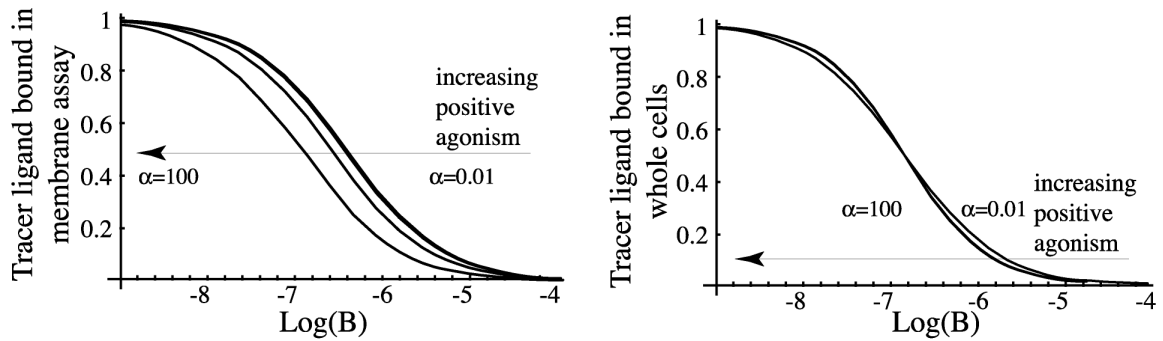


Figure 4.7 Alternate parameter set that exhibits a smaller shift from the whole cell model to the assay model. This scenario may better represent some experimental systems such as the α_{2A} -adrenergic receptor (Wade et al. 2001). Parameters used in this model are the same as in Figure 4.5 except K_G is reduced from $10 \text{ (\#/cell)}^{-1}$ to $0.001 \text{ (\#/cell)}^{-1}$.

Although not included in the model, assays that use membrane preparations may also have access to more G-proteins than would be available in a living cell. In a living cell, G-proteins are associated with the membrane and their locations appear to be regulated. This cellular regulation ensures that at the receptor has access to only a fraction of the total available G-proteins (Neubig 1994). When the cell membrane is disrupted, however, the cytoskeletal elements that maintain this organization may no longer function. Therefore in membrane preparations the receptor may have access to *all* of the G-proteins, thereby affecting the stoichiometry of the system.

4.3.2 Equilibrium analyses: Membrane binding assay can be refocused to detect inverse agonists

The modeling results suggest that the membrane binding assay biases against the detection of inverse agonists, but can the model also suggest solutions? Because the models used in this work are mechanistic, as opposed to “black box” phenomenological models, changes in the signaling pathway can be simulated to see their effects. In the

case of GPCRs, changes in the signaling pathway could include adding a drug that alters the rate of a particular reaction, or changing the concentration of a protein in the pathway. Comparisons between ligand binding in the membrane binding assay and the whole cell assay suggest that by manipulating the G-protein number, the membrane assay can be refocused to detect drugs with a particular efficacy. For example, to refocus the membrane binding assay toward the detection of inverse agonists, the number of G-proteins must be reduced to better match the whole cell binding conditions. Common experimental techniques used to remove G-proteins include chemical inactivation with pertussis toxin or the addition of a non-hydrolyzable GTP analog, such as Gpp[NH]p or GTP γ S. A similar way to remove G-proteins would be to add an excess of GTP—essentially using the “GTP shift” to refocus the assay. Note however, that increased inverse agonist binding affinity due to changing G-protein number comes at the expense of the binding affinity of positive agonists, implying that the assay can only be optimized for a single class of drugs at a time.

Another possibility would be to use the results from two membrane binding assays, each with a different number of G-proteins, to predict the efficacy of a drug. For example, imagine measuring the equilibrium signal drop when G-proteins are present (S_G^+) and when G-proteins are absent (S_G^-). By comparing the values of S_G^+ and S_G^- , the approximate efficacy of the drug could be determined by:

$$S_G^+ = S_G^- \quad \text{neutral antagonist}$$

$$S_G^+ > S_G^- \quad \text{positive agonist}$$

$$S_G^+ < S_G^- \quad \text{inverse agonist}$$

For example, if $S_G^+ = S_G^-$ then ligand binding is insensitive to G-protein concentration, implying that the ligand binds equally well to either the active or inactive receptor conformation—consistent with the binding behavior of a neutral antagonist. Note that these predictions do not require that the absolute number of G-proteins in the system be known, but instead rely on a difference in G-protein number. This approach has the advantages of the simplicity of a binding assay, but would also give functional information about the test ligand.

4.3.3 Equilibrium analyses: Tracer ligand efficacy does not bias the membrane binding assay

In general, screening assays are run using a neutral antagonist as a tracer. Would using a positive or inverse agonist as a tracer affect the bias of the assay toward drugs of a different efficacy? This question can be explored using the analytical results from membrane binding assay to see how tracers with different efficacies would affect the observed equilibrium signal ratio.

As a starting point consider two tracer ligands, a positive agonist (+) and an inverse agonist (-), which both bind to a particular receptor with the same observed affinity, K_{Obs} . If the G-protein concentration can be assumed to be constant, then the analytical results developed earlier can be used to predict equilibrium signal ratio produced when using each tracer ligand. The observed equilibrium constant as defined in Eqn. 4.2 can be related to the parameters in the assay model by:

$$K^+_{obs} = \frac{M^+}{[A^+] N} = K^-_{obs} = \frac{M^-}{[A^-] N} \quad (4.3)$$

where N and M are as given in Eqns. 4.1b and 4.1c. The parameter N only depends on properties of the system (K_{act} , K_G , and $[G]$), and therefore is independent of the tracer ligand used, while the parameter M does depend on a number of ligand-specific parameters (K_a , α , and β) and is therefore denoted as M^+ for the positive agonist and M^- for the inverse agonist. If the concentrations of both tracer ligands are equal[†], $[A^+]=[A^-]$, then by Eqn. 4.3, $M^+=M^-$. If M^+ and M^- are equal, then the equilibrium signal ratio in equation 4.1 must also be equal for both tracer ligands, as shown by

$$\text{Equilibrium signal ratio} = \frac{N + M^+}{N + M^+ + M_B} = \frac{N + M^-}{N + M^- + M_B} \quad (4.4)$$

Thus the efficacy of the tracer ligand will not affect the signal ratio or the efficacy of the ligands detected in an equilibrium binding assay^{††}.

4.3.4 Kinetic analyses: Binding kinetics gives information about ligand efficacy

Thus far we have only examined the membrane binding assay in the equilibrium limit because most high throughput screens are designed as equilibrium assays. Therefore, the results of these assays interpreted using two data points—one before the test ligand is added to establish a base line, and a second after the test ligand has had time to equilibrate with the receptor. Unfortunately, this process has at least two potential

When the concentration of the tracer and test ligands are not equal and yet both ligands bind with the same observed affinity, then binding will favor the most concentrated species, irrespective of either ligand's efficacy.

problems. The first problem is that system may not actually reach equilibrium before the second measurement is taken. In this case, the signal change may appear less than if the assay had been run for a longer time and some potentially important leads may be lost. The second, subtler problem is that equilibrium assays discard valuable kinetic information which can give additional clues about the test ligand.

This additional kinetic information may allow us to predict not only the binding affinity but also the efficacy of a drug. By observing how quickly the signal changes when the test ligand is added, we attempted to distinguish between positive and inverse agonists. Figure 4.8a shows an example of how the signal would change in the membrane binding assay for 5 different test ligands, ranging from a strong positive agonist to a strong inverse agonist. The test ligands were chosen to produce the same drop in signal at long times (approaching equilibrium) and the tracer ligand is a neutral antagonist. Notice that the inverse agonist causes the assay signal to drop slowly, while the positive agonist causes a rapid signal drop. This differential in binding rates between positive and inverse agonists has two important implications. The first is that inverse agonists may be missed by screening assays that are not incubated long enough to allow the system to reach equilibrium. Only those ligands that bind quickly (positive agonists) would be detected. The second implication is that by observing the rate of ligand binding, we can infer the efficacy of the ligand without doing any further tests. Therefore

This result assumes that the total number of free G-proteins does not change appreciably. If this assumption is violated then the efficacy of the tracer ligand *can* affect the equilibrium signal ratio in a system dependent manner. The analytical solution of this more general model is lengthy and is reproduced in Appendix A.

in this system, test ligands that bind slowly but have a large signal drop are most likely inverse agonists while ligands that bind quickly with a large signal drop are most likely positive agonists.

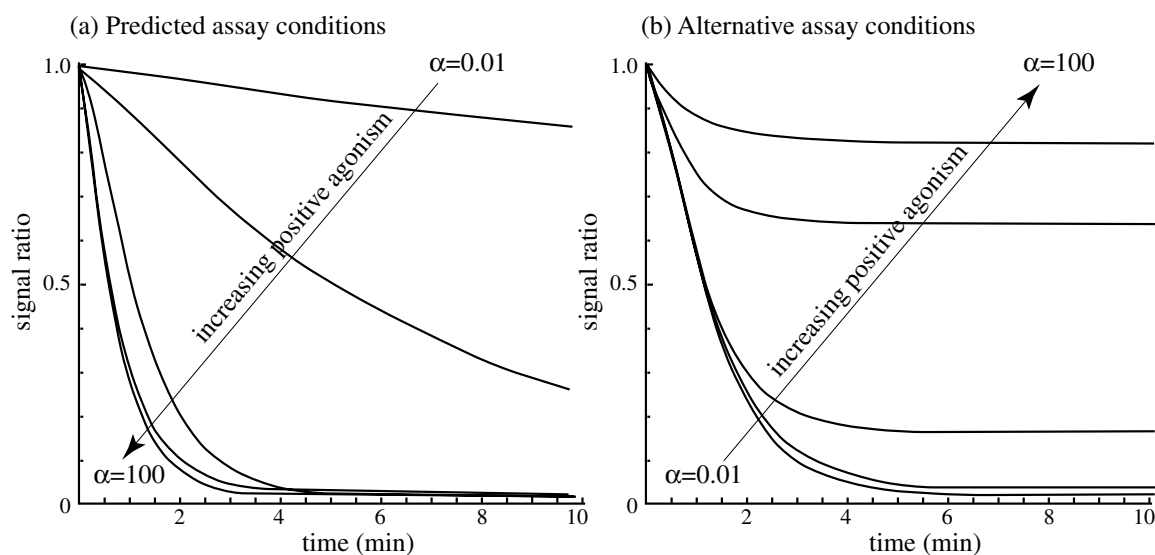


Figure 4.8 Predicted signal as a function of time in the membrane binding assay. Ligands ranging from strong inverse agonists to a strong positive agonists are chosen to all have the same equilibrium signal drop in the assay. The tracer ligand used is a perfect neutral antagonist ($\alpha=1$). (a) Predicted assay conditions: Normally the membrane binding assay is expected to favor the active G-protein bound form of the receptor, R^*G , due to the stabilizing effect of the empty cage state. Under these conditions inverse agonists bind more slowly than positive agonists. (b) Alternative assay conditions: If the assay is modified to stabilize the inactive receptor conformation, R , positive agonists bind more slowly than inverse agonists. Parameters in both plots are the same as those shown in Figure 4.5, except in (b) K_G has been changed to 0.0005.

The reason that inverse agonists are predicted to bind more slowly than positive agonists in the membrane binding assay is illustrated in Figure 4.9. Because the membrane assay contains no GTP, and as such no G-protein activation step, the G-proteins in the assay tend to hold the receptor in the active conformation, R^*G . In modeling terms, this stable bond is described by a large value of the equilibrium G-protein binding constant, K_G . When the tracer ligand is added and the system is allowed

In contrast, if the membrane binding assay begins with receptors primarily in the inactive state, R, then positive agonists will bind more slowly than inverse agonists, as shown in Figure 4.7b. To achieve this reversal, the G-protein binding constant, K_G , was reduced, thereby shifting the equilibrium in Figure 4.6 to the left. Experimentally this could be mimicked by using a receptor with low affinity for G-proteins, adding GTP to the assay, or by removing G-proteins from the assay. The explanation for this phenomenon is similar to that in Figure 4.9, except that now inverse agonists must only traverse two steps to bind, while positive agonists must take four steps. More complicated scenarios such as when more than one reaction rate is limiting are also possible, but are beyond the scope of this work. Analysis techniques for these more complex kinetic systems can be found elsewhere, *e.g.* (Hill 1977; Fogler 1999). Based on qualitative behaviors such as the magnitude of the GTP shift and the speed at which signals are detected by GPCRs, most screening assays are expected to behave similarly to the assay shown in Figure 4.8a.

These results demonstrate that the binding kinetics of a drug can give useful information about the relative efficacy of that drug. The interpretation of the data will vary with the receptor system under study and the assay conditions; experiments with known ligands would be useful to first determine plausible ranges of key parameters based on the overall system behavior. In *all* cases however, kinetic binding data yields valuable information about the efficacy of the ligand.

4.3.5 Kinetic analyses: Tracer ligand efficacy can affect binding kinetics

The efficacy of the tracer ligand can affect the binding kinetics of the test ligand. As discussed above, a positive agonist tracer ligand will hold the receptor in the AR*G

state, allowing positive agonist test ligands to bind more quickly than inverse agonists and giving results similar to Figure 4.8a. Tracer ligands that hold the receptor primarily in other states (e.g. AR) will allow different kinetics of test ligand binding (e.g. Figure 4.8b). These examples require that the tracer ligand exerts a strong influence over the receptor by binding tightly and specifically to primarily one conformation. Finding a ligand that binds with such high specificity is required to overcome the effects of G-proteins on the receptor conformation (the parameter K_G in the model), which may not be possible for some systems. Further, using a tightly binding tracer ligand can be a disadvantage in that the absolute size of the signal drop will be reduced, making it difficult to distinguish signal from noise.

4.4 Conclusions

Our modeling results indicate that current membrane binding assays bias against the detection of inverse agonists, both at long and short assay times. Thus current high throughput screening methods which are based on membrane binding are predicted to miss many inverse agonists. Modifications such as removing G-proteins from the assay or observing the kinetics of ligand binding may help to refocus the assay and also provide functional information about the test ligands. Alternative modifications such as using a tracer ligand with a different efficacy were shown to have no effect on the equilibrium signal when the free G-protein concentration can be assumed constant, but could affect the kinetics of test ligand binding.

Further experimental work will be needed to determine when this bias is significant enough to cause drugs to be missed. For example, the system illustrated in Figure 4.5 shows a robust change in ligand affinity from whole cell binding to membrane

assays, while the system in Figure 4.7 shows a significantly smaller change. Future measurements of the receptor/G-protein binding affinity (K_G) may help to shed light on which systems are prone to the bias described in this work. For systems where ligands ranging from strong agonists to inverse agonists exist, simple binding assays should be sufficient to describe the bias as was done for the α_{2A} -adrenergic receptor (Wade et al. 2001). However by using binding assays one will always be limited to testing ligands that have already been found and may not completely represent what *could* be found using a completely unbiased assay.

This work only represents one example of how modeling can aid in improving our design and understanding of high throughput screening assays. By using modeling, we can explore a wide variety of assay conditions using details known about the system which could be difficult to assess experimentally. As we have shown in the case of GPCRs, modeling can elucidate biases in the screen and suggest ways to correct and or compensate for these biases. Similar techniques might be used to analyze assays on other kinds of receptors or even enzyme assays, such as tyrosine kinase assays (Park et al. 1999). In general, modeling allows us to focus our screens and glean more information from the data with little additional cost.

CHAPTER V
SELF ORGANIZATION OF MEMBRANE BOUND PROTEINS VIA
DIMERIZATION

5.1 Introduction

Dimerization is observed in systems ranging from colloidal suspensions to protein complexes on the cell surface. In this work we first ask how dimerization affects particle organization, and then for biological systems how this organization affects physiology. Heterodimerization is unique in condensed matter physics because it is not a field interaction but instead is a one-to-one interaction. Thus when a dimer forms it becomes inert. Although this type of bond formation is common in biology, little theoretical work has been done to elucidate how dimerization affects particle organization and why this organization is important for the cell. For receptor tyrosine kinase proteins, dimerization is thought to bring reactive species together to transduce a signal (Weiss and Schlessinger 1998), although dimerization alone may not be sufficient to transduce a signal (Burke and Stern 1998). In other systems the physiological role of dimerization is less clear. For example, it has been recently revealed that a large number of G-protein coupled receptors (GPCRs) are able to form homo- and heterodimers (Nimchinsky et al. 1997; Hebert and Bouvier 1998; Gines et al. 2000; Overton and Blumer 2000). In most cases, dimerization of GPCRs does not correlate with signaling, but instead is thought to affect signal cross-talk among receptor types or desensitization

of the receptor via an unknown mechanism (George et al. 2000; Jordan et al. 2001). Similarly, the bacterial receptor Tar (Gardina and Manson 1996), human nerve growth factor receptor (Schlessinger and Ullrich 1992), and the bacterial and plant Photosystem II proteins (Jahns and Trissl 1997) are all able to form transient dimers in the membrane, but the reasons for these interactions are unknown.

Using Monte Carlo simulations, we show that protein dimerization can cause long range ordering within the cell membrane. Although other mechanisms such as lipid rafts may participate in ordering the proteins within the membrane, protein-protein interactions are likely to play a key role in establishing this order and dynamically changing this order over short time spans. The key mechanism for forming extended order via dimerization is partner switching (Fig. 5.1). Here each protein competes to bind with its neighbors before they move too far apart to interact. If this binding and unbinding reaction is fast relative to the diffusion rate, then the proteins can *share* a single bond among multiple proteins and in doing so form a stable oligomer. This bond sharing is analogous to sharing a single electron across many bonds in chemistry. In modeling terms, the translational movement rate is determined by the diffusion coefficient and the rates of

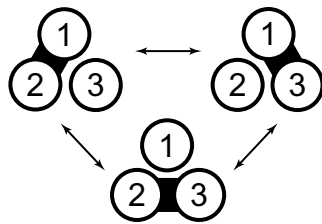


Figure 5.1 Dimerization can lead to the formation of trimers via diffusion-limited partner switching. This same mechanism can be extended to form larger oligomers when more monomers are present.

binding and unbinding can be described by two reaction rate constants, k_{dimer} and k_{mono} in the reaction:



Note that k_{dimer} and k_{mono} are intrinsic rate constants, meaning that they describe the rate at which binding and unbinding take place *after* diffusion has brought them together.

5.2 Methods

5.2.1 Monte Carlo simulations

Simulations were run on a 700 x 700 triangular lattice with periodic boundary conditions and a lattice spacing corresponding to 0.5 nm. Particles were assumed to occupy hexagons with a diameter of 10 lattice spacings, which corresponds to a protein diameter of 5 nm and is approximately equal to the diameter of a single G-protein coupled receptor. During the simulation, particles were picked at random to react and move. If the edges of two particles were separated by an interaction radius of 5 grid spacings (2.5 nm) or less and both were monomers, they were allowed to form dimers with a probability proportional to k_{dimer} . Dimers were allowed to monomerize with a probability proportional to k_{mono} . Particles were allowed to diffuse a single grid spacing in a random direction with a probability proportional to the diffusion coefficient. If the site was occupied, then the move was rejected and not repeated. Single particles within a dimer pair were allowed to move toward or in parallel with each other with the same probability as a single unbound particle. Cluster size was measured by counting the total number of particles that are within the interaction radius of at least one member of the

same cluster. Before statistics were taken, all simulations were allowed to pre-equilibrate, and then at least 500 measurements were made, between which each protein was allowed to move an average two diameters between measurements. Phase diagram simulations were run with 1000 particles corresponding to a surface coverage of 18% and reached equilibrium within 10 ms of simulation time. Runs with two particle species were run with 300 A and 300 B particles with binding parameters set at $k_{\text{mono}}=4.6$ and $k_{\text{dimer}}=46$, thereby placing the ensemble in the oligomer phase. Average separation distance was measured for 10,000 independent runs. Simulations were written in C++ using Metrowerks CodeWarrior and were run on a cluster of Apple PowerPC G4 machines.

5.2.2 Scaling to GPCRs

Dimensionless rates are given relative to a normalized diffusion rate of 1, correlated to the time required for a particle to travel 0.1 particle diameters. This time can be calculated using the diffusion coefficient along a two-dimensional surface:

$$t = r^2 / (4D_t) \quad (5.2)$$

where t is the characteristic time, r is the distance traveled, and D_t is the translational diffusion coefficient. For a GPCR, r is 0.5 nm (10% of the protein diameter) and estimates of D_t range from 10^{-8} to 10^{-11} cm^2/s (Saffman and Delbruck 1975; Shea and Linderman 1997), yielding a characteristic time of 10^{-4} to 10^{-7} seconds. Therefore a normalized dimerization rate of 10 corresponds to $10/10^{-4}$ to $10/10^{-7}$ or 10^5 to 10^8 sec^{-1} . By presenting the results in normalized form, they can be directly applied to any two-dimensional system where dimerization is possible. The GPCR dimerization rate of 10^5

sec^{-1} was estimated using a GPCR rotational diffusion coefficient of $2.7 \times 10^5 \text{ sec}^{-1}$ (Saffman and Delbruck 1975) assuming two proteins must align to within 60° of the protein-protein binding site to dimerize. The monomerization rate, rather than the dimerization rate, was assumed to be receptor specific. For dimerization to take place, two proteins must first rotate to align their binding sites. This step does not directly depend on the receptor type or on the specific state of the receptor. Assuming the time scale for rotational diffusion is limiting, then the subsequent receptor specific binding step will not contribute substantially to the overall dimerization rate. In contrast, monomerization is not affected by the rotational diffusion of the proteins, and as such is fully determined by the identity and state of the receptor.

5.3 Results and Discussion

5.3.1 Dimerization can cause clustering *in vivo*

We first consider the case of one homodimerizing species that is allowed to react and diffuse in two dimensions yielding phase behavior illustrated in Fig. 5.2a.

Depending on the binding kinetics relative to the diffusion rate, the ensemble can exist in a two-dimensional gas of monomers, a two-dimensional gas of dimers, or an intermediate diffusion-limited oligomer state. In the monomer gas state, the ratio of dimerization to monomerization rates is low, driving the equilibrium toward a homogeneous mixture of monomers. In the dimer gas state, the ratio of dimerization to monomerization rates is high, permitting the particles to form stable dimers but lacking any long-range order. Between these two states there exists an intermediate state that orders particles into oligomers via the partner switching mechanism described earlier. Our simulation results

(Fig. 5.2b) demonstrate that this phase behavior does indeed emerge when the contributions of many particles are included. Movies of this interaction can be viewed on the web at www-personal.engin.umich.edu/~pwoolf/dimerization.html. Oligomer size is maximized when the dimerization rate is approximately ten times the monomerization rate, and when both rates are fast relative to the diffusion rate. From inspection of Figure 5.2b, the minimum normalized dimerization and monomerization rate constants required to observe the oligomer phase are approximately $k_{\text{dimer}}=10$ and $k_{\text{mono}}=1$, with larger constants resulting in further increases in oligomer size. When these results are scaled to the diffusion coefficient of GPCRs in the cell membrane, it is found that the oligomer phase should be present if the dimerization rate constant is at least 10^5 sec^{-1} and the monomerization rate constant is at least 10^4 sec^{-1} .

The dimerization and monomerization rate constants for GPCRs have not been directly measured, but our estimates suggest that diffusion-limited oligomers are present in the cell. The dimerization rate constant can be estimated based on the rotational diffusion coefficient of a GPCR to be on the order of 10^5 sec^{-1} , thereby allowing the system to access the oligomer phase. The monomerization rate constant is specific to the receptor species and its activation state, likely varying from nearly zero to much larger values and thus allowing for monomer, dimer, and oligomer phases to be present.

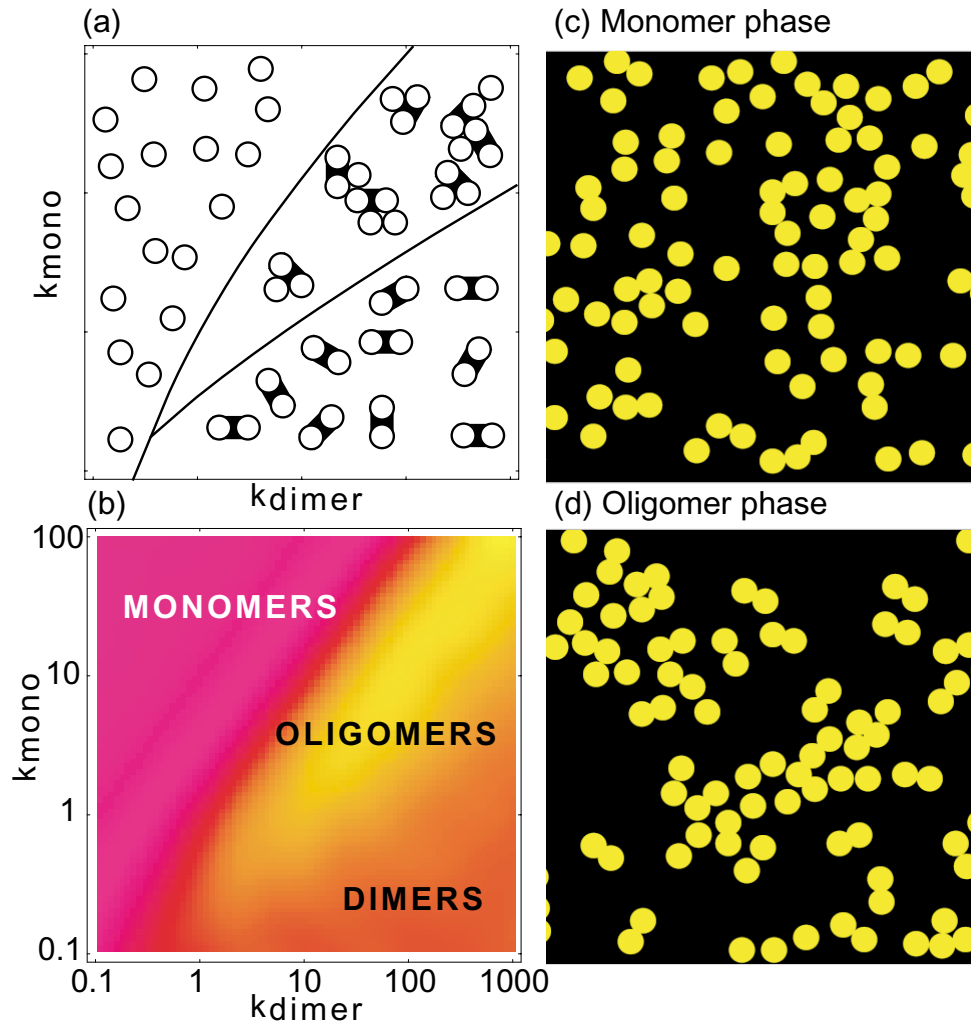
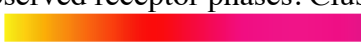


Figure 5.2 (a) Schematic phase behavior of a dimeric species to indicate three phases: a two-dimensional monomer gas, a two-dimensional dimer gas, and a diffusion-limited oligomer phase. (b) Simulation results that show how the cluster size varies with k_{mono} and k_{dimer} normalized to a diffusion rate constant, k_{move} , of 1. The labels on the diagram denote the three observed receptor phases. Cluster size is indicated by color and varies from 4.2 to 1.9 (4.2  1.9) particles per cluster. (c) Sample image of particle location in the monomer gas phase. (d) Sample image of particle location in the oligomer phase. Note that the particles are more clustered in the oligomer phase than they are in the monomer phase, as is reflected quantitatively in the phase diagram.

Increased mobility of the receptor-receptor binding surface or local structures in the lipid bilayer could also act to increase k_{dimer} (Gheber and Edidin 1999) and in doing so further favor the oligomer phase. Experimentally, membrane preparations of GPCRs

including the D₃ dopamine, δ -opioid, and μ -opioid receptors have been shown to form trimers and even tetramers in spite of their being monovalent proteins (Nimchinsky et al. 1997; George et al. 2000). It has been difficult to explain why these proteins form larger oligomers, but this finding is consistent with the diffusion-limited oligomerization proposed here.

Receptor organization could be altered by the presence or absence of ligands. Experimental data have shown that GPCRs respond to ligands by dimerizing or monomerizing (Hebert et al. 1996; Gines et al. 2000); therefore ligand binding could change k_{mono} to push a system from, for example, a monomer gas state to an oligomer state. Samples of how these two states might appear on the cell membrane are shown in Figures 5.2c and d. By clustering proteins together in the oligomer phase, a ligand could indirectly influence how the cell responds. For example, clustering could reduce local diffusion limitations for secondary messengers such as G-proteins, or for proteins involved in the desensitization pathway such as receptor kinases. Thus at the physiological level, receptor signaling efficiency and desensitization could in part be modulated by ligand induced changes in dimerization.

The average oligomer size increases by increasing the protein density or by adding inert proteins to the system. For example, increasing the active or “dimerizable” protein density from 18 to 37% coverage results in an average oligomer size 50% over what would be seen if no dimerization were present. Similarly, adding inert proteins that do not form dimers up to a 37% surface coverage causes the average oligomer size to increase by approximately 15% (Figure 5.3). In the typical eukaryotic cell, proteins occupy between 20 and 50% of the membrane surface area (Gennis 1989); therefore the

protein densities tested in the simulations are physiologically realistic. Both increased active protein density and increased inert protein concentration effectively reduce the observed diffusion rate of proteins within the membrane, driving the system into a more diffusion-limited regime that favors oligomerization. In the phase diagram in Figure 5.2b, this decrease in diffusion coefficient corresponds to shifting the results to the upper right, thereby favoring an increase in oligomerization. It is important to note that the effect of density is local. Thus, although the active receptor may be expressed at low densities on the cell surface as a whole, the receptors could be limited to high density domains due to corralling or association with membrane lipid islands, thereby favoring oligomerization (Gennis 1989; Saxton 1989; Gheber and Edidin 1999; Pralle et al. 2000).

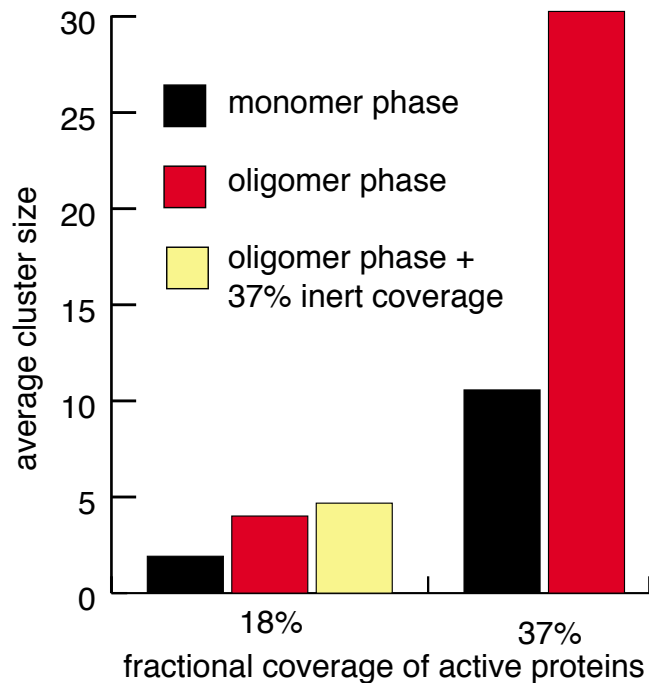


Figure 5.3 Effects of increasing active and inert particle density on the average cluster size. Cluster size always increases with particle density due to simple crowding; however, oligomers increase their cluster size more quickly due to a reduction in the apparent diffusion coefficient at high particle density.

5.3.2 Dimerization influences receptor cross-talk

Next, receptor cross-talk was examined by simulating the interaction between two different protein species. For GPCRs, one type of cross-talk takes place when two receptors interact with a common G-protein. For example, the μ - and δ -opioid receptors both act through the G_i form of the G-protein, but respond to different ligands (George et al. 2000). This kind of cross-talk can be beneficial because it allows many receptors to activate a common signal transduction pathway and thereby ensures that the signal will be transmitted; however, in other cases cross-talk could be harmful because it prevents the cell from discriminating between distinct pieces of information about the environment. Therefore, a mechanism for dynamically regulating receptor cross-talk would be of benefit to the cell.

Cross-talk at the receptor level depends on how the receptors associate with each other. We examined the interaction of two receptor species, A and B, under three different association rules: no dimerization (A and B are inert); homodimerization (A binds with A; B binds with B); and heterodimerization (A binds with B). Examples of each of these cases have been experimentally observed for GPCRs (George et al. 2000; Gines et al. 2000; Jordan et al. 2001). As a measure of receptor cross-talk we calculated the minimum distance separating two different species of receptors on the assumption that receptors spaced more closely would have more cross-talk via secondary messengers.

In the oligomer and dimer gas phases, changing the receptor-receptor association rules affected receptor cross-talk (Fig 5.4). No dimerization led to a well-mixed system and the separation between A and B took on an intermediate value. Heterodimerization coupled dissimilar receptor species, resulting in a short separation distance between A

and B and presumably increased cross-talk. In contrast, homodimerization caused like receptor species to separate themselves into distinct islands, increasing the separation distance between A and B and reducing cross-talk. Therefore treatments that alter the receptor-receptor association rules, such as the presence of ligands that induce or inhibit dimerization, could affect receptor cross-talk and any ensuing physiological responses.

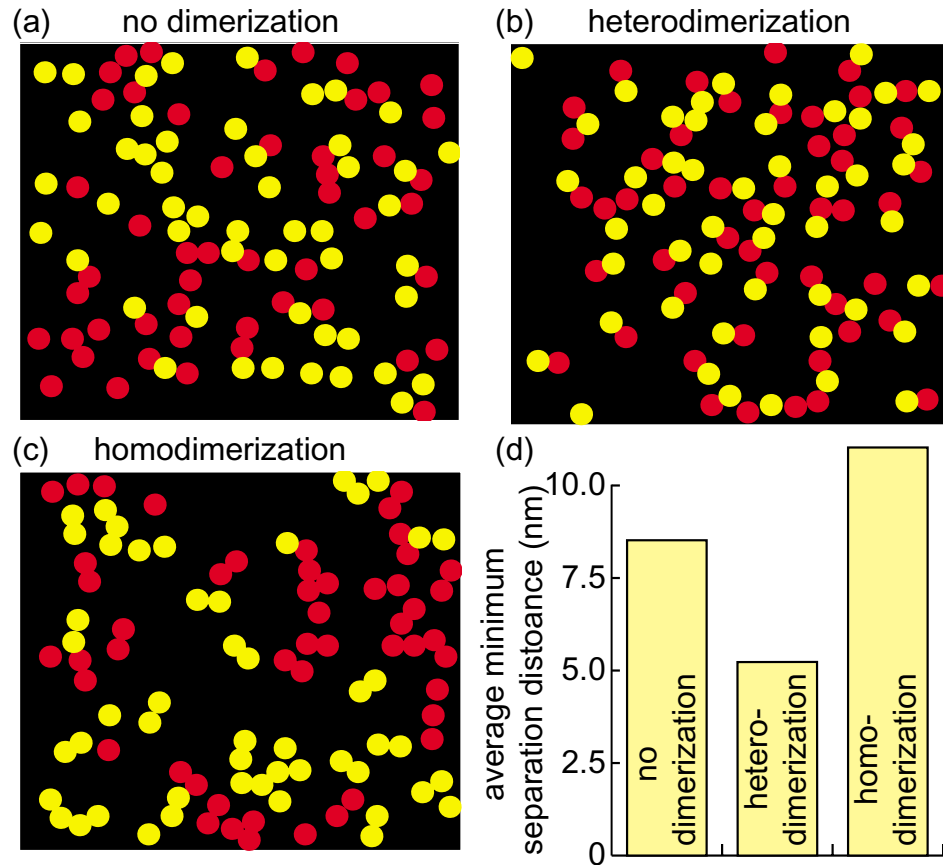


Figure 5.4 Snapshots of the positions of two protein species in yellow and blue under the following protein-protein association rules: (a) No interaction between proteins; (b) Heterodimerization; (c) Homodimerization. (d) Average minimum separation distance between two dissimilar neighbors quantifies what can be observed visually in figures a, b and c, implying that heterodimerization enhances cross-talk while homodimerization represses cross-talk.

The effects of receptor-receptor association rules on cross-talk are most pronounced in the oligomer phase. For example, when receptors associate as homodimers they form extended homogeneous islands in the oligomer phase, but only

form stable pairs in the dimer gas phase. As such, homodimerization in the oligomer phase isolates dissimilar receptors more effectively than homodimerization in the dimer gas phase, presumably leading to reduced cross-talk. When receptors associate as heterodimers, cross-talk becomes sensitive to the concentration of each receptor species. In the dimer gas phase, any deviation from a 1:1 concentration ratio leaves uncoupled receptors, resulting in poor mixing and less cross-talk. In contrast, receptors in the oligomer phase use the partner switching mechanism (Fig. 5.1) which is less sensitive to the concentration ratio, resulting in better mixing over a wider range of conditions and more cross-talk. These results may explain why evolution has favored dimerization in so many receptor systems and suggest that these receptor systems should operate in the oligomer phase for improved control of cross-talk.

Further exploration of this topic will be described in the following chapter.

5.3.3 Dimerization rules describe a spatial grammar

Because ligands to GPCRs alter the dimerization state of their receptors, we propose a higher level abstraction of receptor signal regulation through a form of *spatial grammar*. In linguistics, a grammar describes how words are linked together to express a concept. Similarly, in signal transduction a spatial grammar describes how receptors link together to create a functional pattern. For example, Figures 5.4a,b, and c show three qualitatively different patterns that two receptor species can assume depending on the specific grammar. Shorthand representations of those grammars are

<u>Grammar</u>	<u>Pattern</u>	<u>Meaning</u>
A B	Figure 5.4a	medium cross-talk
A•B	Figure 5.4b	high cross-talk
A•A B•B	Figure 5.4c	low cross-talk

where A and B represent different receptor types, and the • symbol indicates receptor association. In each case the cell will receive a different signal depending on the specific grammar. The following statements illustrate the analogous case in English

<u>Grammar</u>	<u>Pattern</u>	<u>Meaning</u>
they are here	.	factual statement
are they here	?	question
here they are	!	explicative denoting a change

All of these cases are rearrangements of the same three words to express different meanings. Therefore ligands that affect receptor association rules are in effect changing the grammar of their signal and in doing so altering the meaning. Although illustrated with only two receptor types, a spatial grammar can also describe the interaction of many species, thereby providing a useful analogy to help extend our understanding of GPCR signal transduction beyond the single protein level to the more global system level.

We have demonstrated a new emergent property of dimerization with implications for signal transduction and membrane organization. Oligomerization via dimerization extends protein-protein interactions beyond single protein behavior and as such may explain why dimerization is so prevalent among membrane receptors. This result also has implications for drug design. If a drug is developed that alters the associative rules of the receptor then that drug may also affect how the receptors localize themselves on the cell membrane, and in doing so influence how the signal is interpreted by the cell. Oligomerization via dimerization is not only applicable to membrane proteins but can be generalized to other non-biological systems. For example, heteroflocculation in colloidal suspensions is used industrially to control material properties (Asselman and Garnier 2000). This process may employ similar partner switching mechanisms and therefore would have a grammar that could be manipulated to alter the behavior of the resulting

materials. Similarly, these results could be extended to apply to polyvalent particles, assuming that bond formation is reversible and that the rates of bond formation and destruction are fast relative to the diffusion rate. Finally, understanding protein organization and its effects on signal transduction in terms of a linguistic grammar provides a powerful analogy to extend our understanding of signal transduction from the level of single proteins to the broader system level. It is through this more complete view of signal transduction that we can begin to understand how the cell integrates diverse stimuli to arrive at a coherent response.

CHAPTER VI
ACTIVATION, SELF—ORGANIZATION, AND CO—REGULATION OF
RECEPTOR DIMERS

6.1 Introduction

What is the physiological consequence of receptor dimerization if dimerization does not catalyze a reaction? The current dogma is that most proteins bind with other proteins to either catalyze or inhibit reactions. However this explanation for protein binding does not explain the apparent ubiquity of protein—protein interactions that do not affect the active site of the protein nor the binding that takes place between proteins with seemingly unrelated functions. Another explanation for protein bonds is that they allow proteins to form extended structures; however many proteins have only one binding site and therefore can only form dimers. In this work we use computer modeling to show that dimerization can organize multiple receptor species on the cell membrane. We also show that dimerization induced organization affects receptor cross—talk and internalization rates in a way that depends on the logical rules that govern receptor hetero— and homodimerization.

As a sample case we have chosen to focus on the G—protein coupled receptor (GPCR) family. Many GPCRs have been shown to form homo— and heterodimers, but dimerization does not appear to cause receptor signaling as reviewed in (Gomes et al. 2001). Experimental evidence indicates that dimerization might affect GPCR desensitization or localization, but there was no known physical mechanism for this observation. Therefore, in this work we have attempted to see if dimerization could have

a physiologically observable effect by basing our model on known physical properties of GPCRs.

GPCRs and receptors in general provide a particularly interesting case for the study of dimerization because these proteins change conformation upon ligand binding. This change in conformation not only allows the receptor to activate secondary messengers, but also affects receptor internalization and possibly dimerization. For example, it has been shown that ligand binding affects the dimerization of the SSR5 receptor (Rocheville et al. 2000), the bradykinin B₂ receptor (AbdAlla et al. 1999), and the β_2 AR receptor (Angers et al. 2000). Therefore, binding a ligand to a receptor may not only change the activity of the receptor but also the dimerization induced organization of the receptor in its environment.

In chapter 5, I demonstrated that dimerization alone can exhibit phase behavior in which membrane proteins can exist in a monomer gas, dimer gas, or mixed gel phase depending on the kinetics of the system. In the gel phase, membrane proteins form extended clusters that are capable of self—organization. The clusters in the gel phase are able to form by using a partner switching mechanism in which a single dimer bond can be rapidly shared among many membrane proteins within the cluster. As an analogy, consider a cocktail party in a ballroom where each guest can only hold the attention of one other guest at a time. If the guests in the party are not talkative, then everyone in the room will wonder aimlessly and never form any structure, thereby forming the analogous monomer gas phase. On the other hand, if the guests become engrossed in their own focused conversations, then everyone in the room will explore the room as tight pairs, akin to the dimer gas phase. However if the guests discuss topics familiar to everyone, such as the weather, then any speaker may be able to effectively hold the attention of more than one person at a time by rapidly shifting focus from person to person. If the speaker is able to perform this shift faster than the guests can escape, then the speaker has

effectively made a trimer using only a dimer interaction. This last case characterizes the gel phase.

The organization that results from dimerization is not static but instead is dynamic. Following the cocktail analogy above, clusters of guests in the gel phase do not form rigid and unchanging groups but instead constantly break down and regroup into different combinations. This kind of organization is qualitatively different from the organization observed in most engineered systems in that it is probabilistic. In an engineered system, such as a car or a building, the parts are connected together in a precise and rigid way that either does not change with time or changes only along a limited pathway. In contrast, dynamic organizations such as cocktail parties or proteins in the cell membrane do not have set, permanent connections.

Two related advantages of a dynamic organization are that it is robust to changes in the system and it can self—organize. Small changes in a rigid system, such as removing a gear from a car, can cause the whole system to fail. In contrast, removing a small number of proteins from the cell membrane has little effect on the overall functioning of the system. The reason the dynamic organization is more robust to these changes is that the rules that govern this organization also allow the system to self—organize. Therefore small changes in the protein expression level cause the proteins within the system to reorganize to compensate for the loss. In biological systems, this level of robustness is needed to cope with noise ranging from thermal fluctuations to stochastic protein binding events and therefore is an integral part of the cell's functioning.

In this chapter I model GPCRs in the gel phase to explore the physiological consequences of dimerization. In each case I present simulation data that is experimentally accessible and provides intuition to expand our understanding of the importance of spatial localization for signal transduction. The framework presented here will help experimentalists to organize new findings on receptor dimerization and should provide new avenues for future research.

The objective of this work was to determine how dimerization affects receptor organization and cell signaling. To achieve this objective I have chosen to use mechanistic computer models of receptors reacting and diffusing on the cell membrane. Models are useful for this kind of study because they allow us to isolate a single phenomenon such as dimerization to determine what, if any role it could play in the real system. Modeling results are also general. Thus the findings in this work not only apply to GPCRs but also to other membrane proteins, or even broader classes of systems such as reactants on a catalytic surface. Because these models only account for a small part of the cell's machinery, our results will not predict the cell's behavior exactly. However, models can help to determine what is and is not possible and can suggest experimentally useful and testable trends that may be difficult to uncover using experimental techniques alone.

The modeling results focus on three main areas. First, one to three different receptor species were simulated under all combinations of dimerization rules to determine how the logical rules that govern dimerization can affect the global organization of proteins on the membrane. Second, the degree of cross-talk between receptors was measured as a function of the dimerization rules. Third, the effect of dimerization on receptor internalization was examined. With these results in hand, I next discuss the implications of these findings for cell physiology and drug development. Finally three experimental examples from the literature are provided in the light of our dimerization findings. This work provides experimentally testable hypotheses and valuable rules of thumb for interpreting dimerization interactions.

6.2 Methods

Simulations of receptor reaction and diffusion were run using a Monte Carlo approach. To begin the simulation, receptors were placed at random on a two

dimensional 400 by 400 triangular grid with periodic boundary conditions. In all experiments, 100 of each receptor species was present, allowing the total receptor count to range from 100 receptors for simulations of only one species to 300 when three species were simulated. Each particle had a radius of 5 grid spacings (occupied 91 vertices) corresponding to a diameter of 5 nm approximately the diameter of a GPCR. If two receptor monomers were separated by less than one receptor radius then dimerization was possible. Monomers were allowed to diffuse in a random direction with a probability proportional to the diffusion rate. If the chosen random site was occupied the move was rejected and no further attempts at movement were made. Diffusion of a receptor within a dimer was similar to the monomer case except when the receptor attempted to move away from or overlap with its binding partner. If the receptor attempted to move away from or overlap its partner, the partner would attempt to move in parallel with the receptor. If the new position of both receptors did not overlap with other receptors in the system the move was allowed; otherwise it was rejected and no further moves were tried. All simulations used a normalized diffusion rate of 1, normalized dimerization rate of 46.41, and normalized monomerization rate of 4.64, thereby placing the ensemble of membrane proteins in the gel phase (see chapter 5 for discussion). These normalized rates correspond to physical rates of $D=10^{-10}\text{cm}^2 \text{sec}^{-1}$, $k_{\text{dimer}}=10^6 \text{sec}^{-1}$, and $k_{\text{mono}}=10^7 \text{sec}^{-1}$ which is approximately that of a GPCR (see sample calculation in Chapter 5). An iteration is defined as the time required for each particle to move one particle diameter. Simulations are pre-equilibrated for 40 thousand iterations and then 200 thousand measurements are taken over the next 400k iterations for each experiment. Measurements include counting the number of bonds and calculating average shortest distance between species.

The interaction between multiple species is expressed in the form of a *dimerization rule* and multiple dimerization rules are expressed as a *dimerization network*. Dimerization rules are expressed using a compact notation in which I indicate

that two species can form dimers by dotting them together. Thus the rule $A \nabla B \nabla C$ indicates that the dimers AB and BC can form, but not the dimers AC, AA, BB, or CC nor any trimer species. Multiple rules including interconverting species can be nested into a dimerization network. For example, if A^* is the active state of A then the two dimerization rules $A^* \nabla A^* \nabla B$ and $A \nabla B$ can be expressed in the dimerization network $A^* \nabla A^* \nabla B \nabla A$.

These dimerization rules represent extreme cases in which binding can or cannot occur, while in the real case the binding probability most likely changes with the receptor species. This extreme case is useful for these initial studies because it allows us to cast dimerization rules in general terms. However as more experimental data becomes available these simulations can be modified to include different dimerization probabilities between different species

To describe the ordering of an ensemble, the average shortest radius between each pair of species was calculated. Thus, for three species the average shortest radius was calculated between AA, AB, AC, BA, BB, BC, CA, CB, and CC. The average shortest radius from A to B and from B to A are not equivalent and each provides a unique descriptions of the system. For example, imagine a single B particle surrounded by a sea of A particles. For each A particle, the single B is the closest B, while for B there is only one nearby A that is closest.

Signaling was simulated by counting the number of secondary messengers located adjacent (within one grid spacing) to an active receptor. This model of signaling assumes that active receptors and secondary messengers do not form stable bonds but instead need only to bump into each other to propagate the signal.

Receptor internalization was also modeled by assuming that if a receptor is internalized and it is dimerized, then its dimerization partner will also be internalized. In the simulations, measurements of initial internalization rates were made by choosing at random an active species and targeting it plus its partner for internalization. This

selection process was repeated 1000 times on a variety of ensembles to gather statistics on the average internalization rate for each species. At no time were particles actually removed from the simulation because this would alter the rates of other processes; thus only the initial rate of internalization was recorded.

To ensure that the results presented here are not an artifact of the parameter set, parameter sweeps of k_{dimer} , k_{mono} , D , and particle densities were also run. In each of these cases the qualitative trend did not change, however the magnitude did. Thus changes that tended to push the system farther into the gel regime (increased k_{dimer} and k_{mono} , or reduced D) tended to amplify the effects of receptor organization, while changes that made the system more homogeneous (lower particle density, increased D) attenuated the effects of the dimerization rules.

6.3 Results

Three sets of simulation results are used to demonstrate how dimerization can impact signaling. In the first set, the interactions between one, two, and three distinct particle species are simulated under different dimerization rules to gather experimentally accessible statistics describing the ensemble. In the second set, the interactions between two receptor species and a common secondary messenger are simulated under different interaction rules to determine how dimerization influences cross—talk. In the third set, hetero— and homodimerization is shown to integrate signals via receptor internalization.

6.3.1 Dimerization rules affect global organization

Although a local reaction, dimerization can also influence global membrane protein organization particularly when many protein species are present. To demonstrate this organization, we simulated the interaction of one, two, and three generic particle species under different dimerization rules. Qualitative aspects of the particle organization

are shown by comparing single frames from an equilibrated ensemble. Average quantitative measures of particle organization are also made to reveal less apparent changes in organization in response to different dimerization rules. These simulations show that an intermediate level of organization involving between 3 and 8 receptors is measurable and has global effects.

Changes in dimerization rules can cause a qualitative change in particle organization as shown in Figure 6.1. In each panel a different dimerization rule is applied for two or three species. These images represent what would be observed experimentally if each receptor could be tagged and colored according to its identity. In

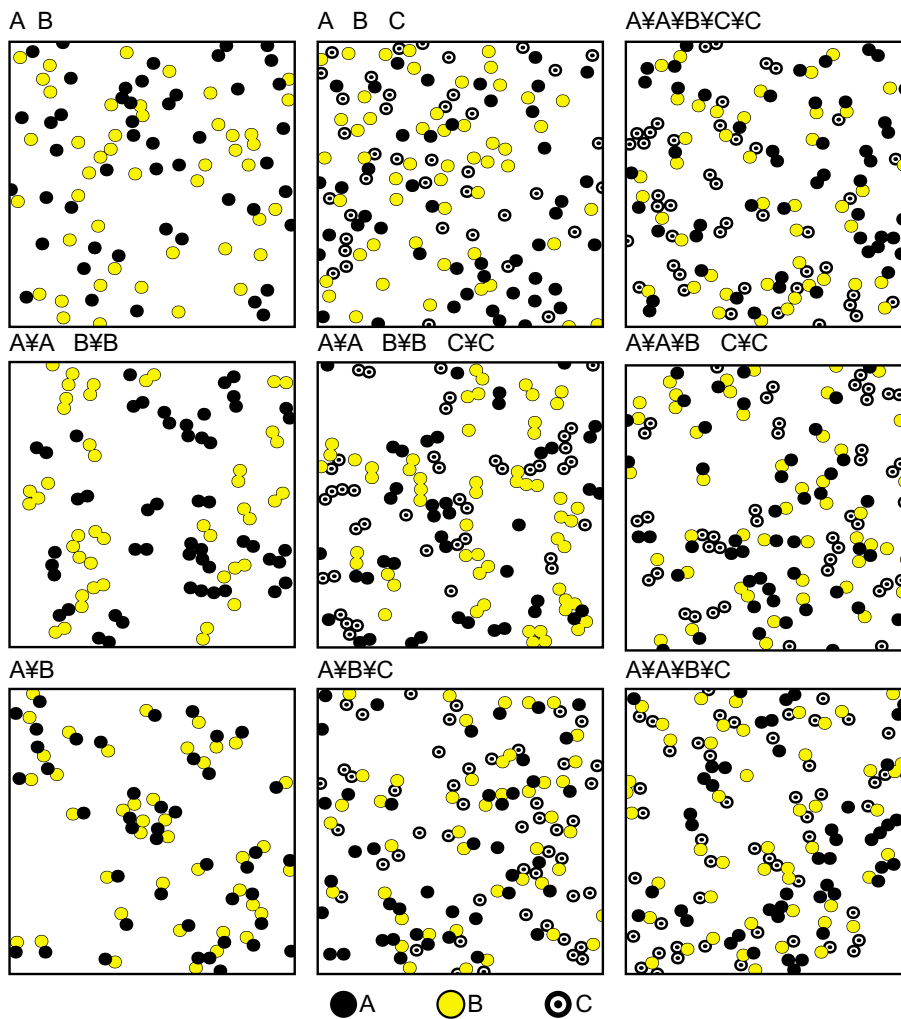


Figure 6.1 Representative receptor organizations under different dimerization rules.

some cases, the effect of a dimerization rule on organization is immediately apparent. For example, compare the case of two non-reactive species (A B) with two homodimerizing species (A•A B•B). The non-reactive species are evenly mixed and exhibit no apparent clumping or organization. In contrast, the two homodimerizing species show marked clustering, self-segregating themselves into distinct homogeneous islands. In other cases, however, the change in organization is less apparent. For example, the dimerization rules A•A•B•C•C and A•A•B C•C lead to structures that are superficially similar, although closer inspection will reveal that A and B are more isolated from C under the latter rules.

To quantify particle organization, the average shortest distance between particle species was measured (Table 6.1). Average shortest distance was chosen because it not only indicates the degree of clustering, but also the identity of particles involved in the cluster. By presenting an average value over many readings I overcome random error associated with looking at a single image. The results are color coded by relative separation distance to make broad patterns more discernable; thus a change in color pattern indicates a change in organization. Note that in some cases the addition of a single bond can significantly alter the organization. For example, compare the rules A•A•B•C•C and A•A•B C•C (interactions 15 and 19 in Table 6.1). As previously noted, these two dimerization rules yield similar qualitative results (see Figure 6.1) although quantitatively the two pictures are easily discernable. Therefore the quantitative data provides a higher degree of resolution to describe the equilibrium organization of the ensemble.

The results presented here are cross-comparable and interconvertible. Although the simulations are run with between one and three species, the density of each species present does not change from simulation to simulation. Therefore, results obtained for the interactions of a single species can be meaningfully cross-compared to results with more species. For example the average shortest radius between A particles does not

change between the ensembles A, A B, and A B C because in all cases the density of A particles remains the same although the total density triples when three species are present. Note also that only a fraction of the possible interactions have been simulated, but more can be generated by interconversion. For example, the interaction $A \bullet A \bullet B \bullet C$ can be interconverted to $A \bullet B \bullet C \bullet C$ by swapping A and C. Using this procedure, the subset of interactions presented in Table 6.1 can generate every unique set of rules for three or fewer particles.

Experimental measurements of dimerization can be interpreted using the average shortest radius data in Table 6.1. Techniques such as fluorescence energy transfer (FRET) essentially measure the average shortest radius between tagged species and are already in use for identifying receptor—receptor dimerization (Angers et al. 2000; Cornea et al. 2001). If the separation distance between multiple membrane bound proteins are measured, then the pattern of radii can be directly compared to the data in Table 1 to predict a dimerization rule. This rule in turn can be used to make predictions about other properties of the system such as internalization rate and signal cross—talk, as described below. Because the minimum separation distance is also affected by particle density, stoichiometry, dimerization rate, and monomerization rate (see Chapter 5) the values reported in Table 6.1 are only quantitatively accurate for one particular system; however the pattern of each dimerization rule is unique, independent of the system parameters. Including information about a particular experimental system into the model will allow the simulation predictions and experimental data to be compared directly.

Interaction	average shortest radius between particles (nm)								
	AA	AB	AC	BA	BB	BC	CA	CB	CC
1) A	11								
2) A•A	5								
3) A B	11	11		11	11				
4) A•B	11	5		5	11				
5) A•A B	5	11		13	11				
6) A•A B•B	6	23		23	6				
7) A•A•B	11	6		6	11				
8) A•A•B•B	8	8		8	8				
9) A B C	11	11	11	11	11	11	11	11	11
10) A•A B•B C•C	5	14	14	14	5	14	13	14	5
11) A•A B•B C	5	14	11	14	5	11	13	13	11
12) A•B•C	11	7	11	8	12	8	11	7	11
13) A•A•B C	10	6	11	6	11	11	11	11	11
14) A•A•B•C	7	10	11	11	11	6	12	6	11
18) A•B•B•C	11	7	11	8	11	8	11	7	11
16) A•A•B•B•C•C	8	9	13	10	10	9	13	9	8
17) A•A•B•B•C	7	10	11	11	11	7	13	6	11
15) A•A•B•C•C	8	8	12	8	11	9	12	8	8
19) A•A•B C•C	10	6	13	6	11	13	12	11	5
20) A•B C	11	5	11	5	11	11	11	11	11
21) A•B C•C	11	5	14	5	11	14	11	12	5
23) B•A•C•B	11	8	8	8	11	8	8	8	11
24) B•A•A•C•C•B	10	9	9	9	11	7	9	7	11
25) B•A•A•C•C•B	10	8	10	8	11	8	10	8	10
26) B•B•A•C•B•B	11	9	7	9	10	9	7	9	11
27) B•B•A•A•C•B•B	10	10	8	10	10	8	8	8	11
22) all to all	9	9	9	9	9	9	9	9	9

Far (>12)
Intermediate
Close (<10)

Table 6.1 Average shortest separation radius between particle types for all combinations of 1 through three particle species.

6.3.2 Dimerization as a route to control cross—talk

One form of signal cross—talk takes place when multiple receptor species use a common second messenger. Because signals are propagated by the encounter between a receptor and second messenger, I propose that cross—talk among multiple receptor species

will depend on the spatial organization of membrane proteins and as such should be sensitive to changes in dimerization rules. This form of cross-talk has been demonstrated experimentally with the somatostatin and dopamine receptors (Rocheville et al. 2000) and is likely to play a role in other receptor systems. To explore how this cross-talk takes place I simulated the interaction between two receptors (R_1 and R_2) and a common second messenger (S) under a variety of dimerization rules. The activity contribution of each receptor species was measured as the fraction of secondary messenger adjacent to that species. Thus secondary messengers adjacent to R_1 were counted as signals from R_1 and secondary messengers near R_2 as signals from R_2 . Note that with this scheme it is possible for both R_1 and R_2 to claim a secondary messenger if all three species were closely localized. This model of secondary messenger activation would closely approximate the initial rate of secondary messenger activation.

The simulation results show that changing the dimerization rule affects both the total signal and the relative contribution of each receptor type (Figure 6.2). The total signal varied by as much as 30% depending on the specific dimerization rule. The relative contribution of R_1 and R_2 to the total signal ranged from 1:1 for the $R_1 R_2 S$ rule to approximately 3:2 for the $R_1 R_2 \nabla R_2 S$ rule.

Changes in dimerization rules affect cross-talk primarily because of clustering and competition effects. This pattern is most easily uncovered by examining pairs of rules that differ by only one bond. For example, the rules $R_1 R_2 S$ and $R_1 \nabla R_2 S$ differ only by one $R_2 R_1$ bond, however the $R_1 \nabla R_2 S$ rule gives a significantly smaller total signal. Under the $R_1 \nabla R_2 S$ rule, receptors can form heterodimers and as such will tend to cluster into islands that exclude S, thereby decreasing the total signal. Note that this finding assumes that receptors and G-proteins can not occupy the same x,y position on the membrane.

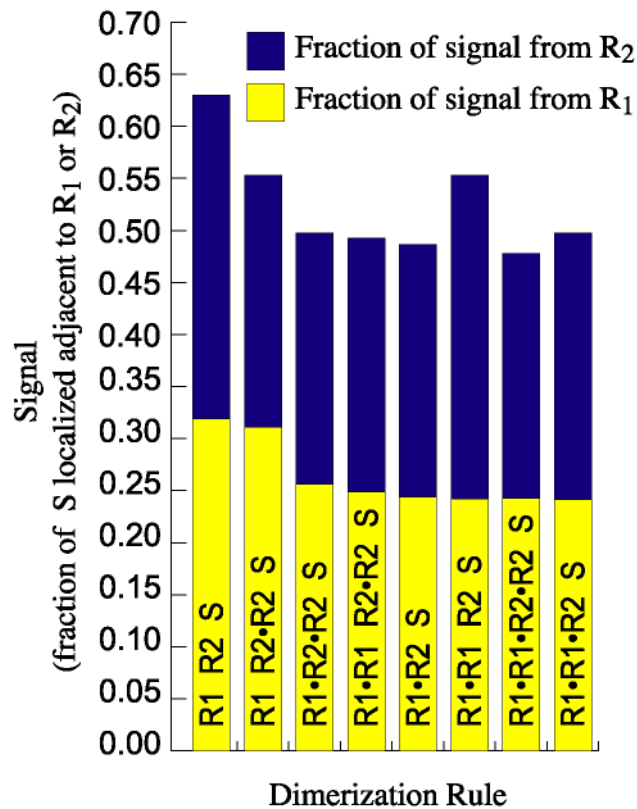


Figure 6.2 The effect of changing dimerization rules on the signaling capability of each receptor type.

6.3.3 Receptor number co—regulation via dimerization

Receptor number and dimerization rules can change in response to ligand stimulation. To link these two processes I propose that if a receptor within a dimer is active and therefore targeted for internalization, then its binding partner will also be targeted for internalization. This connection has been experimentally demonstrated with heterodimers of β_2 —adrenergic receptors and δ —opioid receptors (Jordan et al. 2001). This assumption is not dependent on the dimerization rate because in all cases dimerization alone will tend to co—localize proteins and as such cause both to be

trafficked together. Using this information I have simulated the interaction between an active receptor species (R_1) and an inactive receptor species (R_2) to find the initial rate of internalization for both species under various dimerization rules.

The internalization rates of both the active and inactive species change in response to different dimerization rules (Figure 6.3). Because R_1^* is the only active species, only monomeric R_1^* and the dimers $R_1^*R_1^*$ and $R_1^*R_2$ can be internalized. Therefore, any dimerization rule that favors the formation of the $R_1^*R_2$ dimer causes more R_2 to be co—internalized. Similarly, because only one R^* is targeted for internalization at a time, rules that favor the formation of the dimer $R_1^*R_1^*$ accelerate the internalization of R_1^* by the same co—internalization mechanism.

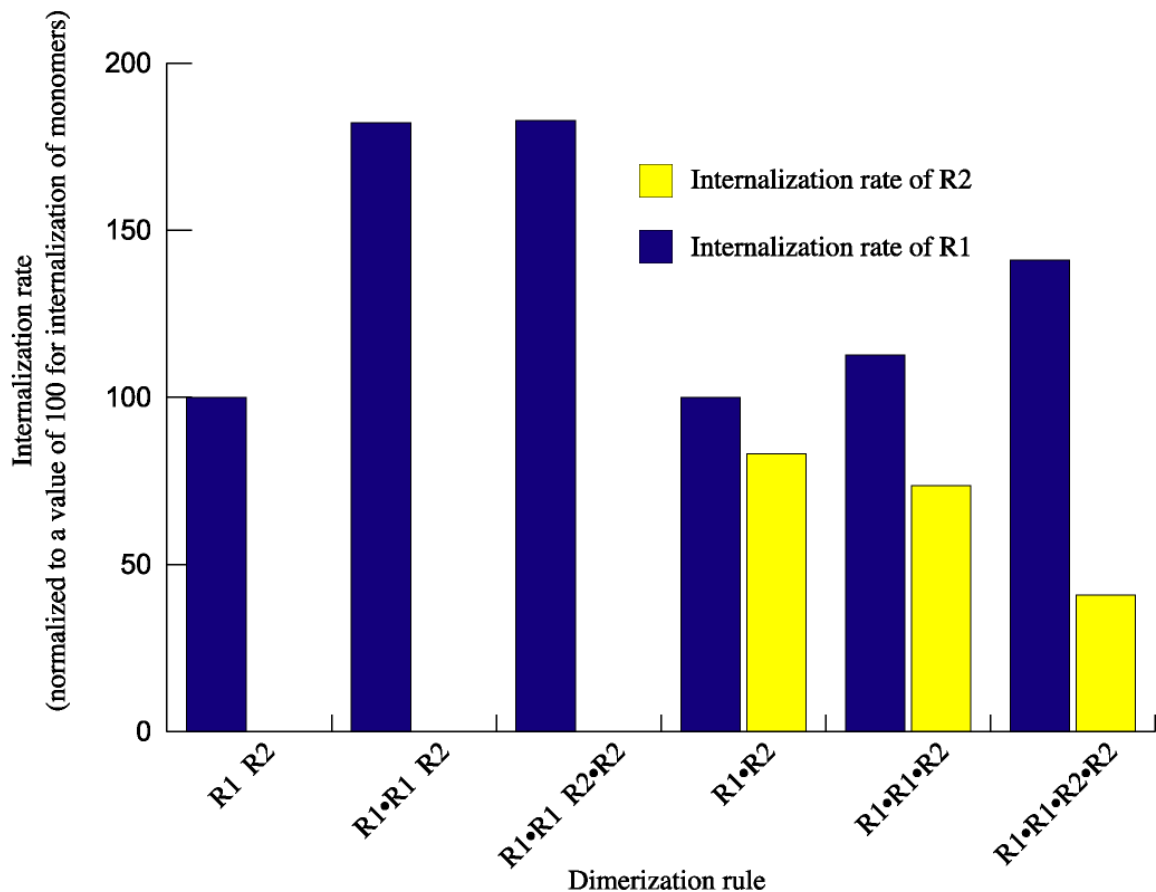


Figure 6.3 Internalization rates of two receptor species under different dimerization rules. For these internalization studies, it is assumed that the receptor R_1 is active and R_2 inactive..

6.4 Discussion

The simulation results demonstrate that dimerization has system wide effects and cannot be examined solely at the one or two protein level. Therefore this work presents a new viewpoint to examine the collective behavioral changes induced by dimerization.

The effects of changing dimerization rules are complicated and can be difficult to predict *a priori*. For example, moving from the rule $A\text{---}B\text{---}C$ to $A\text{---}B^{\circ}\text{---}C$ (see Table 6.1 and Figure 6.1) involves forbidding a bond between C and B. As expected this move increases the average shortest distance between C and B, but it also changes the distances between nearly every other species too. The reason that the whole system changes is that the addition or removal of a single dimer combination adjusts the number of available binding partners to a species, which in turn affects its local environment. This change in local environment then causes a global organizational change to emerge.

Other methods of receptor organization that involve receptor attachment to the cytoskeleton or trafficking via lipid rafts are also possible but are less complete than the dimerization mechanism proposed here. Receptor attachment to the cytoskeleton is a plausible way to localize receptors, but it is saturable and requires that the distinct parts of the cytoskeleton are themselves spatially segregated. Therefore small changes in the expression level of either cytoskeletal proteins or receptors could cause the system to become disordered. Lipid rafts have the disadvantage that they too are saturable. Furthermore rafts are also fairly nonspecific and slow to reorganize in response to a signaling event. In contrast, dimerization based methods of receptor organization are not strongly affected by changes in receptor expression level, can quickly reorganize in response to small changes in receptor conformation, and are very specific to a near infinite palette of protein—protein binding surfaces. Therefore dimerization acts by decentralizing control of the receptor organization. In doing so, dimerization makes the signaling system both more responsive and more stable.

In the following sections I demonstrate that changes in dimerization rules can have physiological implications and that these changes are observable in experimental systems. The simulation results are used to show that dimerization can result in emergent behaviors that could not be detected by studying a single protein or single dimer. This emergent behavior has direct applications to drug development and in particular provides a novel pharmacological route to modulate receptor internalization. Finally these emergent properties are discussed in light of three experimental receptor systems. In total, this work provides experimentally testable hypotheses and valuable rules of thumb for interpreting dimerization interactions.

6.4.1 Dimerization networks exhibit physiologically relevant emergent properties

Regulation and integration of a signal transduction pathway is generally thought to involve a number of levels of cellular control; however, the simulations used in this work indicate that at least some of these processes can be controlled at the receptor level using dimerization alone. Two processes of interest are the regulation of receptor number via internalization and integration of signals from multiple active receptors. By including dimerization in these processes I have found emergent properties that have physiological relevance. In this section, each of these properties will be explored separately and then brought together to show how a dimerization network alone can be used to infer regulatory behavior.

Dimerization provides a novel route to modulate the receptor internalization rate. Common wisdom says that ligand binding to a receptor only affects the internalization rate of that single receptor; however, in experimental systems such as the β_2 AR and V_2 receptor systems it appears that the internalization rates of multiple receptor species are linked (Klein et al. 2001). The simulation results demonstrate that dimerization can cause ligand induced receptor internalization to be non—reciprocal in much the same way

as the experimental system. Non—reciprocal internalization means that a ligand to R_1 may induce R_1 and R_2 to internalize, but a ligand to R_2 may only cause R_2 to internalize. An explanation for this asymmetry is that the dimerization rules for receptor can change in response to ligand binding. For example, let R_1^* and R_2^* denote active, ligand bound receptors, and R_1 and R_2 denote inactive receptors. If only the ligand for R_1 is present then a dimerization rule such as $R_2 \rightleftharpoons R_1^* \rightleftharpoons R_1^*$ may apply, whereas if only the ligand for R_2 is present then the dimerization rule may change to $R_1 \rightleftharpoons R_2^*$. In the first case, activation of R_1 would cause both R_1 and R_2 to internalize because the $R_2R_1^*$ dimer would pull in R_2 via a co—internalization mechanism. In contrast, only R_2 would be internalized in the second case (see Figure 6.3). The result is that ligand binding causes asymmetric internalization.

Two other cases are possible when ligands to both R_1 and R_2 are present or no ligand is present, revealing a more general four species dimerization network. One dimerization network that is consistent with the example above is $R_1 \rightleftharpoons R_2 \rightleftharpoons R_1^* \rightleftharpoons R_2^*$. When only the ligand to R_1 is present then all R_1 is converted to R_1^* , returning the dimerization rule $R_2 \rightleftharpoons R_1^* \rightleftharpoons R_1^*$. When only the ligand to R_2 is present, we recover the rule $R_1 \rightleftharpoons R_2^*$. Note that the dimerization network must be internally consistent. Therefore the network $R_1 \rightleftharpoons R_1^* \rightleftharpoons R_2 \rightleftharpoons R_1^* \rightleftharpoons R_2^*$ is not valid because the dimerization rule when only R_2 is active is $R_1 \rightleftharpoons R_2^*$, implying that inactive R_1 cannot form homodimers.

Physiologically, non—reciprocal internalization produces a unique form of signal transduction cross regulation. In one case, receptor activation down regulates and hence desensitizes only one signaling pathway as is normally expected. However, if a receptor can form heterodimers then non—reciprocal internalization is possible, implying that a second, seemingly unrelated pathway could also be down regulated. This kind of cross regulation of receptor expression could be used in development, for example, where activation of one receptor may cause a short term response, while activation of a different

receptor may cause a global change in phenotype that modulates the response of many signaling systems.

Nonlinear receptor cross—talk can also emerge when dimerization is included. Nonlinear receptor cross—talk implies that the signal produced when two receptor species are active does not equal the sum of the signals produced if each receptor is active alone. The particular behavior that two receptors will exhibit depends on the dimerization network. This is shown for one particular case in Figure 6.4. Cases I and III illustrate linear cases while cases II and IV illustrate nonlinear cases. Using experimental methods alone, understanding this nonlinear cross—talk could be difficult to explain because the two receptors are only related via a common secondary messenger. For example, if the effect of activating R_2 were under study, then the activity of R_1 could play a large or small role depending on the dimerization network. Under the network in Case II, the coactivity of R_1 would play a large role, increasing the observed signal by approximately 150% if R_1 were active.

Knowing the dimerization network of a set of receptors is sufficient to derive useful information about receptor internalization and cross—talk. Take for example the dimerization network and its associated rules shown in Figure 6.5(a). The individual dimerization rules for this network could have been derived from protein—protein binding assays or from the literature for many receptor species. Even if only some of the dimerization rules were available, partial information could be used to define a subset of possible dimerization networks, while if all of the rules were immediately available then a single dimerization network could be derived. Because each dimerization rule exhibits a characteristic organization as shown in Table 6.1, it may also be possible to determine the dimerization rule directly from a multi—signal FRET type assay too. Using the dimerization network, the relative signals of each receptor type can be predicted using the

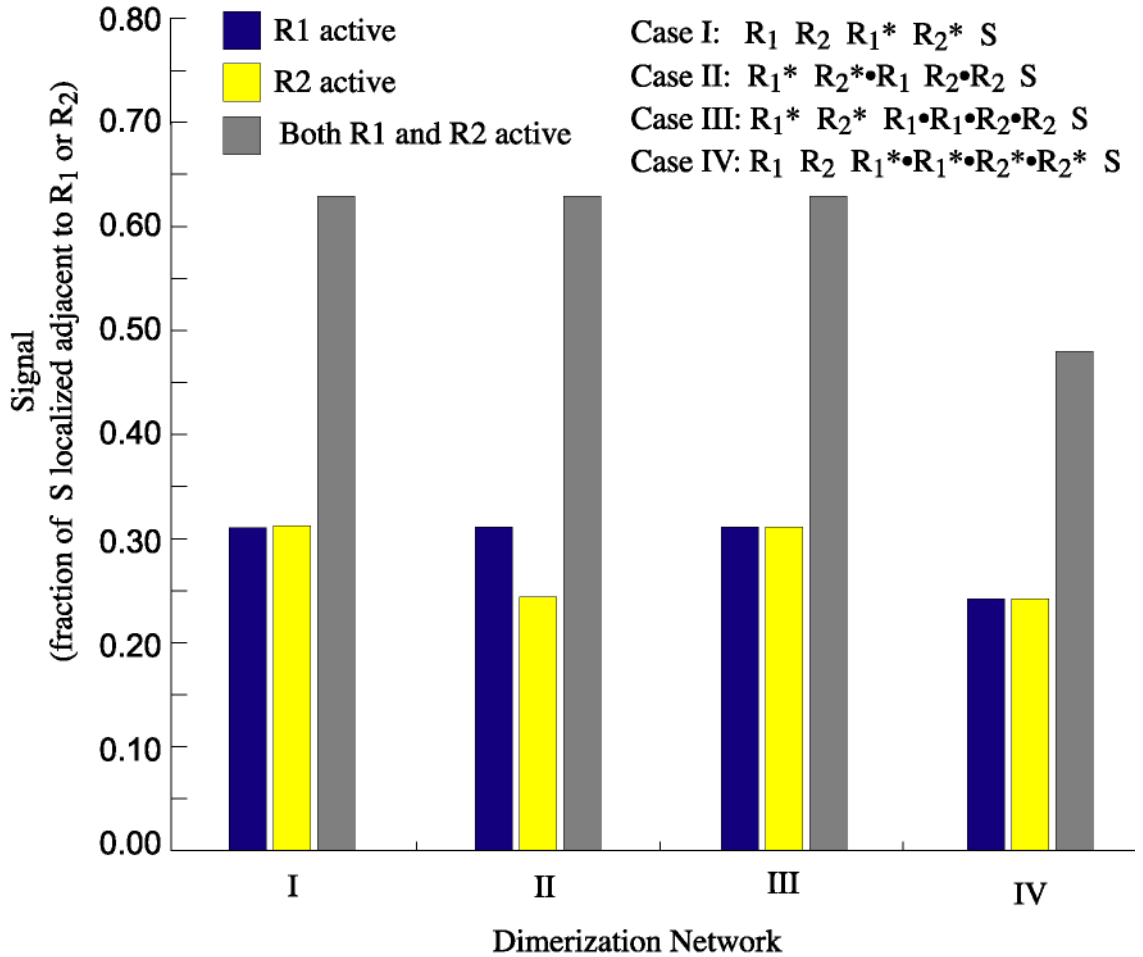


Figure 6.4 Drug induced signals under different dimerization networks when two receptors share a common secondary messenger. Here R1 and R2 are receptors and S is the secondary messenger.

data in Figure 6.2. The dimerization network in Figure 6.5(a) is predicted to generate the mixed positive/inverse agonist behavior described in Figure 6.5(b). Changes in internalization rates in response to receptor activation can also be predicted using the data in Figure 6.5c. In some cases the internalization will exhibit no cross regulation, while in others, receptors may co—internalize in complicated ways. For example, in Figure 6.5(c) the internalization rates of R_1 and R_2 change depending on the activation state of each receptor. Because the models used in this work assume full activation of a receptor species, the changes in internalization rate are solely due to the dimerization rules. Therefore in some cases the dimerization rules may not only convey information that

would be difficult to obtain from experimental measurements alone, it may also be the *only* way to explain certain findings.

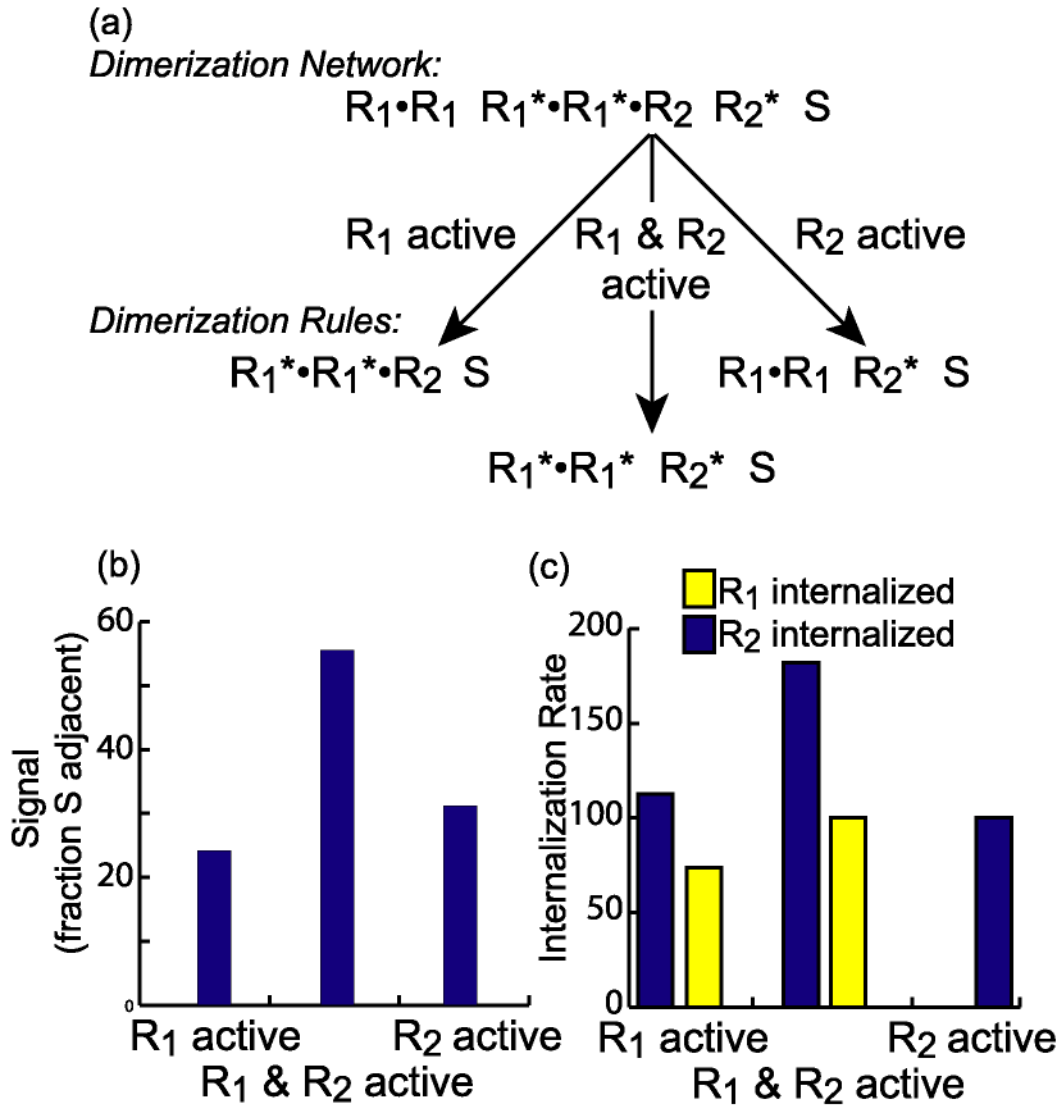


Figure 6.5 Example of how dimerization can be used to infer properties of a signaling system. (a) Deriving dimerization rules from a dimerization network. (b) signal for each dimerization rule (c) internalization rate for each dimerization rule.

6.4.2 Dimerization as a tool for drug development

Receptors change dimerization state in response to drug binding. Therefore, drug designers may be able to harness dimerization as a tool to control the cell's response to a

drug. The simulation results have shown that the dimerization state of a receptor should affect signaling and internalization, both of which strongly influence the cells eventual response. By creating drugs that induce receptor heterodimerization with specific partners or homodimerization, drug designers could tailor drugs to have unique properties that are not currently accessible.

In this work, for simplicity I have assumed that a drug causes all of a single receptor species to become 100% active. Therefore all of the observed changes in signaling and internalization are due to changes in localization *alone*. This point is important because it shows that drug induced changes in dimerization rules can have significant effects at the physiological level. For example, consider the dimerization networks shown in Figure 6.4. When only one receptor species is active, the maximum possible signal for the system varies considerably depending on the drug induced dimerization rule. This effect is likely magnified by further amplification steps downstream of the secondary messenger, meaning that the dimerization network selected by a drug could be sufficient to decide if a drug does or does not signal.

The internalization rates of many receptor species may also be affected by the drug acting on a single receptor. For example consider the dimerization rules in Figure 6.3. Moving from the rule $R_1 \rightleftharpoons R_1 \rightleftharpoons R_2$ to $R_1 \rightleftharpoons R_1 \rightleftharpoons R_2$ involves changing the conformation of R_1 such that it forms both homo— and heterodimers. As a result of this change, the internalization rate of R_1 nearly halves and the internalization rate of R_2 substantially increases. In some cases this co—internalization of different receptor species could manifest itself as an undesirable side effect of the drug a property that could be removed by changing the drug such that it did not allow heterodimers to form.

Alternatively the slower internalization rate could also be useful in some applications. Receptor internalization is a primary mechanism for long-term desensitization to a drug (Tsao and von Zastrow 2000). Therefore reducing the rate of receptor internalization may also extend the useful life of the drug in the body before desensitization takes over.

Controlling drug-induced dimerization may also provide a novel method for controlling receptor expression levels. Inverse agonists and some antagonists have been implicated in increasing the expression levels of receptors on the cell surface. For example, a common postoperative treatment for heart failure involves a regimen of beta-blockers which antagonize the β_2 -adrenergic receptor (β_2 AR). Unfortunately, after extended beta-blocker treatment, removal of the drug causes hypersensitivity to endogenous β_2 AR agonists such as adrenaline due to an increased expression rate of β_2 AR receptors, putting the patient at risk once more (Strauer 1990). If the goal were to develop a drug to safely return the patient to a normal β_2 AR expression level, then the ability of the drug to induce dimerization could play an important role. Ideally, one would like the receptor number to drop quickly but without stimulating a response from the receptor. As demonstrated in Figure 6.2, ligands that induce homodimerization of their target should cause a smaller response. Therefore a drug that caused β_2 AR to dimerize would be preferred. Similarly, drugs that induce homodimerization also cause more internalization (Figure 6.3). Therefore homodimerization is once again preferred. A completely different approach of activating a receptor that heterodimerizes with the β_2 AR such as the δ - or κ -opioid receptor (Jordan et al. 2001) could also reduce β_2 AR expression without any activation at all. This approach may cause other problems due to

activation of the opioid receptor, but these may be less dangerous than the presenting problem.

Receptor dimerization may provide a novel pharmacological handle to control drug activity. To efficiently screen for drugs that cause a desirable dimerization network, high throughput FRET assays could be used in much the same way as other fluorescence based drug screens that are currently in use.

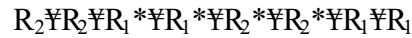
6.4.3 Biological systems affected by receptor organization

The effects of dimerization predicted by our simulations have been observed in a number of experimental systems. Here three examples are provided that demonstrate different aspects of how dimerization might influence cellular response. In each case the base model described in this work is compared to available experimental findings. Because the base model only roughly approximates the receptor—receptor stoichiometries and receptor dimerization kinetics, it is not reasonable to expect an exact agreement between experimental and modeling results. That said, the agreement between experiment and model results is surprising, indicating that dimerization most likely works both *in silico* and *in vivo*.

6.4.3.1 Localization and Signal Regulation of Dopamine and Somatostatin Receptors

Rocheville *et al.* demonstrated that the dopamine D₂ receptor and the somatostatin receptor SSTR1 form functionally interacting heterodimers (Rocheville *et al.* 2000). Both receptors belong to the GPCR family and both share a common G—protein, G_i, implying that they might exhibit receptor level cross—talk. Previous experimental work has shown that the dopamine and somatostatin receptors form homodimers (Rocheville *et al.* 2000; Armstrong and Strange 2001). Rocheville *et al.* use FRET to show that the two

receptors form heterodimers when at least one receptor species is active. These experimental findings suggest the following dimerization network



where $R_1 = \text{SSTR1}$ and $R_2 = \text{D}_2$. Using this network, dimerization rules can be derived for any receptor activation case. Each rule in turn can be used to predict the separation distance, signaling level, and internalization rate of each receptor species.

The separation distance between dissimilar receptor species is predicted for each rule using the data in Table 6.1 and found to compare favorably to the experimentally observed FRET efficiency as shown in Table 6.2. As predicted by the model, when at least one receptor species is active the FRET efficiency drops indicating a shorter separation distance. Although the model captures the general experimentally observed trend, it does not predict a measurable difference between having one or both receptors active. The reason for this discrepancy could be experimental, but is more likely because the model assumes that all receptor—receptor dimers bond with equal strength. If FRET data were also available for homodimers, this discrepancy could be examined quantitatively. However, using the available FRET data in combination with the simulation results leads us to predict that the strength of dimer bonds goes as $R_1 R_2$ heterodimers $>$ R_1 homodimers $>$ R_2 homodimers. This series would explain why any receptor activation that allows heterodimers to form causes a large change in FRET signal (separation distance). The series also predicts that active R_1 competes with R_2 more effectively for R_2 bonds than active R_2 competes with R_1 for R_1 bonds, producing the observed change in FRET efficiency.

Condition	Rule	Mean separation distance (nm)	FRET efficiency
R ₁ & R ₂ inactive	R ₁ ∅R ₁ R ₂ ∅R ₂	23	2 – 2%
R ₁ active	R ₁ *∅R ₁ *∅R ₂ ∅R ₂	8	18 – 2%
R ₂ active	R ₁ ∅R ₁ ∅R ₂ *∅R ₂ *	8	16 – 2%
R ₁ and R ₂ active	R ₁ *∅R ₁ *∅R ₂ *∅R ₂ *	8	20 – 2%

Table 6.2 Separation distance from simulations compared to FRET efficiency. Separation distance data taken from Table 6.1. FRET data taken from (Rocheville et al. 2000).

When bond strengths between dimer species are not equal, the modeling results can still provide insight. For example, a strong R₁R₂ heterodimer and a less strong R₂ homodimer may give a rule that is an equal mix between R₁∅R₂∅R₂ and R₁∅R₂°R₂ resulting in a mean separation distance part way between 6 and 12 nm (see Table 6.2), or 9 nm. This separation distance is slightly larger than the dual homodimer case in Table 6.2 and could account for the small drop in FRET efficiency that is observed experimentally.

Model predictions and experimental data for receptor signaling also show a similar trend as shown in Table 6.3. Because both receptors use a common second messenger, the cross—talk data in Figure 6.2 was used to predict signal strength. The model underpredicts the signal when only one receptor is active. This is most likely because the model only measures the initial rate of secondary messenger activation, while in a real system one would measure the signal over a finite time. However, the model predicts the overall trend of the experimental result, lending support to the models applicability to real biological systems.

Similar to the separation distance results presented above, activation of either R₁ or R₂ gives an identical signal in the model, but gives a different signal experimentally. If we allow the homodimer and heterodimer bond strengths to differ, then the same bond strength series presented for the separation distance data (R₁R₂ heterodimers > R₁ homodimers > R₂ homodimers) best fits the experimental signaling data too. In general, second messenger activation is favored by fewer receptor—receptor bonds and more

Condition	Rule	Second messenger activation	Observed signal
R_1 & R_2 inactive	$R_1 \nrightarrow R_1 \quad R_2 \nrightarrow R_2 \quad S$	0%	0%
R_1 active	$R_1 * \nrightarrow R_1 * \nrightarrow R_2 \nrightarrow R_2 \quad S$	24%	36 – 3%
R_2 active	$R_1 \nrightarrow R_1 \nrightarrow R_2 * \nrightarrow R_2 * \quad S$	24%	39 – 3%
R_1 and R_2 active	$R_1 * \nrightarrow R_1 * \nrightarrow R_2 * \nrightarrow R_2 * \quad S$	48%	52 – 4%

Table 6.3: Predicted activation level of secondary messenger as compared to an experimentally observed signal increase. Second messenger activation taken from Figure 6.2. Observed signal increase taken from (Rocheville et al. 2000).

active receptors. Thus activating either R_1 or R_2 will produce equal numbers of active receptors, but active R_2 receptors will be more accessible than the active R_1 receptors because R_2 has a weaker homodimer bond than R_1 . Therefore activation of R_1 alone should cause a smaller signal than activation of R_2 .

Although the internalization rate of each receptor species was not experimentally measured, internalization can be predicted from the dimerization network alone as is shown in Table 6.4. Because of the structure of the dimerization network, one would expect that both receptor species would be internalized when only one species was active, but the active species would be internalized more rapidly than the inactive species. If bond strengths are assumed to be unequal then the trend of internalization rates will be slightly shifted from the results in Table 6.4. Using the bond strength series consistent with activation and separation distance data (R_1R_2 heterodimers $>$ R_1 homodimers $>$ R_2 homodimers) the R_1 internalization rate may be higher when R_1 alone is active and when both receptors are active. When R_2 alone is active, the R_1 internalization rate is expected to be lower and the internalization rate of R_2 higher. The reason for these shifts is that the internalization rate of a receptor depends in part on its probability of being bound to a receptor that is about to be internalized. Thus, if the R_1 homodimer bond is stronger than the R_2 homodimer bond, then active R_1 is more likely to co—internalize another R_1 than an R_2 . These results demonstrate how a dimerization network can be used to infer behaviors about a signaling system when experimental data is not available. Presumably,

more accurate stoichiometry and receptor—receptor binding data could be used in the model to allow more precise predictions.

Condition	Rule	Internalization rate of R ₁	Internalization rate of R ₂
R ₁ & R ₂ inactive	R ₁ ↔R ₁ R ₂ ↔R ₂	0	0
R ₁ active	R ₁ *↔R ₁ *↔R ₂ ↔R ₂	140	40
R ₂ active	R ₁ ↔R ₁ ↔R ₂ *↔R ₂ *	40	140
R ₁ and R ₂ active	R ₁ *↔R ₁ *↔R ₂ *↔R ₂ *	180	180

Table 6.4 Predicted internalization rates of each receptor species under different receptor activation conditions. Note that the internalization rates are normalized to a value of 100 for an active non—dimerizing receptor species.

6.4.3.2 Dimerization Limited Cross—Talk among α_b —Adrenergic, M Muscarinic, and δ —Opioid Receptors

The α_{2b} —adrenergic, m muscarinic, and δ —opioid receptors all share a common secondary messenger, G_i, and yet exhibit no cross—talk among pools of this secondary messenger (Graeser and Neubig 1993). Therefore, activation of one receptor species depletes the second messenger pool for only that species and does not strongly affect the signaling capability of the other two species. One explanation for this finding may be that these three receptor species are localized to spatially distinct regions on the membrane. Such localization may be due to any one of a number of mechanisms; here I explore the possibility that dimerization is the cause.

Because dimerization can affect receptor localization as shown in Figure 6.1 and Table 6.1, I hypothesized that dimerization could be responsible for the lack of cross—talk between these three species. Experimental work indicates that the α_{2b} and δ —opioid receptors form homodimers (Venter et al. 1983; Venter et al. 1984; Wade et al. 1994; George et al. 2000) (Cvejic and Devi 1997). Within the muscarinic receptor family, the m3 and m2 receptor subtypes have been shown to form homodimers (Zeng and Wess 1999) (Maggio et al. 1999), suggesting that the m4 may also form homodimers although

this has not been experimentally confirmed. Ligand activation of the δ -opioid receptor causes a small shift toward monomers (Cvejic and Devi 1997), while the effects of receptor activation on the other two receptors has not been determined. Finally, no heterodimers between these three receptor species have been reported. This list of interactions suggests the dimerization network



Therefore, depending on the activity levels of the receptors, one of the general dimerization rules $A \rightleftharpoons B \rightleftharpoons C$ or $A \rightleftharpoons B \rightleftharpoons C$ apply.

Using either dimerization rule, our simulations indicate that dimerization alone could be responsible for the compartmentalization of receptors and the resulting lack of cross-talk among G-protein pools. Figure 6.1(e) qualitatively shows that the dimerization rule involving only homodimerization will cause the receptor species to self-segregate into homogeneous islands. Table 6.1 confirms this observation and also shows that both dimerization rules isolate each receptor species more effectively than any other rules involving dimerization of three species. This self-segregation of receptors could be confirmed experimentally using a FRET assay. The dimerization rule could also be tested indirectly by comparing the predicted receptor internalization rates and signaling levels for the rule to experimental findings.

6.4.3.3 Co-Regulation of κ -, δ -, and μ -Opioid Receptors via Dimerization

The three opioid receptor subtypes, κ , δ , and μ , have been shown to form a complex network of homo- and heterodimers, but why? Presumably if this interaction were unnecessary then it along with many other dimerization networks in the cell would be selected out, but instead it persists. Using the framework presented in this work, the dimerization rule for the opioid receptors can be derived from already known interactions among receptor species. The κ -, δ -, and μ -opioid receptors have been shown to form

homodimers (Cvejic and Devi 1997; Jordan and Devi 1999; George et al. 2000); the κ — and δ —opioid receptors form heterodimers (Jordan and Devi 1999); and the μ — and δ —opioid receptors also form heterodimers (George et al. 2000; Gomes et al. 2000)

Together these observations suggest the following dimerization rule:

$\kappa\kappa\delta\delta\mu\mu$

The resulting organization of this dimerization rule is described by the average minimum separation distance data for the rule $A\forall A\forall B\forall B\forall C\forall C$ in Table 6.1 and could be confirmed experimentally using an assay such as FRET.

One reason for this complicated dimerization rule may be to allow dynamic co—regulation of receptor expression levels. Assuming receptor activation does not significantly change the dimerization rule, the simulations predict that activation of the δ —opioid receptor should cause internalization of all three subtypes, while activation of the κ —opioid receptor should internalize only the κ — and δ —opioid receptors. By linking the expression level of multiple receptors, the cell can dynamically adjust its sensitivity to a variety of stimuli simultaneously. This result is experimentally testable by tracking receptor expression after prolonged treatment with agonists specific to each receptor species.

6.5 Conclusion

This work demonstrates that dimerization can play a critical function in regulating information within the cell and may have important implications for drug discovery. Future experimental work is needed to determine which receptors form hetero— and homodimers and under what conditions. These data will contribute to a more complete vision of how proteins within the membrane are dynamically localized which in turn will describe how signaling is regulated by the cell.

Although the dimerization networks studied in this work contain a maximum of three species, the simulations developed here can easily be extended to accommodate more species to model more physiologically complete systems. Linking together currently known receptor—receptor homo— and heterodimer combinations (Gomes et al. 2001), dimerization networks involving at least different GPCR species and a variety of different G—proteins can be derived. If all interactions were accounted for, then most likely the dimerization network would be even larger. The interconnectedness of these systems implies that spatial localization does have a significant biological role and as such must be considered when discussing cellular communication.

CHAPTER VII

UNTANGLING LIGAND INDUCED RECEPTOR ACTIVATION AND DESENSITIZATION

7.1 Introduction

How do drug properties influence desensitization? Drug development often focuses on optimizing potency and activity, while desensitization is seen as a side effect. Using computer simulations I have explored how drug specific properties influence desensitization with the goal of seeing if drug desensitization and drug activity can be decoupled, potentially allowing drug designers to optimize both properties independently.

For GPCRs, the process of receptor desensitization can be broken up into the three steps shown in Figure 7.1. In the first step (Fig. 7.1a) ligand binds to the receptor to stabilize or select for a specific receptor conformation. Using a simplified view of this interaction, ligand binding to the receptor can be described by the association rate constant, k_{on} , dissociation rate constant, k_{off} , and the conformational selectivity factor, α . These three parameters are specific to the drug's interaction with the receptor, and as such can be manipulated directly by changing the chemical structure of the ligand. Historically drug design has focused on increasing α and thereby making the drug more active or on increasing the ratio between k_{on} and k_{off} such that the ligand binds to the receptor with higher affinity. However in this chapter I will argue that the magnitude of k_{off} also plays a role and can be used to directly affect desensitization.

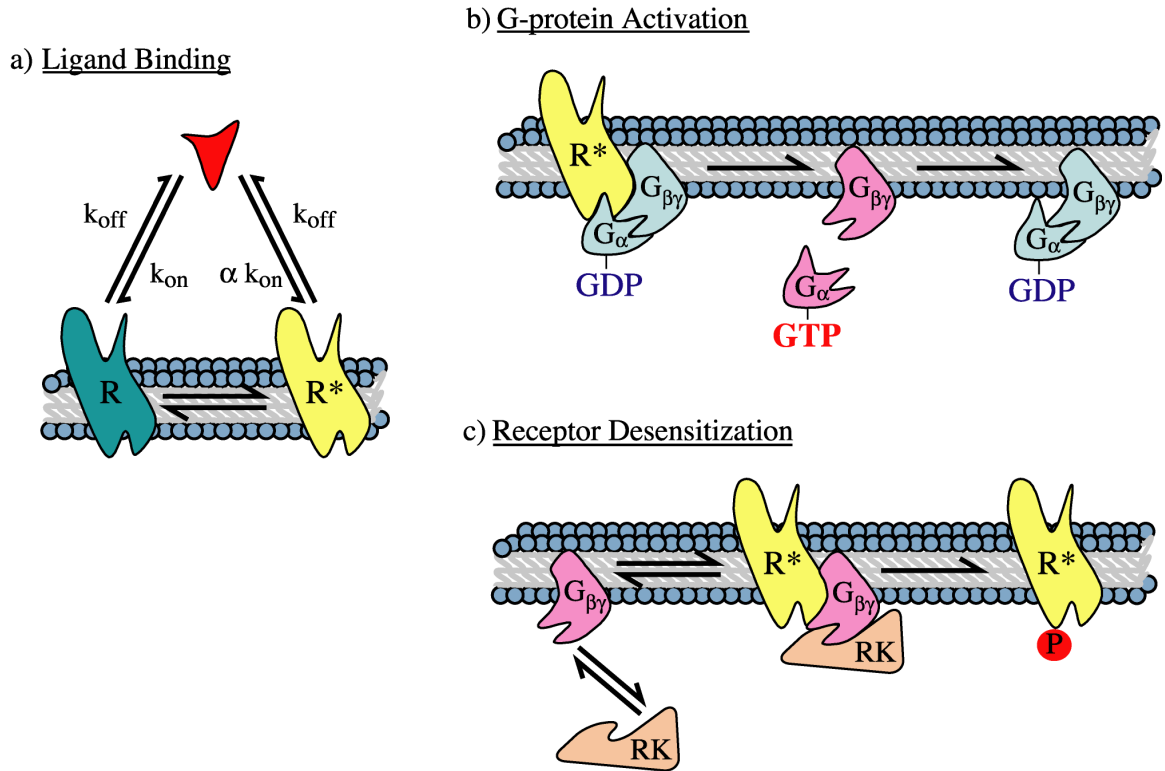


Figure 7.1 Three processes that affect GPCR desensitization. a) Receptors sense the environment via ligand binding. The ligand binding rate constant (k_{on}) is modified by the conformational selectivity factor, α , to determine the preferred receptor state, active (R^*) or inactive (R). b) Active receptor conformations can bind to and activate the G-protein trimer. Because the G_α subunit possesses an intrinsic GTPase activity, with time the subunit will cleave GTP into GDP, thereby allowing the inactive G_α subunit to recombine with $G_{\beta\gamma}$ to recover the inactive G-protein. c) Receptor desensitization is initiated by receptor kinase (RK) binding to the active $G_{\beta\gamma}$ subunit of the G-protein. This complex can then phosphorylate the active receptor, thereby targeting the receptor for internalization and desensitization.

In the second step (Fig. 7.1b), the active receptor can bind to and activate G-proteins within the cell membrane. In the inactive state, G-proteins exist as a GDP bound trimer. Upon activation by a receptor, the G-protein exchanges its GDP for a GTP molecule and breaks into two signaling subunits, G_α -GTP and $G_{\beta\gamma}$. Due to an intrinsic GTPase activity of the G_α subunit, the signaling G_α -GTP automatically reverts to an inactive G_α -GDP and then can rebind with the membrane bound $G_{\beta\gamma}$ subunit to recover

the inactive G-protein (Taylor 1990). Using this mechanism the cell is able to detect and amplify small signals and also reset when the signal is removed.

In the third step (Fig. 7.1c), the active receptor is phosphorylated and targeted for desensitization. Active GPCRs are phosphorylated by receptor kinase proteins recruited to the cell membrane by active $G_{\beta\gamma}$ subunits. Once phosphorylated, the receptor can be bound by arrestin proteins, which are thought to target the receptor for internalization and desensitization (Krupnick and Benovic 1998).

Because receptor activation is required for both G-protein activation and receptor desensitization, it is tempting to conclude that activation and desensitization are simply linearly related. In this view, receptor activation causes G-protein activation which in turn causes receptor kinase recruitment that leads to phosphorylation and desensitization. Thus, any drug that increases G-protein activation should similarly increase receptor desensitization. However this view assumes that the time delay between G-protein activation and receptor phosphorylation is negligible, which may or may not be the case depending on the drug and cell system.

In some experimental systems such as the β_2 -adrenergic receptor, desensitization and activation show a strong correlation (Figure 7.2a) (Benovic et al. 1988). In systems such as these, the primary determinant of both ligand induced activity and desensitization is likely the conformational selectivity factor, α , because this parameter determines the fraction of receptors in the active conformation. However the m-opioid and dopamine D_{1A} receptors do not exhibit a strong correlation between activation and desensitization (see Figure 7.2b), implying that other ligand properties can determine the relative activation to desensitization ratio.

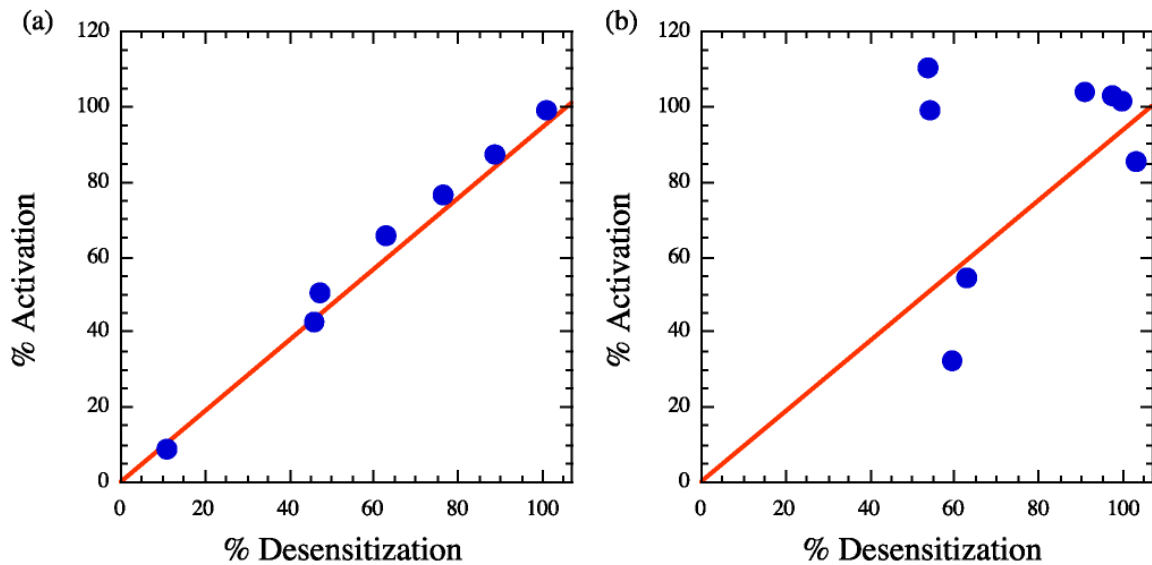


Figure 7.2 Comparison of activation and desensitization profiles for a variety of drugs (blue circles) on two different receptor systems. (a) Seven drugs acting on a β_2 -adrenergic receptor in reconstituted system (Benovic et al. 1988) show a strong correlation between receptor activation and desensitization. (b) Eight drugs to the dopamine D_{1A} receptor in C-6 glioma cells (Lewis et al. 1998) exhibit a weak correlation between activation and desensitization. Figures modified from (Riccobene et al. 1999).

Theoretical work using a simplified ordinary differential equation model of receptor activation and desensitization has confirmed the importance of α in systems such as that shown in Figure 7.2a (Riccobene et al. 1999). However this earlier work fails to explain uncorrelated systems such as is shown for the dopamine D_{1A} receptor in Figure 7.2b. In uncorrelated systems, G-protein activation and receptor desensitization are not related and as such cannot be simply explained by the effect of α alone.

One possible reason that earlier work was not able to account for this lack of correlation was that it did not include spatial effects. Therefore this work seeks to extend earlier work by including spatial effects and discrete dynamics with the goal of explaining both correlated and uncorrelated activation/response data.

Discrete spatial models have suggested that the ligand association and dissociation rates can affect G-protein activation (Mahama and Linderman 1994). To understand this mechanism, which has been termed “switching” (Stickle and Barber 1989), consider the two extremes of irreversible receptor–ligand binding (Figure 7.3a) and fast receptor–ligand binding and unbinding (Figure 7.3b). In both cases the ligand is bound to only one out of three receptors at any time; therefore only the rate of ligand movement among individual receptors changes. In the irreversible binding case, the ligand bound receptor can activate all of the G-proteins local to the receptor but no more. In contrast, a ligand with a large dissociation rate constant can rapidly switch from receptor to receptor while activating many of the local G-proteins and then moving on.

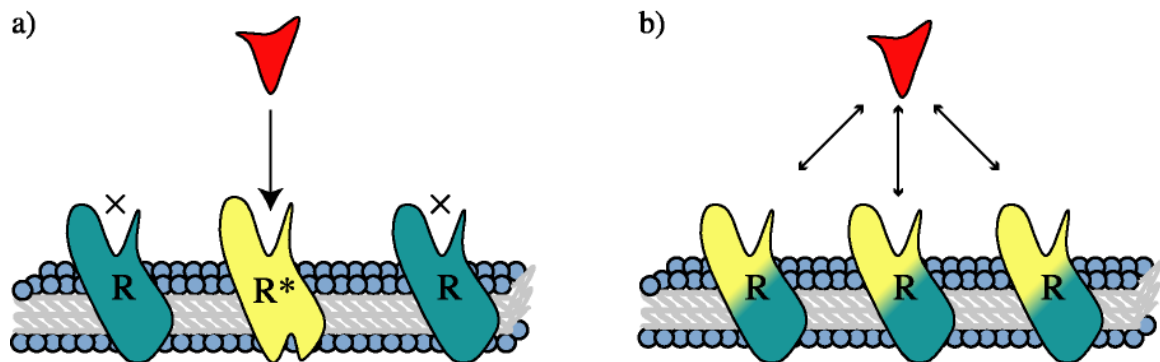


Figure 7.3 Three receptors binding with a single ligand molecule under two limiting kinetic cases. a) Ligand binds irreversibly to one receptor, leaving the other two receptors permanently inactive. b) Ligand binding and unbinding is fast; thus, each receptor is only occupied 33% of the time.

Previous Monte Carlo simulations indicate that increased ligand switching will lead to an increase in overall G-protein activation (Mahama and Linderman 1994; Shea and Linderman 1997). By rapidly switching from receptor to receptor, the ligand does not permit local depletion zones to form around the receptor and thereby ensures that a large signal is generated. These simulation results have been corroborated by some experimental findings (Stickle and Barber 1989; Stickle and Barber 1992; Mahama and

Linderman 1995), although more experimental work needs to be done to determine the generality of these findings.

If switching affects G-protein activation then it may also affect receptor desensitization. As shown in Figure 7.1, G-protein activation and receptor desensitization are sequentially linked because the G-protein must be activated before receptor kinase can be recruited to the membrane. Therefore, changes in G-protein activation should affect receptor phosphorylation, although not necessarily at the same time scale.

As an analogy, compare desensitization to opening a door. Although it may be possible to grip the door knob (ligand binding) and turn it (G-protein activation) over a short time scale, actually opening the door (desensitizing the receptor) takes a significantly longer time. Therefore, a knob turn will not always result in an opened door, particularly if we do not hold onto the handle for long enough (large k_{off}).

The purpose of this chapter is to determine how the kinetics of ligand-receptor interactions differentially affect receptor desensitization and G-protein activation depending on the cellular environment. This relationship will first be explored using a computational model of receptor activation and desensitization and then compared to experimental data.

7.2 Methods

In this work I use Monte Carlo simulations to determine how the ligand conformational selectivity, association, and dissociation rate constants affect G-protein activation and desensitization. Monte Carlo simulations were used so that the state and location of each protein could be followed, thereby making the most realistic predictions possible with a simplified model. The cell membrane was modeled as a two dimensional triangular grid with periodic boundary conditions. To initialize the simulation, receptors and G-proteins were placed on the grid at random non-overlapping locations. Both receptors and G-proteins had a diameter of two grid spacing, making a single grid spacing approximately 2 nm. Proteins were allowed to interact if they were separated by one grid spacing or less. Simulations were run on a 3000 by 3000 grid with 50 receptors and 500 G-proteins, consistent with experimentally observed receptor densities (Stickle and Barber 1989; Rousseau et al. 1997).

The simulation contained nine distinct species: R, R_p, LR, LR_p, G, G_α-GTP, G_α-GDP, G_{βγ}, G_{βγ}-RK. Each species is described in more detail Table 7.1 and the interaction network of these species is shown in Figure 7.4. Note that G_α-GTP and G_α-GDP are cytosolic species and as such their positions were not followed. G-protein activation and receptor phosphorylation are assumed to be diffusion-limited reactions (Shea and Linderman 1997), and as such are modeled as collision coupled.

Initially, non-ligand bound receptors were assumed to be completely inactive while the ligand bound receptor were fully active, corresponding to a strong positive agonist. Later simulations included an explicit conformational selectivity factor, such that partial agonists could also be tested in the model.

Species Name	Description	Location
R	Inactive receptor	membrane
R _p	Phosphorylated receptor	membrane
LR	Ligand bound receptor	membrane
LR _p	Ligand bound phosphorylated receptor	membrane
G	Inactive G-protein trimer	membrane
GαGTP	Active alpha subunit of the G-protein	cytosol
GαGDP	Inactive alpha subunit of the G-protein	cytosol
Gβγ	Active beta-gamma subunit of the G-protein	membrane
GβγRK	Beta gamma subunit bound to receptor kinase	membrane

Table 7.1 Identities of species used in the desensitization model.

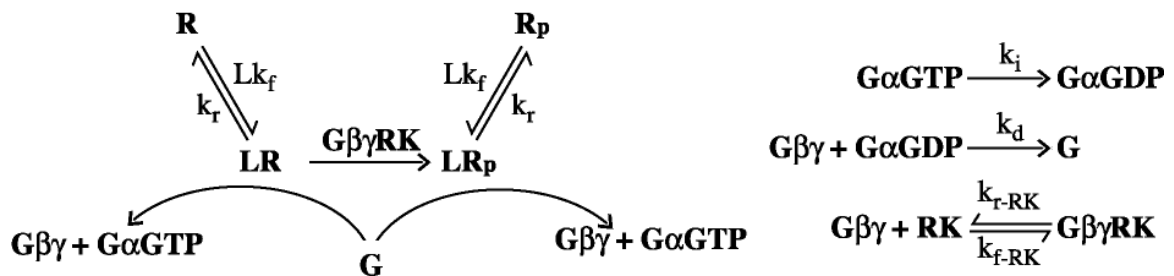


Figure 7.4 Interaction network of the GPCR signaling and desensitization pathways.

Following the mechanism in Figure 7.4 mechanism, only the LR and LR_p species can activate G-protein and only the LR species can be phosphorylated. In agreement with experimental findings (Jin et al. 2000), phosphorylated and non-phosphorylated receptors are assumed to signal with equal activity. In a living cell, receptor phosphorylation would eventually lead to receptor internalization and desensitization (Krupnick and Benovic 1998). However these later desensitization events would take place at a much longer time scale, and as such are not explicitly modeled here. Instead, I

assume that the rate of receptor phosphorylation is proportional to the desensitization rate.

The simulation dynamics were governed by the parameters listed in Table 7.2. In most cases these parameters are available directly from the literature, however two parameters had to be estimated. The receptor kinase association rate constant was estimated to be approximately equal to the G_{α} - $G_{\beta\gamma}$ association rate constant because in both cases proteins are recruited from the cytosol to $G_{\beta\gamma}$ in the cell membrane. The receptor kinase dissociation rate constant was estimated by assuming that the receptor kinase binds to $G_{\beta\gamma}$ with a high equilibrium affinity. Future experimental work will help to refine the estimates. The effect of changing k_{f-RK} on the signaling profile is examined as a cell property later in this work.

Constant	Description	Value	Reference
L	Ligand concentration	10^{-10}M	(Riccobene et al. 1999)
k_f	Ligand association rate constant	$10^8 \text{ M}^{-1} \text{ sec}^{-1}$	(Riccobene et al. 1999)
k_r	Ligand dissociation rate constant	0.37 sec^{-1}	(Riccobene et al. 1999)
α	Conformational selectivity factor		Assumed perfect positive agonist
k_i	Alpha subunit inactivation rate constant	1 sec^{-1}	(Shea et al. 2000)
k_d	Inactive G—protein association rate constant	1000 sec^{-1}	assumed rapid (Shea et al. 2000)
k_{r-RK}	Receptor kinase dissociation rate constant	100 sec^{-1}	Value not known
k_{f-RK}	Receptor kinase association rate constant	1000 sec^{-1}	Value not known
D	Receptor and G-protein diffusivity in the membrane	$10^{-11} \text{ cm}^2 \text{ sec}^{-1}$	(Shea and Linderman 1997)

Table 7.2 Parameters used in model. Parameters taken the literature except for the receptor kinase association and disassociation rate constant which are unknown. Note that here the conformational selectivity factor (α) only affects the receptor conformation and not the ligand binding rates to ensure that ligand-receptor dissociation and receptor activation can be controlled independently.

The simulation was run by allowing the proteins to diffuse and react according to the reaction rules presented in Figure 7.4. To begin each iteration, a particle is chosen at random. This particle is given the opportunity to diffuse and carry out its reactions in a random order to eliminate any unintended bias. For example, the ligand bound receptor, LR, may diffuse in a random direction and may also dissociate from its ligand.

Rates of G-protein activation and receptor desensitization were calculated from average measurements of initial rates. Simulations were run for 3000 iterations, corresponding to between 16 and 60 seconds depending on the parameters chosen. After each iteration, the total numbers of phosphorylated receptors and activated G-proteins were stored. At the end of the simulation, the initial rates of phosphorylation and activation were calculated by assuming the initial rates to be linear and fitting the rate data to a straight line. In general, the assumption of a linear initial rate was excellent for the G-protein activation rate (r^2 values > 0.95) and adequate for receptor phosphorylation rate (r^2 values > 0.8). Each simulation was repeated a total of 100 times to determine the mean and standard deviation of each rate.

To determine the effect of ligand binding kinetics, each simulation condition was run using 8 ligand dissociation rate constant (k_{off}) values (46, 93, 190, 370, 925, 1900, 2800, 3700 sec^{-1}). The ligand association rate constant (k_{on}) was then scaled to ensure that the equilibrium ligand occupancy remained at a low and constant value of 2.5%, similar to the physiological levels of many drugs in the body.

Simulations were run to see the effect of the conformational selectivity factor (α), diffusivity (D), G-protein inactivation rate constant (k_i), and receptor kinase association rate constant ($k_{\text{f-RR}}$). These simulations were able to show the effect of ligand specific

parameters ($\alpha, k_{\text{on}}, k_{\text{off}}$) and how these behaviors changed with changes in the cellular signaling machinery ($D, k_i, k_{f\text{-RK}}$).

Simulations were written in C++ and run on a cluster of Apple Macintosh G4 machines. Each simulated condition took approximately 6 hours to gather 100 runs.

7.3 Results

The results of the Monte Carlo simulations are divided into two categories. First I test the effects of ligand specific properties on G-protein activation and receptor desensitization. These ligand specific properties include $k_{\text{on}}, k_{\text{off}}$, and α . Next I simulate the effects of changing the cell properties D, k_i , and $k_{f\text{-RK}}$. Together these results give a detailed picture of how desensitization and activation interrelate.

7.3.1 Effects of Ligand Properties $k_{\text{on}}, k_{\text{off}}$ and α

In the simplified model of drug—receptor interaction shown in Figure 7.1, the drug can be completely described by the three parameters $k_{\text{on}}, k_{\text{off}}$ and α . Each of these parameters in turn directly relate to the chemical structure of the ligand and its interaction with the receptor.

Figure 7.5 shows the effects of α and the ligand dissociation rate constant on activation and desensitization. As shown in Fig. 7.5a, in all cases increases in the ligand dissociation rate constant and α result in increased G-protein activation. The data show almost no difference in behavior between a ligand with an α value of 10^7 and ∞ implying that the ligand activity is nearly saturated at this value. These findings are consistent with

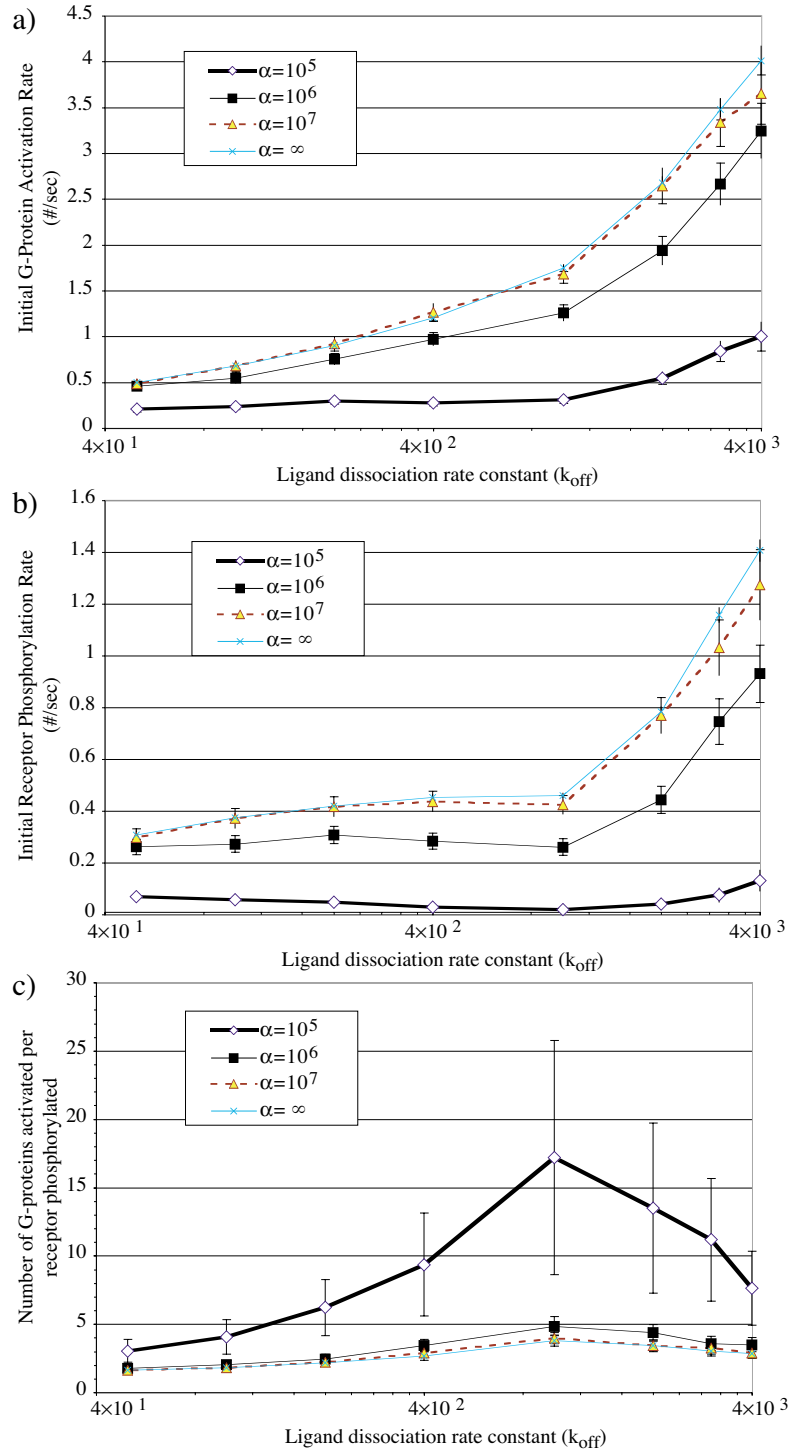


Figure 7.5 Effects of ligand dissociation rate constant and α on G-protein activation and receptor phosphorylation rates. Values of $\alpha = 10^5$, 10^6 , 10^7 , and ∞ represent LR complexes that are active 10%, 50%, 90%, and 100% of the time respectively. The data in a) and b) are combined into c) to directly show the relationship between the G-protein activation rate and receptor phosphorylation rate.

previous work on ligand switching (Mahama and Linderman 1994; Shea and Linderman 1997).

The rate of receptor phosphorylation also increases with α , but varies nonlinearly with ligand dissociation rate constant as shown in Fig. 7.5b. Interestingly, at low values of α , the rate of receptor phosphorylation passes through a minimum when $k_{\text{off}} = 930 \text{ sec}^{-1}$, while at greater values of α the receptor phosphorylation rate becomes flat at $k_{\text{off}} = 930 \text{ sec}^{-1}$.

The rates of G-protein activation and receptor phosphorylation are compared in Figure 7.5c. This value is generated by dividing the rate of G-protein activation by the rate of receptor phosphorylation to obtain the number of G-proteins activated for each receptor phosphorylated. Therefore large values on Figure 7.5c indicate that the drug causes a disproportionate amount of activation, while low values indicate more phosphorylation than desensitization. These results confirm the presence of a local maximum in G-protein activation versus receptor phosphorylation for ligands with a dissociation rate constant of approximately 930 sec^{-1} , which although high for most drugs is possible. The presence of this maximum is independent of the α value, but is most pronounced at lower values of α .

Note that in all cases simulations were run to ligand dissociation rate constants as low as 0.37, but at values below 37, both the G-protein activation rate and the receptor phosphorylation rates became independent of the ligand dissociation rate constant. From inspection of the simulation data, the activation and desensitization rates stop changing at low k_{off} values because the mean ligand residence time exceeds the mean time required to

phosphorylate the receptor and to establish a G-protein activation steady state. Therefore, at small k_{off} values, nearly all LR complexes become phosphorylated.

7.3.2 Effects of Cell Properties k_i , D , and $k_{f\text{-RK}}$.

Cell properties clearly influence signal transduction, and as such may account for some of the variation in activation and desensitization. Therefore, in this section I vary three cell specific properties k_i , D , and $k_{f\text{-RK}}$ to see how they affect the balance between activation and desensitization. In each simulation I have included one base case using the parameters listed in Table 7.2 for comparison.

Using the same procedure from Figure 7.5c, the relative number of G-proteins activated per phosphorylated receptor was used to compare different conditions. Figure 7.6a shows that the relative activation versus desensitization increases as the G-protein inactivation rate constant, k_i , increases. Also the location of the maximum appears to shift to larger ligand dissociation rate constants as k_i increases. The effects of diffusion on activation and desensitization are shown in Figure 7.6b. As the diffusivity decreases, the location of the maximal activation peak shifts left. Finally, Fig. 7.6c shows that decreasing the receptor kinase association rate strongly increases the relative activity of the ligand, but does not shift the peak to the left or right.

Inspection of the raw data reveals that in all cases increasing k_{off} caused an increase in G-protein activation; therefore, the local maximum in Figure 7.6 is primarily due to changes in the receptor phosphorylation rate.

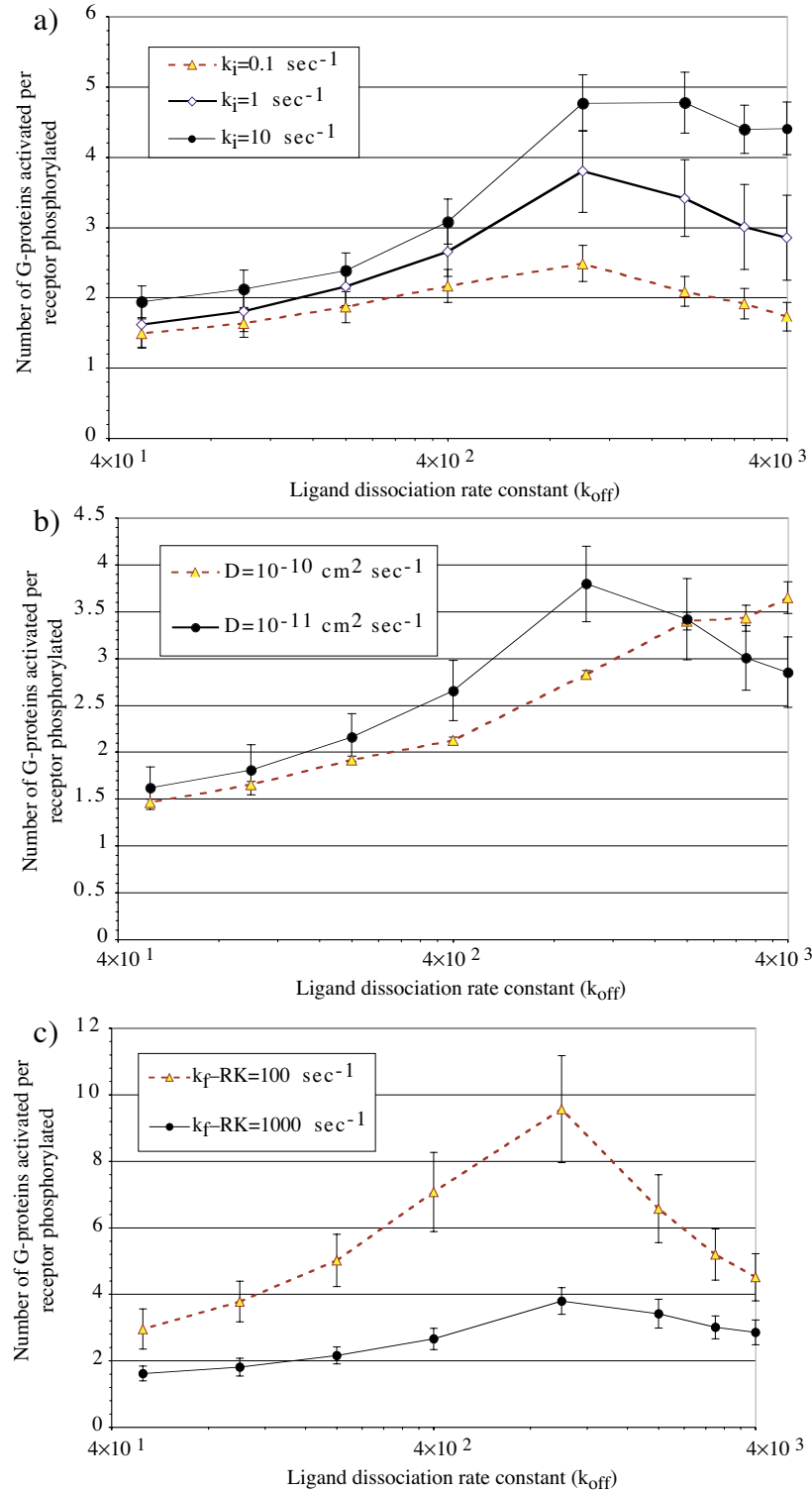


Figure 7.6 Effects of cell properties on G-protein activation and receptor phosphorylation rates.

7.4 Discussion

This modeling work was motivated by the observation that G-protein activation and receptor phosphorylation are sometimes but not always proportional (see Figure 7.2). I speculated that activation and desensitization could become decoupled if spatial events and discrete dynamics were included, thereby more accurately modeling the system and allowing switching to take place.

The results from Figure 7.5 and 7.6 show for the first time that changes in the ligand dissociation rate constant can alter the proportion of G-protein activation and receptor phosphorylation. In Figure 7.7, data in Figure 7.5c is replotted in the same format as Figure 7.2 to show this relationship more clearly. This finding implies that activation and desensitization can be partially decoupled in some systems by changing the conformational selectivity factor, α , and ligand dissociation rate constant. These results have implications for our general understanding of receptor dynamics as well as for drug design. In the following sections I will discuss why this noncorrelated behavior emerges and provide a physiological example from the literature that demonstrates similar behavior.

7.4.1 Effect of α on the Relative Phosphorylation Rate

The conformational selectivity, α , has a nonlinear effect on the receptor phosphorylation rate. In the Monte Carlo simulations, small values of α always cause less G-protein activation (Fig. 7.5a) and hence less receptor desensitization (Fig. 7.5b), however Fig. 7.5c shows low α values tend to have a disproportionately low phosphorylation rate relative to G-protein activation.

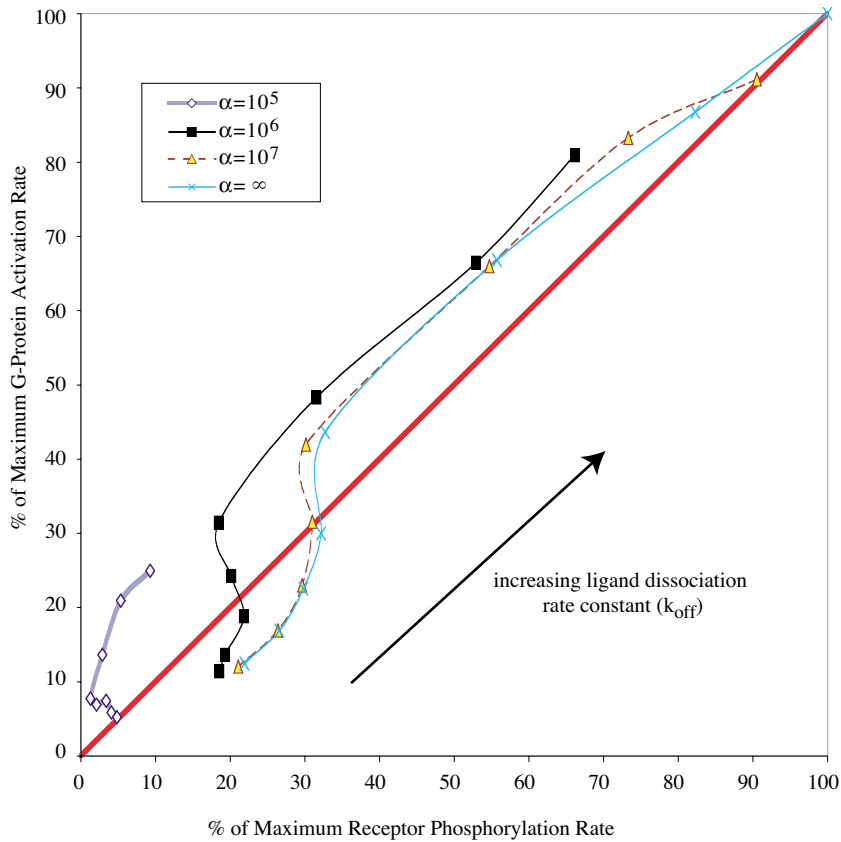


Figure 7.7 Activation versus desensitization simulation results for drugs with a variety of different dissociation rate constants and α values. Note that the simulations do not predict that activation and desensitization are proportional.

This bias toward reduced phosphorylation at low α values likely takes place because the time delay between G-protein activations is long under these conditions. Recall from Figure 7.1b, that the active G-protein contains an intrinsic GTPase activity and as such acts as a timed molecular switch. Thus if the mean lifetime of an active G-protein is t_G , then ligands that do not activate receptors for intervals longer than t_G will tend to cause less phosphorylation.

The simulations suggest that this low relative phosphorylation rate could also be observed with an ultra low concentration ligand with a large α value. In this case any time the ligand bound to the receptor it would cause a response, but ligand binding would

be so infrequent that the ligand would cause very little desensitization. The tradeoff for using this strategy for drug design is that the ligand causes only a very small overall response.

7.4.2 Minimum Receptor Phosphorylation Rate

In all of the simulations run, spatial effects cause a local minimum in the receptor phosphorylation rate when $k_{\text{off}} = 930 \text{ sec}^{-1}$. This minimum in receptor phosphorylation is responsible for the maximum in the relative number of G-proteins activated per phosphorylated receptor shown in Figures 7.5c, 7.6a, 7.6b, and 7.6c.

The minimum in receptor phosphorylation rate can be explained by tracking the source of receptor kinase near a ligand bound receptor as shown in Figure 7.8. The receptor kinase proteins near a LR complex are there either because 1) that LR complex activated a G-protein that recruited a kinase to the membrane or 2) another LR complex activated a G-protein that recruited a kinase to the membrane. In the second case, the receptor kinase was most likely not activated near the receptor and as such had to diffuse to get there.

The proportion of receptor kinases near to the receptor depends on the ligand dissociation rate. If the ligand dissociation rate is slow, then the ligand-receptor bond is long lived (see Fig. 7.3a) and most of the receptor kinases near the receptor were recruited by that receptor. In contrast, if the ligand dissociation rate is fast, then the ligand can accurately modeled using a field approximation and the Monte Carlo simulation results approach the result that would be predicted using partial differential equation (PDE) model (see Fig. 7.3b). In this PDE limit there is little receptor kinase

recruitment at any one receptor, but significant overall recruitment from other receptors.

The result in Figure 7.8a shows that the total receptor kinase level, and hence the receptor phosphorylation level reaches a minimum at an intermediate ligand dissociation rate.

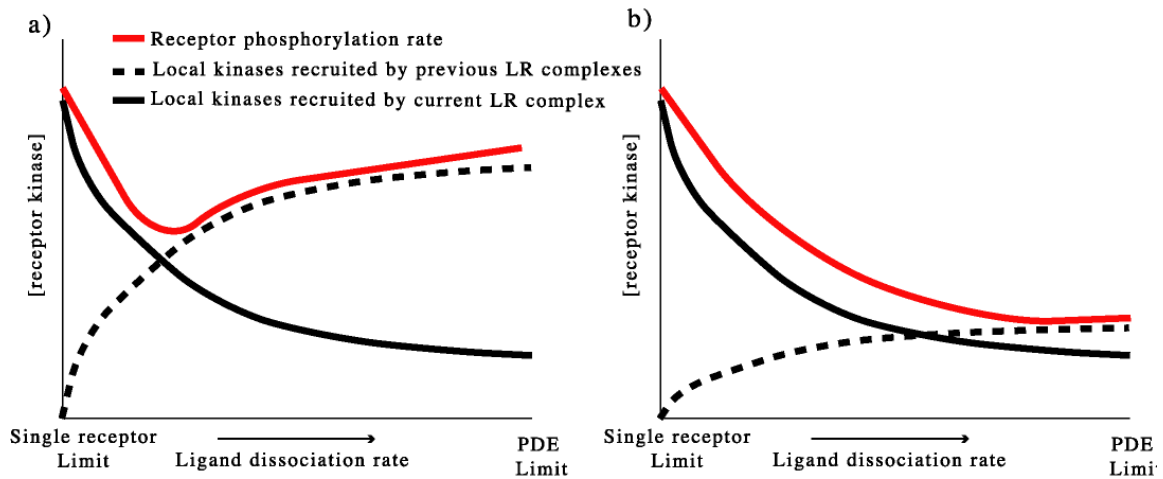


Figure 7.8 Schematic of the source of receptor kinase near a receptor as a function of the ligand dissociation rate constant. a) Conditions that produce a local minimum in receptor kinase concentration and hence minimum in receptor phosphorylation rate. b) Conditions in which receptor kinases activated by other receptors do not affect the phosphorylation rate of the ligand bound receptor tend should show no minimum in phosphorylation and less phosphorylation at higher rates.

The shape of the kinase profiles depends on the system that is being tested.

Therefore, if the concentration of receptor kinases recruited by other receptors is low due to slow diffusion, for example, then the total receptor kinase level may decrease slowly and have only a shallow minimum (Fig. 7.8b). The effects of cell properties on desensitization will be discussed in more detail in the next section.

7.4.3 Cell specific effects on desensitization

Not only do ligand properties influence desensitization, but also the properties associated with the cell should also play a role. These cell properties might include

different receptor types, changes in local receptor environments, or different signal transduction kinetics. These differences associated with the cell could help to explain why in some systems activation and desensitization are proportional for all known ligands, while other systems they are not.

To test the effect of changing cell properties, various values of the G—protein inactivation rate (k_i), diffusion rate (D), and receptor kinase association rate (k_{F-RK}) were tested to see their effect on the relative desensitization rate (see Figure 7.6). The G—protein inactivation rate could vary from system to system either due to variations in each subtype of G—protein or could be adjusted dynamically via regulators of G—protein signaling (RGS) proteins (Berman and Gilman 1998). Figure 7.6a shows that increasing k_i also increases the relative number of G—proteins activated per phosphorylated receptor. The reason for this increase is that a larger k_i results in a shorter active G—protein lifetime, thereby limiting the radius that an active G—protein can diffuse. Because active G—proteins are responsible for recruiting receptor kinase to the membrane, a shorter active G—protein lifetime directly translates to a shorter receptor kinase lifetime and therefore less desensitization.

The effects of changing k_i on G—protein activation have recently been demonstrated experimentally and are supported by our simulations (Zhong et al. 2001). This work shows that the concentration of active G—proteins is constant near the receptor for any k_i , but the radius of active G—proteins increases with decreasing k_i . Therefore by modulating the G—protein inactivation rate, one can alter the interaction range of an active receptor. Zhong *et al.* suggest that this altered range forms a kinetic scaffolding that dynamically structures the signaling environment in the cell. In terms of

desensitization, kinetic scaffolding can be extended to include the effects of RGS on receptor kinase induced receptor phosphorylation. Thus, RGS proteins not only limit the radius of active G-proteins around an active receptor, but they also effectively limit the range of $G_{\beta\gamma}$ bound receptor kinase proteins.

Decreasing the diffusion coefficient (D) causes the system to be better mixed, and as such causes more phosphorylation as is shown in our model results in Figure 7.6b. However at very high ligand dissociation rates ($\sim 10^3$), the relative number of G—proteins activated per phosphorylated receptor is greater for larger diffusion coefficients. This increase in relative G—protein activation takes place because each receptor can effectively activate more G—proteins when diffusion is fast because no local depletion zones form. The diffusion coefficient can change due to changes in membrane compositions, or changes in receptor localization both of which would depend on the specific receptor type and cellular environment

Perhaps surprisingly, decreasing the receptor kinase association rate constant caused a dramatic increase in the relative number of G—proteins activated per receptor phosphorylated (see Fig. 7.6c). The reason for this increase is that a reduced receptor kinase association rate results in fewer receptor kinase proteins on the membrane, and therefore less overall receptor phosphorylation.

7.4.4 μ —Opioid Receptor Activation and Desensitization

Experimental work with the μ -opioid receptor has provided some evidence in support of the hypothesis that activation and desensitization can be varied independently via ligand dissociation rates. The ligands morphine, etorphine, buprenorphine, and

DAMGO all exhibit qualitatively different G-protein activation, desensitization, and dissociation rates, and as such can be compared directly to predictions made by the Monte Carlo simulations. The properties of each ligand are summarized in Table 7.3.

Ligand	G-Protein Activation	Dissociation rate	Receptor Desensitization	References
morphine	high(?)	fast	low	(Rothman et al. 1995; Blake et al. 1997; Zhang et al. 1998)
etorphine	high	slow	high	(Blane et al. 1967; Rothman et al. 1995; Zhang et al. 1998)
buprenorphine	intermediate	slow	high	(Rothman et al. 1995; Blake et al. 1997)
DAMGO	high	fast	intermediate	(Tolkovsky 1982; Scheibe et al. 1984; Yu et al. 1997)

Table 7.3 Activation and desensitization profiles for four common ligands to the μ -opioid receptor. Table modified from (Riccobene 1999).

In qualitative terms, the data in Table 7.3 suggest that ligands with a faster dissociation rate will tend to have less desensitization, while drugs with a slow dissociation rate will cause more desensitization. This finding is in agreement with the relative data in Figure 7.5c, lending experimental support to the hypothesis that desensitization can be affected by ligand dissociation rate.

Quantitative data on μ -opioid receptor activation and desensitization for a number of drugs have been experimentally measured (Yu et al. 1997) and are directly compared to the simulation results in Figure 7.9. Both the simulation results and the experimental data predict that at high G-protein activation rates there should be proportionally less desensitization for most drugs. In terms of the door analogy discussed above, this result is sensible. Because G-protein activation must precede desensitization, switching events

that take place at a time scale faster than desensitization will tend to favor activation. However the model using the current parameter set is not able to fully account for the small desensitization caused by morphine.

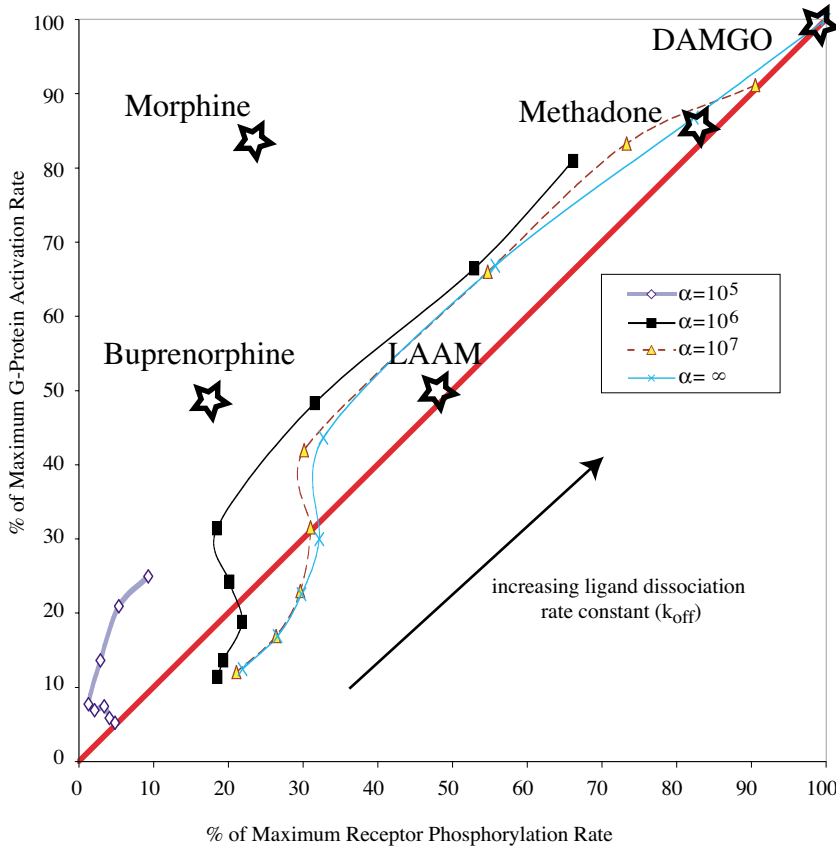


Figure 7.9 Comparison of simulation results to the relative activation and desensitization profiles of five drugs to the μ -opioid receptor expressed in h μ CHO cells. Data taken from (Yu et al. 1997). Note that literature values of the activity of morphine vary significantly depending on the experimental system (Zhong et al. 2001).

Clinical work with the μ -opioid receptor by Shen *et al.* (Shen and Crain 1997)

has demonstrated that co-administration of low doses of a neutral antagonist along with an agonist can cause the agonist signal for a longer period before becoming desensitized.

This phenomenon is shown in a mouse model in Figure 7.10

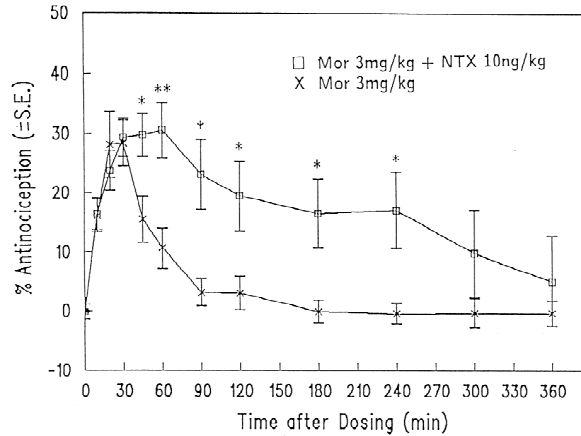


Figure 7.10 In a mouse model, treatment with morphine (Mor) and a neutral antagonist naloxone (NTX) results in a longer effect than morphine alone would produce. (Figure taken from (Shen and Crain 1997)).

By blocking receptors with the neutral antagonist, Shen *et al.* have essentially limited the amount of switching that is possible in the system (akin to Figure 7.3a) without affecting the agonist dissociation rate. This change is equivalent to reducing the density of receptors available for agonist binding. In terms of Figure 7.8, this reduction in effective receptor density reduces the concentration of receptor kinase proteins recruited by other LR complexes, thereby reducing the overall desensitization rate. Other mechanisms such as G-protein cross-talk could also play a role in extending the lifetime of the agonist when co-stimulated with an antagonist (Crain and Shen 2000), but these mechanisms are complicated and require a much more detailed knowledge of the signal transduction pathways before they can be confirmed.

7.5 Conclusions

By modeling the spatial aspects of desensitization, I have shown that receptor desensitization and G-protein activation can be partially decoupled. The simulations

show that at an intermediate ligand dissociation rate, the relative number of G-proteins activated per receptor phosphorylated should reach a maximum.

These results open the possibility that drugs could be tailored to have varying amounts of desensitization. For example, one could design drugs with a high dissociation rate and low α that would signal, but not desensitize—similar to the mechanism proposed here for morphine. Alternatively, one could design drugs with small dissociation rate constants and high α values to cause large amounts of desensitization.

More experimental work is needed to confirm the predictions made by this model. The primary need is for quantitative measures of G-protein activation, receptor desensitization, and ligand dissociation for a number of ligands that bind to the same receptor. Table 7.3 lists only qualitative trends, and as such cannot be directly compared to experimental findings. Although the agreement between experiment and theory is intriguing, more experimental data is needed to prove that the ligand dissociation rate is controlling.

CHAPTER VIII

CONCLUSIONS AND FUTURE DIRECTIONS

G—protein coupled receptor signaling is a primary route the cell uses to gather information about its environment. The cell in turn uses this information to determine how to respond, and in doing so affects the physiological state of the organism. Therefore through gaining a deeper understanding of GPCR signaling, we aid the development of new therapies for human disease.

In this thesis I have uncovered a number of emergent properties associated with G-protein coupled receptor signaling. In many cases these findings have direct pharmacological implications and can be immediately implemented in drug discovery and development. In addition to the applied uses of this work, these findings contribute to the framework of our understanding of cellular communication and biology in general. In the following sections I will discuss some of the key findings made in this thesis and will highlight areas that may lead to interesting and fruitful future research.

8.1 Receptor dimerization

It is now well demonstrated that GPCRs, along with many other proteins, form dimers, but the question is why? One of the most significant findings of this thesis is that dimerization alone can cause proteins to localize into clusters larger than two proteins. When put into the context of receptor mediated signaling, I have shown that dimerization

induced clustering could significantly affect how signals are both transmitted and regulated. These physiological effects of clustering could in part explain why dimerization is so ubiquitous throughout biology and why this ability has been evolutionarily conserved.

Because the goal of the dimerization work presented in this thesis was to determine if dimerization could affect receptor localization, the models were simplified to include only a few receptor species. However, experimental work using high throughput protein-protein binding assays has indicated that vast networks of protein dimerization interactions exist. For example, Figure 8.1 shows the dimerization interaction of approximately one thousand proteins in the yeast genome. Networks like these suggest that dimerization interactions throughout the cell are a primary mechanism for organizing proteins within the cell. If true, then future proteomics work will need to develop completely new tools to analyze, interpret, and simulate the behavior of these networks.

A key challenge that will need to be overcome when analyzing dimerization in more general terms will be the issue of dimensionality. Throughout the cell there are examples of three-dimensional volumes (cytoplasm), one-dimensional lines (actin filaments), and even locally fractal surfaces (the rough ER or the lining of a mitochondria). In each environment, proteins should exhibit different reaction kinetics (Savageau 1998), which includes protein-protein interactions. These changes in reaction kinetics could drive the formation of signaling complexes that include a mixture of dimensions, such as that illustrated in Figure 8.2.

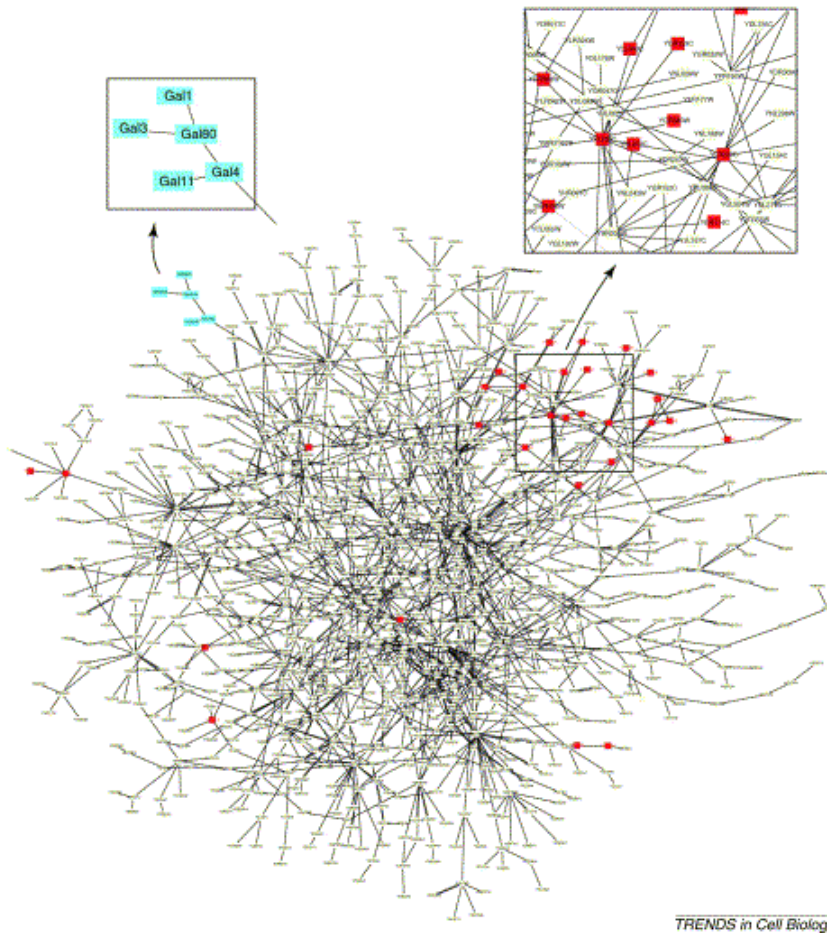


Figure 8.1 Protein-protein interaction map for approximately one thousand proteins in the yeast genome. Figure copied from (Tucker et al. 2001).

I suspect that the cell uses these changes in dimensionality as a general mechanism for specifically localizing proteins in the cell membrane. Using the simulation environment developed in this thesis, I have generated preliminary simulations of dimerization on non-flat surfaces. The results of these simulations are presented in Appendix B. Unfortunately, these results are not completely convincing because they are run on a grid that may bias the simulation when run on a distorted surface. However future simulations on a continuously varying surface may prove more compelling.

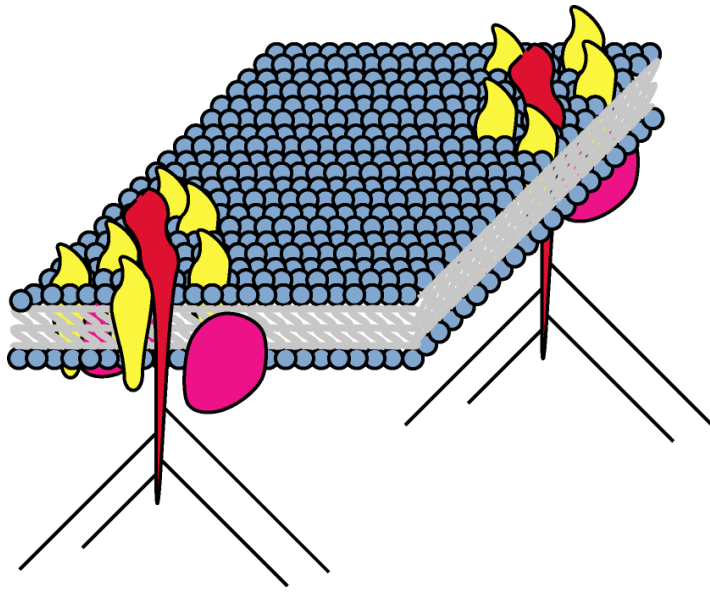


Figure 8.2 Dimerization induced localization could organize a large number of species together, including parts of the cytoskeleton.

Beyond the mechanistic arguments of how dimerization could be affected by dimensionality, dimerization also provides a simple and elegant way to control protein positions. In a dimerization based localization scheme, control is distributed among the individual proteins. Thus there is no need for a complicated, all knowing centralized controller within the cell. Controlling protein positions with dimensionality also has the advantage that it is dynamic. For example, if it were found that some proteins tended to cluster at small radius of curvature surfaces, then the cell could use this property to rapidly and automatically redistribute receptors to pseudopods that probe the environment for nutrients. If nutrients were found, this could then cause more receptors to cluster in this area, providing the cell with a clear indication of where to move.

This dimerization work fits into a larger class of problems known as diffusion limited aggregation (reviewed in (Sander 2000)). The canonical example of diffusion

limited aggregation involves single particles that randomly diffuse toward a stationary cluster. Once the particle encounters the cluster it sticks and another free particle is added. With time this cluster grows into a fractal, snowflake like structure. The dimerization models presented in this work follow in the same framework except that here the binding is reversible and all particles are allowed to diffuse. However, the resulting structures produced by diffusion limited aggregation and dimerization induced clustering are similar in that they are irregular and self-assembling. Therefore the methods used to analyze diffusion limited aggregates may be helpful for future analytical work on dimerization.

8.2 Desensitization

The second major finding in this thesis is that G-protein activation and receptor desensitization can, in some cases, be controlled independently via the ligand dissociation rate. Experimental work in some systems has demonstrated that in general G-protein activation and desensitization increase with each other. However, in a number of significant receptor systems, activation and desensitization appear to be only loosely correlated. The modeling work in this thesis is able to account for the behavior of both systems based on the properties of the ligand and signal transduction system.

This finding has an immediate pharmacological impact, for it implies that drug desensitization can be tailored for a specific application by changing the dissociation rate. Drug development currently focuses on maximizing ligand binding affinity and efficacy, however when desensitization is considered this approach may not be optimal. As shown in Chapter 7, the relative G-protein activation rate to receptor phosphorylation rate

reaches a maximum for ligands with a large dissociation rate constant. Therefore optimizing a drug for high binding affinity may also be inadvertently optimizing for a maximum desensitization rate. If instead, drug designers focused less on binding affinity and more on toxicity, then it may be possible to develop drugs that desensitize less quickly and have fewer side effects.

On the other extreme, this work opens the possibility of developing a completely new class of drugs that cause only receptor desensitization without activating G-proteins. These drugs would act by reducing the number of receptors on the cell surface, thereby making the cell less sensitive to endogenous ligands. This kind of therapy could be helpful in cases where a genetic defect or disease causes receptor over expression, such as congenital night blindness or some forms of cancer (Milligan and Bond 1997). It is likely that there are already a small number of commercially available drugs that have their primary effect via desensitization of a receptor or receptor subtype. However, knowing that this ability to desensitize is related to the ligand dissociation rate allows for the rational design and dosing this unique class of drugs.

This work has demonstrated that desensitization can, in principle, be controlled by the dissociation rate, but this needs to be confirmed experimentally. The experimental data shown in Chapter 7 suggest that the opioid and dopamine receptor systems can show differing levels of G-protein activation and desensitization, and could provide a fruitful system for future desensitization research. However, to convincingly demonstrate the relationship between the activation and desensitization profiles of a drug, we primarily need quantitative measures of the ligand dissociation rate constants. With these

dissociation rate constants in hand, it would be possible to confirm that increased dissociation rates generally lead to decreased desensitization.

8.3 Drug Screening

By nature, high throughput drug screens are empirical and are not generally subject to modeling scrutiny. However, in Chapter 4 of this work I demonstrated that some screens are inherently biased against certain classes of drugs, indicating that modeling can and should play a role developing and interpreting screening assays. By uncovering this screening bias, this work not only highlighted a possible shortcoming of the assay system but it also suggested new ways to run the assay such that the assay could be focused toward detecting only drugs with desirable properties.

Although we generally lack precise parameter values for our models, models of screens can still provide useful insight about invariant properties of a system. For example, in Chapter 4 I show that the assay signal drop will always bias towards positive agonists in a membrane based assay, although in some cases the magnitude of this drop may be too small to measure. This kind of invariant information can still be helpful because it alerts the designers of drug screens that a bias is possible and suggests methods to correct for the bias if it is detected.

In light of the dimerization and desensitization work done in this thesis, membrane based screens could also be used to discover drugs that uniquely affect these processes too. Both receptor dimerization and desensitization are processes that take place at the level of the receptor, and as such are likely strongly influenced by ligands. One could envision modifying the receptors in an assay such that dimerization could be

measured using a FRET signal. This dimerization information could then be used to infer information about the internalization rate and potential for cross-talk caused by the ligand. Similarly, if the ligand desensitization rate correlates to the desensitization rate, then screens could be developed to search for drugs with desirable desensitization profiles. Ideally these measurements could be combined into a small number of assays that could be performed in a high throughput environment without significant protocol changes. An illustration of how this assay might look is shown in Figure 8.3.

This new class of screens would be fundamentally different from current screening assays because they would allow the selection of lead compounds based on multiple criteria. For example, current screening assays only detect compounds that bind tightly to the receptor on the assumption that tight binding is key for a viable drug. However, the desensitization work presented in this thesis suggests that drugs with a large dissociation rate constant could cause less desensitization and as such could be useful for certain disorders. In searching only for tight binding drugs, current screens probably miss other drugs that have useful properties. Using a composite screen, these drugs could be detected and their properties assessed early in the drug discovery process.

8.4 Future Pharmacological Models

Where will pharmacological modeling take us in the future? Our ultimate goal is to develop predictive pharmacological models that bridge molecular biology (e.g. the details of the receptor-ligand interaction) and cellular biology (e.g. the ultimate cellular response generated by ligand binding). I envision that we will eventually create predictive models would give us a clear view of how a drug affects a cell, allowing us to

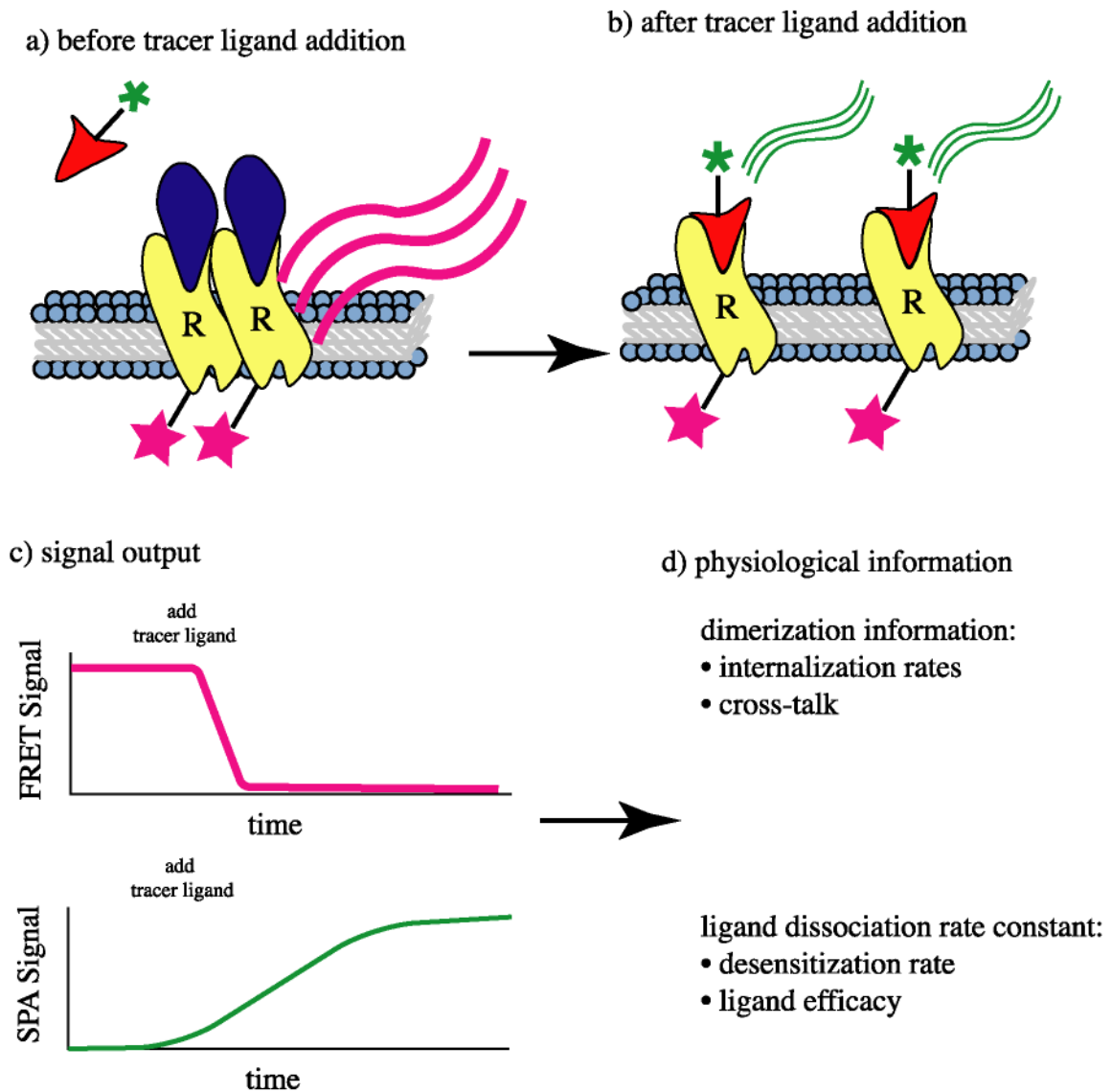


Figure 8.3 A hypothetical composite screening assay. The assay merges a FRET assay to measure protein dimerization and an SPA ligand binding assay. a) Before the tracer ligand is added the test ligand is allowed to equilibrate with the receptor to gather a base FRET and SPA signal. b) Addition of the tracer ligand will displace the test ligand, causing the SPA signal to rise. If the tracer ligand does not induce dimerization, then the FRET signal will drop. c) Hypothetical signal traces for the FRET and SPA signals. d) Using the tools developed in this thesis, physiological information such as receptor internalization rates and desensitization rates could be inferred from the FRET and SPA signals.

relate individual drug parameters such as the conformation selectivity parameter α to cellular behavior. Such models would be useful in drug screening as well as for testing complicated drug therapies.

In this thesis, I have discussed a number of ways to model the role of receptor/ligand/G-protein interactions in determining how a cell will respond to a drug, but these models can make only limited predictions because they are based in part on assumptions that make the problem simpler to solve. For example, sometimes we assume that a particular molecular species is in present at a constant concentration (i.e. no depletion/no species conservation) in complex models in order to find a simple solution. These limitations are required in light of the relatively small amount of quantitative data describing these systems, however as more data becomes available larger, more complete models can be constructed.

One of the clearest assumptions made in current GPCR models is that we can accurately model response using only the receptor, ligand, and G-protein in isolation from the rest of the cell. To some extent this approximation is reasonable: the ligand initiates the signaling cascade, and therefore events that take place soon after ligand binding are the events that are most influenced by the specific properties of that ligand. However, the activity of many other proteins inside the cell can have a profound effect on how the receptor's signal is interpreted. In the case of GPCRs, it is known that the receptor is phosphorylated by a number of receptor kinases (Krupnick and Benovic 1998; Lefkowitz 1998) and then binds to adapter proteins, which may have further signaling ability (Lefkowitz et al. 1992; Zuker and Ranganathan 1999). Later protein—protein binding events then lead to receptor internalization. Eventually, these other steps could be included in a more complete version of the cubic ternary complex model as shown in Figure 8.4, yielding a more accurate representation of GPCR signaling once the parameters describing this system are known. However these extra steps will require

additional experimental measurements to accurately and meaningfully predict the dynamics of this system.

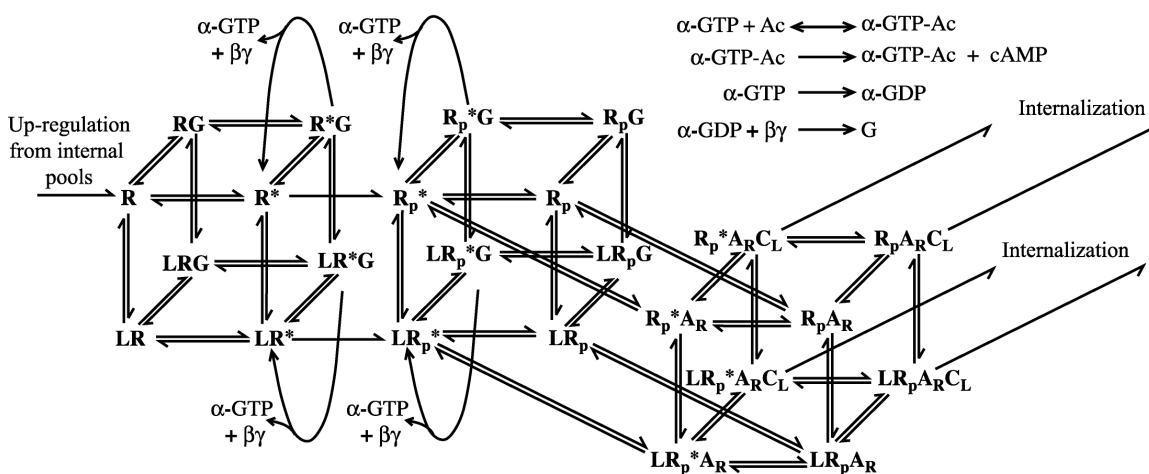


Figure 8.4 Extension of the cubic ternary model of GPCR signaling to include reactions farther down the signal transduction pathway including receptor up-regulation, internalization, arrestin binding (A_R), clathrin binding (C_L), and adenylyl cyclase activation (A_C).

Proteins downstream of the receptor may also be regulated thereby changing how a particular cell will respond to a drug (Bond et al. 1995). For example, downstream proteins may ultimately provide the feedback that regulates the G-protein concentration, possibly causing agonist inversion via the mechanism described in Chapter 3. By including the effects of these other proteins into future models, we will gain a more realistic picture of how the cell interprets its world.

In the modeling work in this thesis, I have assumed that the receptor has only two states, active and inactive, however it is quite possible that the receptor has a wider variety of states available. For example, experimental work has shown that for some receptor systems, different drugs seem to activate different signal transduction pathways more effectively, causing some to suggest that GPCRs would be better modeled with a

three state model (Scaramellini and Leff 1998). From a theoretical standpoint, this change from a two state to a three state receptor would change the space of possible receptor conformations from a line of possible states (shown in Figure 1.2) to a surface of possible states, shown schematically in Figure 8.5. The inclusion of additional receptor states would complicate our analysis of signal transduction, but would also open the possibility of new drugs that act with greater precision.

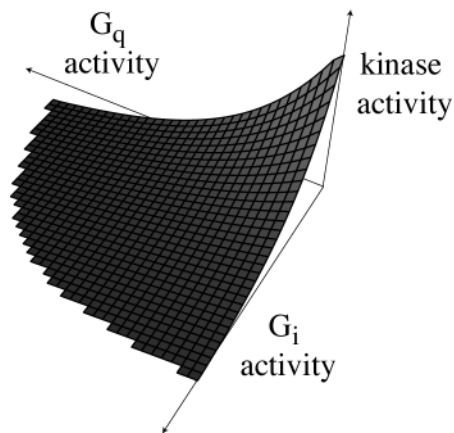


Figure 8.5 A schematic representation of a surface of possible conformations a receptor may occupy. Each axis represents the activity the receptor has for each signal transduction pathway, such as activity of the G—proteins G_i and G_q

An issue not addressed in this work, but relevant to understanding GPCR signal transduction is ligand cross—reactivity. Currently we assume in our models that each ligand affects only one receptor species and that receptor only effects one pathway, but this is clearly not true in many receptor systems. Receptors such as the opiate, muscarinic, and dopamine receptors are actually families of similar receptors interact with similar ligands and G—proteins but have unique individual members within each family with their own behaviors. For example, the κ —opiod receptor of the opiod receptor family is difficult to desensitize, while the δ —opiod receptor rapidly desensitizes (Jordan and Devi 1999; Jordan et al. 2000). The models in this work could be expanded

to include the interaction of multiple ligands with multiple receptors, and even multiple G—proteins to generate a network of interactions similar to a neuronet and shown in Figure 8.6.

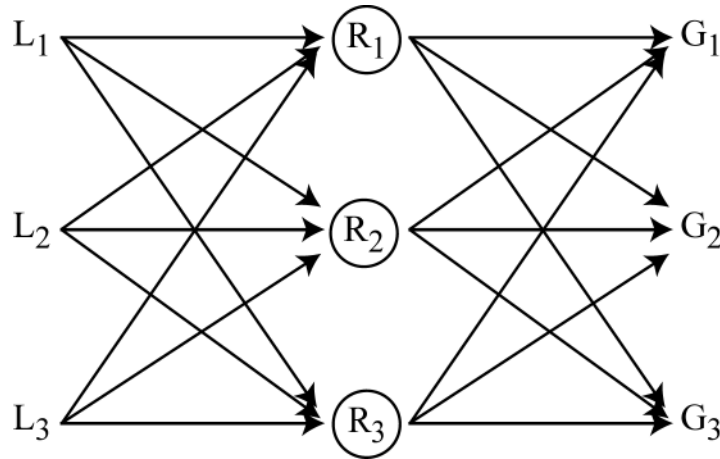


Figure 8.6 Cross—reactivity of ligands, receptors, and G—proteins can produce a more sophisticated information processing system.

Many proteins involved in signal transduction are made up of a number of related protein subunits, leading to a combinatorial effect that could also be explored. In the GPCR signal transduction pathway, the G—protein is made up of a trimer of proteins, each of which has a variety of subtypes (Rahmatullah and Robishaw 1994). Assuming that all of the protein species can bind to each other, we could see at most 480 different G-protein variants, each with their own unique receptor binding and signaling properties. One could explore how the diversity of G—protein combinations is regulated by the cell and how G—protein variation affects cell signaling.

From a modeling point of view, a large number of G—proteins could prove challenging to include. As a first approximation however, one could simply add a small noise term into all of the G—protein specific parameters. This change would effectively spread the data out to account for G—protein variation and even smaller effects such as

thermal fluctuations. However, it is unclear if this addition would significantly enhance our understanding of GPCR signaling.

Eventually it will be possible to include explicitly the effects of each unique G—protein species, but in the short term it may not be required. Changes in G—proteins most likely have subtle effects on the signaling process. Predicting these effects will not be possible until the downstream signaling events are better characterized. As such these subtle changes will have to remain noise.

The more details included in our picture of signaling, the more apparent the value of modeling. By including the roles of many different proteins, we generate a complicated reaction network of time varying reaction and diffusion events a system that is nearly impossible to understand without modeling. This system is not amenable to a reductionist solution, for it is the interaction of these many different proteins that give rise to the cellular response. Therefore, pharmacological models must move toward analyzing the collective behavior of the many parts in this complex system.

APPNDIX A

MODEL EQUATIONS FROM CHAPTER 4

Below I provide additional information about the models and model results generated in Chapter 4. In sections A.1 and A.2, I provide differential material balances for the whole cell model. Note that for simplicity the model in Figure 4.3 only shows ligand A binding, however in the simulations two ligands, A, a tracer, and B, a test ligand are used. The balances include both A and B.

Section A.3 provides the complete analytical solution of the signal response when G-protein conservation is included. This result shows that the efficacy of the tracer ligand can play a role, but in a strongly nonlinear way.

A.1 Differential material balances for the whole cell model

$$\frac{d[R]}{dt} = -k_{fA}[R][A] - k_{fB}[R][B] - k_1[R] + \frac{k_{fA}}{K_{aA}}[AR] + \frac{k_{fB}}{K_{aB}}[BR] + \frac{k_1}{K_{ACT}}[R^*]$$

$$\frac{d[AR]}{dt} = k_{fA}[R][A] + \frac{k_1}{K_{ACT}}[AR^*] - \frac{k_{fA}}{K_{aA}}[AR] - \alpha_A k_1[AR]$$

$$\frac{d[BR]}{dt} = k_{fB}[R][B] + \frac{k_1}{K_{ACT}}[BR^*] - \frac{k_{fB}}{K_{aB}}[BR] - \alpha_B k_1[BR]$$

$$\begin{aligned} \frac{d[AR^*]}{dt} = & \alpha_A k_{fA}[R^*][A] + \alpha_A k_1[AR] + \frac{k_{a1}}{K_G}[AR * G] - \frac{k_{fA}}{K_{aA}}[AR^*] - \frac{k_1}{K_{ACT}}[AR^*] \\ & - \beta_A k_{a1}[AR^*][G] + k_{r1}[AR * G] \end{aligned}$$

$$\begin{aligned} \frac{d[\text{BR}^*]}{dt} &= \alpha_B k_{fB} [\text{R}^*][\text{B}] + \alpha_B k_1 [\text{BR}] + \frac{k_{a1}}{K_G} [\text{BR}^* \text{G}] - \frac{k_{fB}}{K_{aB}} [\text{BR}^*] - \frac{k_1}{K_{ACT}} [\text{BR}^*] \\ &\quad - \beta_B k_{a1} [\text{BR}^*][\text{G}] + k_{r1} [\text{BR}^* \text{G}] \end{aligned}$$

$$\begin{aligned} \frac{d[\text{AR}^* \text{G}]}{dt} &= \beta_A k_{a2} [\text{AR}^*][\text{G}] + \alpha_A \beta_A k_{fA} [\text{R}^* \text{G}][\text{A}] - \frac{k_{fA}}{K_{aA}} [\text{AR}^* \text{G}] \\ &\quad - \frac{k_{a2}}{K_G} [\text{AR}^* \text{G}] - k_{r1} [\text{AR}^* \text{G}] \end{aligned}$$

$$\begin{aligned} \frac{d[\text{BR}^* \text{G}]}{dt} &= \beta_B k_{a2} [\text{BR}^*][\text{G}] + \alpha_B \beta_B k_{fB} [\text{R}^* \text{G}][\text{B}] - \frac{k_{fB}}{K_{aB}} [\text{BR}^* \text{G}] \\ &\quad - \frac{k_{a2}}{K_G} [\text{BR}^* \text{G}] - k_{r1} [\text{BR}^* \text{G}] \end{aligned}$$

$$\begin{aligned} \frac{d[\text{R}^*]}{dt} &= k_1 [\text{R}] + \frac{k_{fA}}{K_{aA}} [\text{AR}^*] + \frac{k_{fB}}{K_{aB}} [\text{BR}^*] + \frac{k_{a1}}{K_G} [\text{R}^* \text{G}] - \frac{k_1}{K_{ACT}} [\text{R}^*] - \alpha_A k_{fA} [\text{R}^*][\text{A}] \\ &\quad - \alpha_B k_{fB} [\text{R}^*][\text{B}] - k_{a1} [\text{R}^*][\text{G}] + k_{r1} [\text{R}^* \text{G}] \end{aligned}$$

$$\begin{aligned} \frac{d[\text{R}^* \text{G}]}{dt} &= k_{a1} [\text{R}^*][\text{G}] + \frac{k_{fA}}{K_{aA}} [\text{AR}^* \text{G}] + \frac{k_{fB}}{K_{aB}} [\text{BR}^* \text{G}] - \alpha_A \beta_A k_{fA} [\text{R}^* \text{G}][\text{A}] \\ &\quad - \alpha_B \beta_B k_{fB} [\text{R}^* \text{G}][\text{B}] - \frac{k_{a1}}{K_G} [\text{R}^* \text{G}] - k_{r1} [\text{R}^* \text{G}] \end{aligned}$$

$$\begin{aligned} \frac{d[\text{G}]}{dt} &= -k_{a1} [\text{R}^*][\text{G}] - \beta_A k_{a2} [\text{AR}^*][\text{G}] - \beta_B k_{a2} [\text{BR}^*][\text{G}] + \frac{k_{a1}}{K_G} [\text{R}^* \text{G}] \\ &\quad + \frac{k_{a2}}{K_G} [\text{AR}^* \text{G}] + k_{c3} [\beta\gamma][\alpha - \text{GDP}] \end{aligned}$$

$$\frac{d[\alpha - \text{GTP}]}{dt} = k_{r1} ([\text{AR}^* \text{G}] + [\text{BR}^* \text{G}]) + k_{r1} [\text{R}^* \text{G}] - k_i [\alpha - \text{GTP}]$$

$$\frac{d[\beta\gamma]}{dt} = k_{r1} ([\text{AR}^* \text{G}] + [\text{BR}^* \text{G}]) + k_{r1} [\text{R}^* \text{G}] - k_{c3} [\alpha - \text{GDP}][\beta\gamma]$$

$$\frac{d[\alpha - \text{GDP}]}{dt} = k_i [\alpha - \text{GTP}] - k_{c3} [\alpha - \text{GDP}][\beta\gamma]$$

A.2 Differential material balances for the membrane binding assay model

$$\frac{d[R]}{dt} = -k_{fA}[R][A] - k_{fB}[R][B] - k_1[R] + \frac{k_{fA}}{K_{aA}}[AR] + \frac{k_{fB}}{K_{aB}}[BR] + \frac{k_1}{K_{ACT}}[R^*]$$

$$\frac{d[AR]}{dt} = k_{fA}[R][A] + \frac{k_1}{K_{ACT}}[AR^*] - \frac{k_{fA}}{K_{aA}}[AR] - \alpha_A k_1[AR]$$

$$\frac{d[BR]}{dt} = k_{fB}[R][B] + \frac{k_1}{K_{ACT}}[BR^*] - \frac{k_{fB}}{K_{aB}}[BR] - \alpha_B k_1[BR]$$

$$\begin{aligned} \frac{d[R^*]}{dt} = & k_1[R] + \frac{k_{fA}}{K_{aA}}[AR^*] + \frac{k_{fB}}{K_{aB}}[BR^*] + \frac{k_{a1}}{K_G}[R^*G] - \frac{k_1}{K_{ACT}}[R^*] - \alpha_A k_{fA}[R^*][A] \\ & - \alpha_B k_{fB}[R^*][B] - k_{a1}[R^*][G] \end{aligned}$$

$$\frac{d[AR^*]}{dt} = \alpha_A k_{fA}[R^*][A] + \alpha_A k_1[AR] + \frac{k_{a1}}{K_G}[AR^*G] - \frac{k_{fA}}{K_{aA}}[AR^*] - \frac{k_1}{K_{ACT}}[AR^*] - \beta_A k_{a1}[AR^*][G]$$

$$\frac{d[BR^*]}{dt} = \alpha_B k_{fB}[R^*][B] + \alpha_B k_1[BR] + \frac{k_{a1}}{K_G}[BR^*G] - \frac{k_{fB}}{K_{aB}}[BR^*] - \frac{k_1}{K_{ACT}}[BR^*] - \beta_B k_{a1}[BR^*][G]$$

$$\begin{aligned} \frac{d[R^*G]}{dt} = & k_{a1}[R^*][G] + \frac{k_{fA}}{K_{aA}}[AR^*G] + \frac{k_{fB}}{K_{aB}}[BR^*G] - \alpha_A \beta_A k_{fA}[R^*G][A] \\ & - \alpha_B \beta_B k_{fB}[R^*G][B] - \frac{k_{a1}}{K_G}[R^*G] \end{aligned}$$

$$\frac{d[AR^*G]}{dt} = \beta_A k_{a2}[AR^*][G] + \alpha_A \beta_A k_{fA}[R^*G][A] - \frac{k_{fA}}{K_{aA}}[AR^*G] - \frac{k_{a2}}{K_G}[AR^*G]$$

$$\frac{d[BR^*G]}{dt} = \beta_B k_{a2}[BR^*][G] + \alpha_B \beta_B k_{fB}[R^*G][B] - \frac{k_{fB}}{K_{aB}}[BR^*G] - \frac{k_{a2}}{K_G}[BR^*G]$$

A.3 Effect of tracer ligand efficacy with G-protein conservation

The equilibrium signal ratio shown in Eqn. 4.4 assumes that the total number of free G-proteins does not change appreciably. If this assumption is violated then the efficacy of the tracer ligand *can* play a role.

Below is the analytical solution of the equilibrium signal ratio when the G-protein concentration is constrained to a total of Gtot.

$$\begin{aligned}
& -((1 + A Kaa + Kact - A^2 Kaa^2 Kact \alpha a^2 \beta a)(-1 + Kact(-1 + Gtot Kg - Kg Rtot) + 2 A^2 Kaa^2 Kact \alpha a^2 \beta a + \\
& \quad A Kaa(-1 + Kact(\alpha a + Gtot Kg \alpha a \beta a)) - \sqrt{(4 Kact Kg Rtot(1 + A Kaa + Kact - A^2 Kaa^2 Kact \alpha a^2 \beta a) + \\
& \quad (1 + Kact + Gtot Kact Kg - Kact Kg Rtot + A Kaa(1 + Kact \alpha a + Gtot Kact Kg \alpha a \beta a))^2})) \\
& (1 + Kact + Gtot Kact Kg - Kact Kg Rtot + A Kaa(1 + Kact(\alpha a + Gtot Kg \alpha a \beta a)) + \\
& \quad B Kab(1 + Kact \alpha b(1 + Gtot Kg \beta b - Kg Rtot \beta b)) - \\
& \quad \sqrt{(4 Kact Kg Rtot(-A^2 Kaa^2 Kact \alpha a^2 \beta a + (1 + B Kab + Kact + B Kab Kact \alpha b)(1 + B Kab \alpha b \beta b) + \\
& \quad A(Kaa + B Kaa Kab \alpha b \beta b)) + (1 + Kact + Gtot Kact Kg - Kact Kg Rtot + \\
& \quad A Kaa(1 + Kact(\alpha a + Gtot Kg \alpha a \beta a)) + B Kab(1 + Kact \alpha b(1 + Gtot Kg \beta b - Kg Rtot \beta b)))^2})) \\
& (A^2 Kaa^2 Kact \alpha a^2 \beta a(1 + Kact(\alpha a + Gtot Kg \alpha a \beta a)) + A Kaa(-1 - B Kab \alpha b \beta b + \\
& \quad Kact^2 \alpha a^2(1 + B Kab \alpha b \beta b + \beta a(-1 + Kg Rtot - B Kab \alpha b + B Kab Kg Rtot \alpha b \beta b)) - \\
& \quad Kact \alpha a \beta a(\alpha a + B Kab \alpha a + Gtot(Kg + B Kab Kg \alpha b \beta b)) - \\
& \quad \alpha a \sqrt{(4 Kact Kg Rtot(-A^2 Kaa^2 Kact \alpha a^2 \beta a + (1 + B Kab + Kact + B Kab Kact \alpha b) \\
& \quad (1 + B Kab \alpha b \beta b) + A(Kaa + B Kaa Kab \alpha b \beta b)) + \\
& \quad (1 + Kact + Gtot Kact Kg - Kact Kg Rtot + A Kaa(1 + Kact \alpha a + Gtot Kact Kg \alpha a \beta a) + \\
& \quad B Kab(1 + Kact \alpha b(1 + Gtot Kg \beta b - Kg Rtot \beta b)))^2})) - \\
& (1 + B Kab \alpha b \beta b)(1 + Kact^2 \alpha a(1 + Kg Rtot + Gtot Kg(-1 + 2 \beta a)) + B Kab \\
& \quad (1 + Kact^2 \alpha a \alpha b(1 + 2 Gtot Kg \beta a - Gtot Kg \beta b + Kg Rtot \beta b) + \\
& \quad Kact(\alpha a + \alpha b + 2 Gtot Kg \alpha a \beta a - Gtot Kg \alpha b \beta b + Kg Rtot \alpha b \beta b)) + \\
& \quad \sqrt{(4 Kact Kg Rtot(-A^2 Kaa^2 Kact \alpha a^2 \beta a + (1 + B Kab + Kact + B Kab Kact \alpha b) \\
& \quad (1 + B Kab \alpha b \beta b) + A(Kaa + B Kaa Kab \alpha b \beta b)) + \\
& \quad (1 + Kact + Gtot Kact Kg - Kact Kg Rtot + A Kaa(1 + Kact(\alpha a + Gtot Kg \alpha a \beta a)) + \\
& \quad B Kab(1 + Kact \alpha b(1 + Gtot Kg \beta b - Kg Rtot \beta b)))^2})) + Kact(1 + Kg Rtot + \alpha a + \\
& \quad Gtot Kg(-1 + 2 \alpha \beta a) + \alpha a \sqrt{(4 Kact Kg Rtot(-A^2 Kaa^2 Kact \alpha a^2 \beta a + (1 + B Kab + \\
& \quad Kact + B Kab Kact \alpha b)(1 + B Kab \alpha b \beta b) + A(Kaa + B Kaa Kab \alpha b \beta b)) + \\
& \quad (1 + Kact + Gtot Kact Kg - Kact Kg Rtot + A Kaa(1 + Kact \alpha a + Gtot Kact Kg \alpha a \beta a) + \\
& \quad B Kab(1 + Kact \alpha b(1 + Gtot Kg \beta b - Kg Rtot \beta b)))^2}))) / \\
& ((1 + Kact + Gtot Kact Kg - Kact Kg Rtot + A Kaa(1 + Kact(\alpha a + Gtot Kg \alpha a \beta a)) - \\
& \quad \sqrt{(4 Kact Kg Rtot(1 + A Kaa + Kact - A^2 Kaa^2 Kact \alpha a^2 \beta a) + \\
& \quad (1 + Kact + Gtot Kact Kg - Kact Kg Rtot + A Kaa(1 + Kact \alpha a + Gtot Kact Kg \alpha a \beta a))^2})) \\
& (-1 - Kact^2 \alpha a(1 + Kg Rtot + Gtot Kg(-1 + 2 \beta a)) + A^2 Kaa^2 Kact \alpha a^2 \beta a \\
& \quad (1 + Kact(\alpha a + Gtot Kg \alpha a \beta a)) - \\
& \quad \sqrt{(4 Kact Kg Rtot(1 + A Kaa + Kact - A^2 Kaa^2 Kact \alpha a^2 \beta a) + \\
& \quad (1 + Kact + Gtot Kact Kg - Kact Kg Rtot + A Kaa(1 + Kact \alpha a + Gtot Kact Kg \alpha a \beta a))^2}) - \\
& \quad Kact(1 + Kg Rtot + \alpha a + Gtot Kg(-1 + 2 \alpha \beta a)) + \\
& \quad \alpha a \sqrt{(4 Kact Kg Rtot(1 + A Kaa + Kact - A^2 Kaa^2 Kact \alpha a^2 \beta a) + \\
& \quad (1 + Kact + Gtot Kact Kg - Kact Kg Rtot + A Kaa(1 + Kact \alpha a + Gtot Kact Kg \alpha a \beta a))^2})) + \\
& \quad A Kaa(-1 + Kact^2 \alpha a^2(1 - \beta a + Kg Rtot \beta a) - Kact \alpha a \beta a(Gtot Kg + \alpha a - \\
& \quad \alpha a \sqrt{(4 Kact Kg Rtot(1 + A Kaa + Kact - A^2 Kaa^2 Kact \alpha a^2 \beta a) + (1 + Kact + Gtot Kact Kg - \\
& \quad Kact Kg Rtot + A Kaa(1 + Kact \alpha a + Gtot Kact Kg \alpha a \beta a))^2}))) \\
& (A^2 Kaa^2 Kact \alpha a^2 \beta a - (1 + Kact + B(Kab + Kab Kact \alpha b))(1 + B Kab \alpha b \beta b) - \\
& \quad A(Kaa + B Kaa Kab \alpha b \beta b)) \\
& (2 A^2 Kaa^2 Kact \alpha a^2 \beta a + A Kaa(-1 + Kact(\alpha a + Gtot Kg \alpha a \beta a))(1 + B Kab \alpha b \beta b) - \\
& \quad (1 + B Kab \alpha b \beta b) \\
& \quad (1 + Kact - Gtot Kact Kg + Kact Kg Rtot + B Kab(1 + Kact \alpha b(1 - Gtot Kg \beta b + Kg Rtot \beta b)) + \\
& \quad \sqrt{(4 Kact Kg Rtot(-A^2 Kaa^2 Kact \alpha a^2 \beta a + (1 + B Kab + Kact + B Kab Kact \alpha b)(1 + B Kab \alpha b \beta b) + \\
& \quad A(Kaa + B Kaa Kab \alpha b \beta b)) + (1 + Kact + Gtot Kact Kg - Kact Kg Rtot + A Kaa \\
& \quad (1 + Kact(\alpha a + Gtot Kg \alpha a \beta a)) + B Kab(1 + Kact \alpha b(1 + Gtot Kg \beta b - Kg Rtot \beta b)))^2})))
\end{aligned}$$

APPENDIX B

EFFECTS OF TOPOLOGY ON DIMERIZATION INDUCED CLUSTERING

B.1 Introduction

In chapter 5 of this thesis, I demonstrated that dimerization alone can induce receptor clustering on a two dimensional surface under diffusion limited conditions. Although this result has direct importance to some receptor signaling processes, it fails to explain how the cell localizes clusters of proteins to a specific *location* on the cell membrane. In some cases this localization is thought to take place around an already existing structure such as part of the cytoskeleton or a cell-cell contact (Bray 1998), although it remains an open question as to why the core structure is where it is.

In this appendix I investigate an alternate route to protein localization driven by dimerization and surface topology alone. The surface of most cells is not a smooth, near flat surface but instead is ruffled with occasional extrusions such as pseudopods and dendrites. One could argue that each of these topological variations is associated with a unique function that would require a unique compliment of proteins. For example, a pseudopod is generally used for both motility and for sensing, thus it might need to have an unusually high density of integrin and chemoattractant receptors in order to be effective.

Intuitively, dimerization induced clustering would seem to be favored on surfaces with a small radius of curvature. For example, consider the hypothetical surface shown

in Figure B1. At the flat part at the base, diffusing receptors would essentially see a 2D environment and as such diffuse fairly rapidly. However, as receptors travel up the surface to smaller radius of curvature areas their local environment transitions from a 2D world to a more 1D world. In this 1D environment, diffusion can only take place along one axis, causing particles to block each other more often and thereby slowing their net movement.



Figure B1 Cell membrane surface that smoothly changes from a two-dimensional surface to a one-dimensional line.

As an analogy, consider merging traffic as shown in Figure B2. Moving from a large ten-lane highway into a small one lane country road results in an increase of traffic density and a greater propensity for traffic jams. Like the receptor case, at low traffic densities, changing from a ten lane to a one lane highway will cause no problems, while at high traffic densities the effects will be more significant. The reason for more traffic problems on the one lane road versus the highway is that on the highway there are more ways to pass each other, thereby relieving any local blockage that may randomly form.

This traffic analogy assumes that receptors have a discrete size on the order of the size of their environment and as such change behaviors at higher receptor densities.

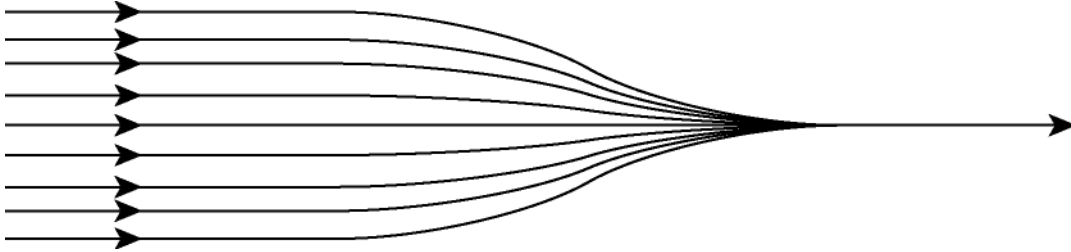


Figure B2 Traffic analogy to illustrate the effect of dimensionality on transport. Moving from a highway with many lanes (two dimensional surface) to a single lane road (one dimensional line) results in a backup of traffic, thereby creating a local change in particle density.

B.2 Discrete and Continuous Diffusion Models

To determine the effect of topology on diffusion, I have employed two spatial modeling approaches which both yielded different results. In the first approach I have used a partial differential equation that describes diffusion to show how a particle should diffuse along a distorted surface. This model predicts that the receptor density should be even at all points. Next I used a Monte Carlo approach to model diffusion with the addition of dimerization to find that receptors should be unevenly distributed along the surface. Both these approaches are widely used in engineering and physics, and therefore present an intriguing contradiction for future research.

As a sample case, imagine a cell membrane defined by the two-dimensional surface of a pyramid as shown in Figure B3. Receptors can be placed on the membrane and allowed to diffuse to observe where they localize. My goal is to find out how the receptors will distribute themselves at equilibrium. I will use PDE, ODE, and MC

methods to analyze this question. The MC work will show how a single particle, then multiple particles will distribute themselves on the membrane. Finally the effects of dimerization will be included. Analytical results will be given where possible.



Figure B3 A two dimensional surface model of a four sided pyramid. This image represents the pyramid from above. This surface can be discretized as five points, with four on the edges and one in the center.

B.2.1 PDE Model of diffusion

This 2D diffusion problem is easily solved using a PDE model. Using Fick's Law, equilibrium diffusion in 2D can be expressed as:

$$\frac{\partial C}{\partial t} = 0 = D \left(\frac{\partial^2 C}{\partial x^2} + \frac{\partial^2 C}{\partial y^2} \right) \quad (\text{B1})$$

Where C is the concentration of the receptor, t is time, x and y are spatial coordinates, and D is the diffusion coefficient. The solution to this equation is a uniform concentration profile across all of x and y for any geometry and is independent of the diffusion coefficient D.

Intuitively this result makes sense. In the mathematically analogous problem of heat conduction, if a block of well-insulated material is started with some temperature gradient, then at infinite time (equilibrium) the block will have a uniform temperature.

B.2.2 ODE Model of Diffusion

This diffusion problem can be changed from a PDE problem to an ODE problem by breaking the pyramid in Figure B1 into discrete points and solving an ODE heat balance on each of those points.

By numbering the corners 1-4, and the center point 5, we can write out 5 steady state mass balances for each of the points:

$$\begin{aligned}
 \frac{dQ_1}{dt} &= 0 = -3kQ_1 + kQ_2 + kQ_3 + kQ_5 \\
 \frac{dQ_2}{dt} &= 0 = -3kQ_2 + kQ_1 + kQ_4 + kQ_5 \\
 \frac{dQ_3}{dt} &= 0 = -3kQ_3 + kQ_1 + kQ_4 + kQ_5 \\
 \frac{dQ_4}{dt} &= 0 = -3kQ_4 + kQ_2 + kQ_3 + kQ_5 \\
 \frac{dQ_5}{dt} &= 0 = -4kQ_5 + kQ_1 + kQ_2 + kQ_3 + kQ_4
 \end{aligned} \tag{B2}$$

Where Q_n is the mass at point n , and k is the mass transfer coefficient. The coefficients that modify each contribution are defined by the number of connections that site has to the other sites. Therefore, site 5 (the center point) loses mass to its four neighbors ($-4kQ_5$) while also gaining mass from its neighbors ($+kQ_1+kQ_2+kQ_3+kQ_4$).

When solved for steady state behavior we find that the mass concentration at all sites will be equal. This finding is identical to the results found using the PDE model and is based on similar assumptions.

B.2.3 MC Model for Single Particle Diffusion

Similar to the ODE model, the diffusion problem can be approached using a MC simulation of a single particle exploring the vertices in Figure B3. This simulation can be done by either allowing a single particle to jump from site to site and gathering statistics or it can be done on the basis of probability both of which give the same result.

To follow the probability of finding a particle at any given site, I begin with a particle at any site, say the center (position 5), at time equals zero. In the next time step the particle will be in 1 of 4 of the corners, each with a 25% probability. In the next time step, the particle in the corner then has a 33% probability of moving back to the center,

and a 33% probability of moving to each of its neighboring corners. This process can be iterated until the system reaches steady state. A sample output of an Excel workbook doing this calculation is shown in Table B1 below:

<u>Site 1</u>	<u>Site 2</u>	<u>Site 3</u>	<u>Site 4</u>	<u>Site 5</u>
0	0	0	0	1
0.25	0.25	0.25	0.25	0
0.167	0.167	0.167	0.167	0.333
0.194	0.194	0.194	0.194	0.222
0.185	0.185	0.185	0.185	0.259
0.188	0.188	0.188	0.188	0.247
0.187	0.187	0.187	0.187	0.251
0.188	0.188	0.188	0.188	0.250
0.187	0.187	0.187	0.187	0.250
0.188	0.188	0.188	0.188	0.250
0.187	0.187	0.187	0.187	0.250

Table B1 Numerical output predicting the probability distribution of a single particle on a 5-point grid in Figure B3. Each row represents a single iteration; notice that a steady state is reached. Note that the resulting equilibrium distribution favors the center site (site 5).

The results generated with this MC simulation clearly disagree with the PDE and ODE models because it predicts that the particle will spend more time in the center site than the edge sites!

The procedure used to generate this MC model can be generalized in a graph theoretic way for any system analytically. The way this is done is by counting the number of feeds into a vertex (called valence in graph theoretic terms) and dividing this by the total number of internal feeds in the system (i.e. the total number of arrowheads). For the system in Figure B3, there are a total of 16 feeds (8 lines that connect points, each line has an arrow head at each end). For the center site (site 5) there are 4 feeds in, resulting in a probability of occupancy of $4/16$ or 0.25. For the corner sites there are 3 feeds, resulting in a probability of occupancy of $3/16$ or 0.1875. I have tested this procedure on other systems and have thus far found it to be general.

Which method, MC or PDE, is right? Both MC methods and PDE methods are widely used to simulate diffusion, but they both give different answers. The PDE results make intuitive sense when compared to the heat equation. However, the MC result also makes sense because the center site is the most crossed site (most connected site) and as such would be expected to see the most traffic. The big difference is that the MC system tracks only one indivisible particle, while the PDE/ODE techniques follow a continuum. Is this a disagreement caused by the continuous to discrete assumptions of the models?

B.2.2.1 MC Simulation of two particles

If MC and PDE models diverge because the first is discrete and the second is continuous, adding another particle to the MC model may bring the MC simulation closer to the PDE result.

The techniques used to model two particles are more complicated than for one particle. First I enumerated all of the possible combinations of two particles on a 5-site grid (10 possible configurations). Then I connected these configurations together into a graph of graphs, as is shown in Figure B4.

Using the analytical probability occupancy techniques introduced for a single particle, it is possible to determine the probability of each state in Figure B4, which in turn can be used to predict the probability of occupancy of each site on the 5-site grid. For example, in Figure B4, there are a total of 48 feeds (green arrowheads). States 1-4 each have a valence of 4 (4 feeds in), states 5-8 have a valence of 5, and states 9-10 have a valence of 6. Therefore there is a $4/48$ chance of finding state 1, a $5/48$ chance of finding state 5, and a $6/48$ chance of finding state 9. Because only states 5-8 have a particle in the middle, these states will determine the total probability of finding a particle at this site. The result is that there is a $4*(5/48)=20/48$ probability of finding a particle in the center, versus a $19/48$ probability of finding a particle on the edge.

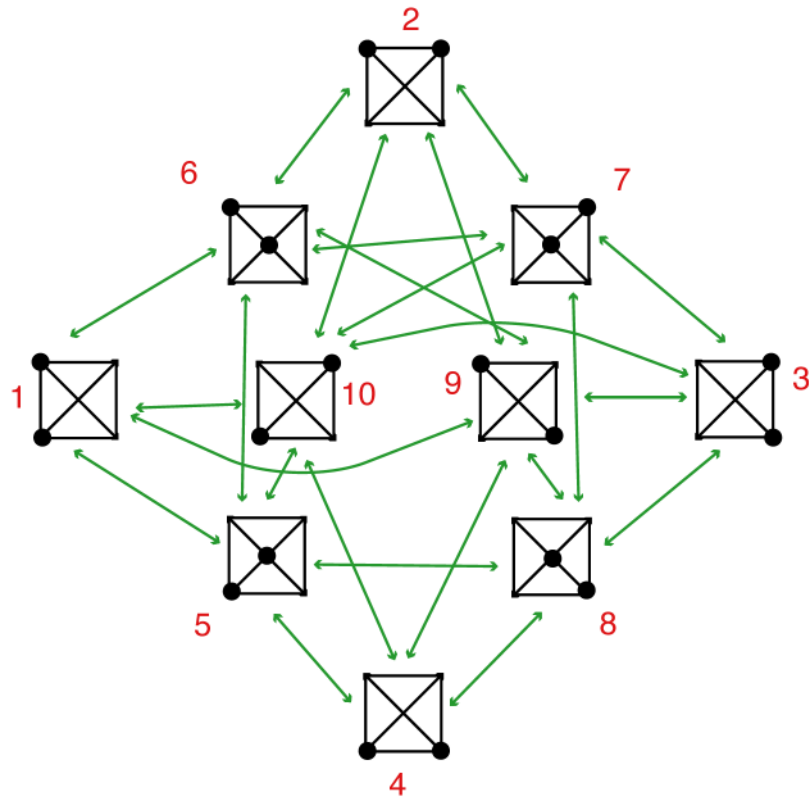


Figure B4 A graphical representation of all of the possible transitions that can be made in a two-particle system on a 5-site grid.

Although this result predicts that there is still an increased likelihood of finding a particle in the center vs. the edge, the magnitude is smaller. Therefore, so called crowding effects in this system seem to drive the result more toward the PDE model, while single receptor dynamics deviate the most from the PDE model.

B.2.2.2 MC model with dimerization:

Dimerization of receptors can be included in this simple 5-site model fairly simply. The easiest case would be to assume irreversible dimerization. Irreversible dimerization eliminates states 9 and 10 from Figure B4. Following the procedure described above I found that dimerization increases the probability of finding a particle on the center site to $4/9$. To compare this to the non-dimerized state we get:

$$P_{\text{center}} \text{ with dimerization} = 4/9 = 0.44444$$

$$P_{\text{center}} \text{ w/o dimerization} = 20/48 = 0.41666$$

Therefore dimerization induces the particle to spend more time at the center site, encouraging a greater divergence with the PDE result.

This model can be modified to include dimerization probabilities by enlarging the graph in Figure B4 to include monomeric and dimeric species along with weighted probabilities for dimerization and monomerization. This work is expected to be tedious to do analytically and would most likely show an intermediate behavior for this system. This result would be interesting for larger systems and is modeled in the next section using MC methods.

B.3 Direct Comparisons of models

To compare different models with different numbers of particles, I will use the *enrichment factor*, ϵ , defined as the increased probability of finding a particle at a particular site or region in comparison to an even distribution. For example, using an MC method, a single particle in a 5-site world has a 25% probability of being in the center versus an 18.75% probability being at the corner. Because there are 5 sites, a PDE model would predict an equal distribution of 20% probability at any site. Therefore the enrichment factor of the center site in the MC over PDE model is $(25/20-1) = 25\%$. This same procedure can be performed for the two-particle system and the MC simulations to get the following results:

Center site of:

PDE/ ODE models	0.000%
5 site MC with 1 particle	25.000%
5 site MC with 2 particles w/o dimerization	4.166%
5 site MC with 2 particles w/ dimerization	11.111%

This same procedure was used on a much larger model with 1119 sites that consisted of a flat region and a thin tube region much like the surface shown in Figure B1. The trend of enrichment factors is the same, although the specific values are different:

Tube fraction from large scale MC simulations:

PDE model	0.000%
1119 site MC with 1 particle	6.413%
1119 site MC with 32 particles w/o dimerization	4.082%
1119 site MC with 32 particles w/ dimerization	5.841%

Therefore at any scale, the relative order of the enrichment factor is the same for all of the systems tested. Single particles deviate most from the PDE models, while multiple particles help to bring the system closer to the PDE solution. Dimerization causes an intermediate solution.

These results show that dimerization **does** cause particles to attract to small radius of curvature areas because it makes them more single-point-like. This effect is not large, but is statically relevant and can be demonstrated for larger systems.

B.2.4 Conclusion

According to the MC simulations performed in this work, particles should self—localize to small radius of curvature areas. This effect is enhanced by dimerization, but is maximal when only one particle is present.

This MC finding is in direct contrast to the PDE prediction, most likely due to the assumptions both models make. A key difference between MC and PDE models is that in MC environment particles have finite areas, while in the PDE model they are infinitely small. From a radius of curvature viewpoint, only particles with finite area can detect a finite change in curvature, while to infinitely small particles all points appear to be flat.

Physically this means that particles in the MC simulation can block each other, while in the PDE they cannot.

The MC approach used in this work was also based on a discrete grid, which may also bias these findings. Future simulations that are run in a continuous environment could remove any uncertainty associated with the grid while also making the findings more palatable to a general audience. I suspect that both on and off the grid, one would find that discrete diffusion will favor locations with a small radius of curvature, but more work needs to be done to validate this hypothesis.

In biological systems, diffusion on nonflat surfaces could play a key physiological role. Small radius of curvature surfaces such as the surface of an endosome or the golgi body may affect the trafficking of single proteins, while larger radius of curvatures such as those on a dendrite may affect larger objects such as protein clusters. Therefore future work will need to focus on finding the relevant length scale where this kind of topology induced clustering takes place.

Thus, although the effects of radius of curvature on diffusion are currently inconclusive, they are intriguing and could provide a major advance to our understanding of protein localization within the cell.

BIBLIOGRAPHY

BIBLIOGRAPHY

- AbdAlla, S., E. Zaki, H. Lothar and U. Quitterer (1999). "Involvement of the amino terminus of the B(2) receptor in agonist-induced receptor dimerization." J Biol Chem **274**(37): 26079-84.
- Adams, J. A., G. M. Omann and J. J. Linderman (1998). "A mathematical model for ligand/receptor/G-protein dynamics and actin polymerization in human neutrophils." Journal of Theoretical Biology **193**(4): 543-560.
- Allison, S. A., S. H. Northrup and J. A. McCammon (1986). "Simulation of biomolecular diffusion and complex formation." Biophys J **49**(1): 167-75.
- Angers, S., A. Salahpour, E. Joly, S. Hilairret, D. Chelsky, M. Dennis and M. Bouvier (2000). "Detection of beta 2-adrenergic receptor dimerization in living cells using bioluminescence resonance energy transfer (BRET)." Proc Natl Acad Sci U S A **97**(7): 3684-9.
- Aragay, A. M., A. Ruiz-Gomez, P. Penela, S. Sarnago, A. Elorza, M. C. Jimenez-Sainz and F. Mayor (1998). "G protein-coupled receptor kinase 2 (GRK2): mechanisms of regulation and physiological functions." Febs Letters **430**(1-2): 37-40.
- Armstrong, D. and P. G. Strange (2001). "Dopamine D2 receptor dimer formation: evidence from ligand binding." J Biol Chem **276**(25): 22621-9.
- Arvanitakis, L., E. Geras-Raaka and M. C. Gershengorn (1998). "Constitutively Signaling G-Protein-Coupled Receptors and Human Disease." TEM **9**(1): 27-31.
- Asselman, T. and G. Garnier (2000). "Mechanism of polyelectrolyte transfer during heteroflocculation." Langmuir **16**(11): 4871-4876.
- Balmforth, A. J., P. Warburton and S. G. Ball (1990). "Homologous desensitization of the D1 dopamine receptor." J. Neurochem. **55**: 2111-2116.
- Barton, A. C. and D. R. Sibley (1990). "Agonist-induced desensitization of D1-dopamine receptors linked to adenylyl cyclase activity in cultured NS20Y neuroblastoma cells." Mol. Pharm. **38**: 531-541.
- Beisker, W. and W. G. Eisert (1985). "Double-beam autocompensation for fluorescence polarization measurements in flow cytometry." Biophys J **47**(5): 607-12.
- Benovic, J. L., C. Staniszewski, F. Mayor, Jr., M. G. Caron and R. J. Lefkowitz (1988). "beta-Adrenergic receptor kinase. Activity of partial agonists for stimulation of

adenylate cyclase correlates with ability to promote receptor phosphorylation." J Biol Chem **263**(8): 3893-7.

Berman, D. M. and A. G. Gilman (1998). "Mammalian RGS proteins: Barbarians at the gate." Journal of Biological Chemistry **273**(3): 1269-1272.

Blake, A. D., G. Bot, J. C. Freeman and T. Reisine (1997). "Differential opioid agonist regulation of the mouse μ opioid receptor." J. Biol. Chem. **272**: 782-790.

Blane, G. F., A. L. Boura, A. E. Fitzgerald and R. E. Lister (1967). "Actions of etorphine hydrochloride, (M99): a potent morphine-like agent." Br J Pharmacol **30**(1): 11-22.

Bokoch, G. M., K. Bickford and B. P. Bohl (1988). "Subcellular localization and quantitation of the major neutrophil pertussis toxin substrate, Gn." J. Cell Biol. **106**: 1927-1936.

Bond, R. A., P. Leff, T. D. Johnson, C. A. Milano, H. A. Rockman, T. R. McMinn, S. Apparsundaram, M. F. Hyek, T. P. Kenakin, L. F. Allen and et al. (1995). "Physiological effects of inverse agonists in transgenic mice with myocardial overexpression of the beta 2-adrenoceptor [see comments]." Nature **374**(6519): 272-6.

Bosworth, N. and P. Towers (1989). "Scintillation proximity assay." Nature **341**(6238): 167-8.

Brauner-Osborne, H. and M. R. Brann (1996). "Pharmacology of muscarinic acetylcholine receptor subtypes (m1-m5): high throughput assays in mammalian cells." Eur J Pharmacol **295**(1): 93-102.

Bray, D. (1998). "Signaling complexes: biophysical constraints on intracellular communication." Annu Rev Biophys Biomol Struct **27**: 59-75.

Burke, C. L. and D. F. Stern (1998). "Activation of Neu (ErbB-2) mediated by disulfide bond-induced dimerization reveals a receptor tyrosine kinase dimer interface." Mol Cell Biol **18**(9): 5371-9.

Chidiac, P., S. Nouet and M. Bouvier (1996). "Agonist-induced modulation of inverse agonist efficacy at the beta 2-adrenergic receptor." Molecular Pharmacology **50**(3): 662-9.

Chuang, T. T., L. Iacovelli, M. Sallese and A. De Blasi (1996). "G protein-coupled receptors: heterologous regulation of homologous desensitization and its implications." Trends Pharmacol Sci **17**(11): 416-21.

- Ciruela, F., C. Saura, E. I. Canela, J. Mallol, C. Lluís and R. Franco (1997). "Ligand-induced phosphorylation, clustering, and desensitization of A1 adenosine receptors." Mol Pharmacol **52**(5): 788-97.
- Collins, F. S. and K. G. Jegalian (1999). Deciphering the Code of Life. Scientific American. **281**: 86-91.
- Colquhoun, D. (1987). Affinity, Efficacy, and Receptor Classification: Is the Classical Theory Still Useful? Perspectives on Receptor Classification. J. W. Black, D. H. Jenkinson and V. P. Gerskowich. New York, Alan R. Liss, Inc.: 103-114.
- Cornea, A., J. A. Janovick, G. Maya-Nunez and P. M. Conn (2001). "Gonadotropin-releasing hormone receptor microaggregation. Rate monitored by fluorescence resonance energy transfer." J Biol Chem **276**(3): 2153-8.
- Costa, T. and A. Herz (1989). "Antagonists with negative intrinsic activity at delta opioid receptors coupled to GTP-binding proteins." Proc Natl Acad Sci U S A **86**(19): 7321-5.
- Cotecchia, S., S. Exum, M. G. Caron and R. J. Lefkowitz (1990). "Regions of the alpha 1-adrenergic receptor involved in coupling to phosphatidylinositol hydrolysis and enhanced sensitivity of biological function." Proc Natl Acad Sci U S A **87**(8): 2896-900.
- Crain, S. M. and K. F. Shen (2000). "Antagonists of excitatory opioid receptor functions enhance morphine's analgesic potency and attenuate opioid tolerance/dependence liability." Pain **84**(2-3): 121-31.
- Cvejic, S. and L. A. Devi (1997). "Dimerization of the delta opioid receptor: implication for a role in receptor internalization." J Biol Chem **272**(43): 26959-64.
- De Lean, A., B. F. Kilpatrick and M. G. Caron (1982). "Dopamine receptor of the porcine anterior pituitary gland. Evidence for two affinity states discriminated by both agonists and antagonists." Mol Pharmacol **22**(2): 290-7.
- Drews, J. (2000). "Drug discovery: a historical perspective." Science **287**(5460): 1960-4.
- Durstin, M., S. R. McColl, J. Gomez-Cambronero, P. H. Naccache and R. I. Sha'afi (1993). "Up-regulation of the amount of Gia2 associated with the plasma membrane in human neutrophils stimulated by granulocyte-macrophage colony stimulating factor." Biochem. J. **292**: 183-187.
- Elorza, A., S. Sarnago and F. Mayor (2000). "Agonist-dependent modulation of G protein-coupled receptor kinase 2 by mitogen-activated protein kinases." Molecular Pharmacology **57**(4): 778-783.

- Fay, S. P., R. G. Posner, W. N. Swann and L. A. Sklar (1991). "Real-time analysis of the assembly of ligand, receptor, and G-protein by quantitative fluorescence flow cytometry." Biochem. **30**: 5066-5075.
- Florio, V. A. and P. C. Sternweis (1989). "Mechanisms of muscarinic receptor action on Go in reconstituted phospholipid vesicles." J Biol Chem **264**(7): 3909-15.
- Fogler, H. S. (1999). Elements of chemical reaction engineering. Upper Saddle River, N.J., Prentice Hall PTR.
- Fonseca, M. I., D. C. Button and R. D. Brown (1995). "Agonist regulation of alpha 1B-adrenergic receptor subcellular distribution and function." J Biol Chem **270**(15): 8902-9.
- Gardina, P. J. and M. D. Manson (1996). "Attractant signaling by an aspartate chemoreceptor dimer with a single cytoplasmic domain." Science **274**(5286): 425-6.
- Gennis, R. B. (1989). Biomembranes: Molecular Structure and Function. New York, Springer-verlag.
- George, S. R., T. Fan, Z. Xie, R. Tse, V. Tam, G. Varghese and B. F. O'Dowd (2000). "Oligomerization of mu- and delta-opioid receptors. Generation of novel functional properties." J Biol Chem **275**(34): 26128-35.
- Gheber, L. A. and M. Edidin (1999). "A model for membrane patchiness: Lateral diffusion in the presence of barriers and vesicle traffic." Biophysical Journal **77**(6): 3163-3175.
- Gines, S., J. Hillion, M. Torvinen, S. Le Crom, V. Casado, E. I. Canela, S. Rondin, J. Y. Lew, S. Watson, M. Zoli, L. F. Agnati, P. Verniera, C. Lluis, S. Ferre, K. Fuxe and R. Franco (2000). "Dopamine D1 and adenosine A1 receptors form functionally interacting heteromeric complexes." Proc Natl Acad Sci U S A **97**(15): 8606-11.
- Gomes, I., B. A. Jordan, A. Gupta, C. Rios, N. Trapaidze and L. A. Devi (2001). "G protein coupled receptor dimerization: implications in modulating receptor function." J Mol Med **79**(5-6): 226-42.
- Gomes, I., B. A. Jordan, A. Gupta, N. Trapaidze, V. Nagy and L. A. Devi (2000). "Heterodimerization of mu and delta opioid receptors: A role in opiate synergy." J Neurosci **20**(22): RC110.
- Graeser, D. and R. R. Neubig (1993). "Compartmentation of receptors and guanine nucleotide-binding proteins in NG108-15 cells: lack of cross-talk in agonist

- binding among the alpha 2-adrenergic, muscarinic, and opiate receptors." Mol Pharmacol **43**(3): 434-43.
- Hall, R. A., R. T. Premont and R. J. Lefkowitz (1999). "Heptahelical receptor signaling: beyond the G protein paradigm." J Cell Biol **145**(5): 927-32.
- Hamm, H. E. (1990). "Surfaces of interaction between Gt and rhodopsin in the GDP-bound and empty-pocket configurations." Adv Second Messenger Phosphoprotein Res **24**: 76-82.
- Hamm, H. E. (1998). "The many faces of G protein signaling." Journal of Biological Chemistry **273**(2): 669-672.
- Hebert, T. E. and M. Bouvier (1998). "Structural and functional aspects of G protein-coupled receptor oligomerization." Biochem Cell Biol **76**(1): 1-11.
- Hebert, T. E., S. Moffett, J. P. Morello, T. P. Loisel, D. G. Bichet, C. Barret and M. Bouvier (1996). "A peptide derived from a beta2-adrenergic receptor transmembrane domain inhibits both receptor dimerization and activation." J Biol Chem **271**(27): 16384-92.
- Hemmila, I., S. Dakubu, V. M. Mikkala, H. Siitari and T. Lovgren (1984). "Europium as a label in time-resolved immunofluorometric assays." Anal Biochem **137**(2): 335-43.
- Hill, C. G. (1977). An introduction to chemical engineering kinetics & reactor design. New York, Wiley.
- Hoffman, J. F., M. L. Keil, T. A. Riccobene, G. M. Omann and J. J. Linderman (1996). "Interconverting receptor states at 4 degrees C for the neutrophil N- formyl peptide receptor." Biochemistry **35**(40): 13047-55.
- Hoffman, J. F., J. J. Linderman and G. M. Omann (1996). "Receptor up-regulation, internalization, and interconverting receptor states. Critical components of a quantitative description of N-formyl peptide-receptor dynamics in the neutrophil." J Biol Chem **271**(31): 18394-404.
- Jahns, P. and H. W. Trissl (1997). "Indications for a dimeric organization of the antenna-depleted reaction center core of Photosystem II in thylakoids of intermittent light grown pea plants." Biochimica Et Biophysica Acta-Bioenergetics **1318**(1-2): 1-5.
- January, B., A. Seibold, B. Whaley, R. W. Hipkin, D. Lin, A. Schonbrunn, R. Barber and R. B. Clark (1997). "beta2-adrenergic receptor desensitization, internalization, and phosphorylation in response to full and partial agonists." J Biol Chem **272**(38): 23871-9.

- Jayawickreme, C. K., S. P. Jayawickreme and M. R. Lerner (1998). "Functional screening of multiuse peptide libraries using melanophore bioassay." Methods Mol Biol **87**: 119-28.
- Jin, T., N. Zhang, Y. Long, C. A. Parent and P. N. Devreotes (2000). "Localization of the G protein beta gamma complex in living cells during chemotaxis." Science **287**(5455): 1034-1036.
- Jordan, B. A., S. Cvejic and L. A. Devi (2000). "Kappa opioid receptor endocytosis by dynorphin peptides." DNA Cell Biol **19**(1): 19-27.
- Jordan, B. A. and L. A. Devi (1999). "G-protein-coupled receptor heterodimerization modulates receptor function." Nature **399**(6737): 697-700.
- Jordan, B. A., N. Trapaidze, I. Gomes, R. Nivarthi and L. A. Devi (2001). "Oligomerization of opioid receptors with beta 2-adrenergic receptors: a role in trafficking and mitogen-activated protein kinase activation." Proc Natl Acad Sci U S A **98**(1): 343-8.
- Kenakin, T. (1995). "Pharmacological proteus?" Trends Pharmacol Sci **16**(8): 256-8.
- Kenakin, T. (1996). "The classification of seven transmembrane receptors in recombinant expression systems." Pharmacol Rev **48**(3): 413-63.
- Kenakin, T. (1997). "Protean agonists. Keys to receptor active states?" Ann NY Acad Sci **812**: 116-25.
- Kenakin, T. P. (1996). "Receptor conformational induction versus selection: All part of the same energy landscape." Trends Pharm. Sci. **17**: 190-191.
- Klein, U., C. Muller, P. Chu, M. Birnbaumer and M. von Zastrow (2001). "Heterologous inhibition of G protein-coupled receptor endocytosis mediated by receptor-specific trafficking of beta-arrestins." J Biol Chem **276**(20): 17442-7.
- Krumins, A. M. and R. Barber (1997). "Examination of the effects of increasing Gs protein on beta2-adrenergic receptor, Gs, and adenylyl cyclase interactions." Biochem Pharmacol **54**(1): 61-72.
- Krupnick, J. G. and J. L. Benovic (1998). "The role of receptor kinases and arrestins in G protein-coupled receptor regulation." Annu Rev Pharmacol Toxicol **38**: 289-319.
- Lauffenburger, D. A. and J. J. Linderman (1993). Receptors: Models for Binding, Trafficking, and Signaling. New York, Oxford University Press.

- Lawson, C. F., R. A. Mortimore, S. K. Schlachter and M. W. Smith (1994). "Pharmacology of a human dopamine D4 receptor expressed in HEK293 cells." Methods Find Exp Clin Pharmacol **16**(5): 303-7.
- Lefkowitz, R. J. (1998). "G protein-coupled receptors III. New roles for receptor kinases and beta-arrestins in receptor signaling and desensitization." Journal of Biological Chemistry **273**(30): 18677-18680.
- Lefkowitz, R. J., S. Cotecchia, P. Samama and T. Costa (1993). "Constitutive activity of receptors coupled to guanine nucleotide regulatory proteins." Trends Pharmacol Sci **14**(8): 303-7.
- Lefkowitz, R. J., J. Inglese, W. J. Koch, J. Pitcher, H. Attramadal and M. G. Caron (1992). "G-protein-coupled receptors: regulatory role of receptor kinases and arrestin proteins." Cold Spring Harb Symp Quant Biol **57**: 127-33.
- Lerner, M. R. (1994). "Tools for investigating functional interactions between ligands and G- protein-coupled receptors." Trends Neurosci **17**(4): 142-6.
- Lesch, K. P. and H. K. Manji (1992). "Signal-transducing G proteins and antidepressant drugs: Evidence for modulation of a subunit gene expression in rat brain." Biol. Psychiatry **32**: 549-579.
- Lewis, M. M., V. J. Watts, C. P. Lawler, D. E. Nichols and R. B. Mailman (1998). "Homologous desensitization of the D1A dopamine receptor: efficacy in causing desensitization dissociates from both receptor occupancy and functional potency." J Pharmacol Exp Ther **286**(1): 345-53.
- Lin, F. T., W. E. Miller, L. M. Luttrell and R. J. Lefkowitz (1999). "Feedback regulation of beta-arrestin1 function by extracellular signal- regulated kinases." J Biol Chem **274**(23): 15971-4.
- Linderman, J. J. (2000). Kinetic approaches to understanding ligand efficacy. The Pharmacology of Functional, Biochemical, and Recombinant Receptor Systems, Handbook of Experimental Pharmacology. T. P. a. A. Kenakin, J., Springer-Verlag. **148**: 119-146.
- Luttrell, L. M., Y. Daaka and R. J. Lefkowitz (1999). "Regulation of tyrosine kinase cascades by G-protein-coupled receptors." Curr Opin Cell Biol **11**(2): 177-83.
- Maggio, R., P. Barbier, A. Colelli, F. Salvadori, G. Demontis and G. U. Corsini (1999). "G protein-linked receptors: pharmacological evidence for the formation of heterodimers." J Pharmacol Exp Ther **291**(1): 251-7.
- Mahama, P. A. and J. J. Linderman (1994). "A Monte Carlo study of the dynamics of G-protein activation." Biophys J **67**(3): 1345-57.

- Mahama, P. A. and J. J. Linderman (1995). "Monte Carlo simulations of membrane signal transduction events: effect of receptor blockers on G-protein activation." Ann Biomed Eng **23**(3): 299-307.
- Mathis, G. (1995). "Probing molecular interactions with homogeneous techniques based on rare earth cryptates and fluorescence energy transfer." Clin Chem **41**(9): 1391-7.
- Milligan, G. and R. A. Bond (1997). "Inverse agonism and the regulation of receptor number." Trends Pharmacol Sci **18**(12): 468-74.
- Nasir, M. S. and M. E. Jolley (1999). "Fluorescence polarization: an analytical tool for immunoassay and drug discovery." Comb Chem High Throughput Screen **2**(4): 177-90.
- Neer, E. J. (1995). "Heterotrimeric G proteins: Organizers of transmembrane signals." Cell **80**: 249-257.
- Nestler, E. J. and G. K. Aghajanian (1997). "Molecular and cellular basis of addiction." Science **278**(5335): 58-63.
- Neubig, R. R. (1994). "Membrane organization in G-protein mechanisms." Faseb J **8**(12): 939-46.
- Neubig, R. R. and L. A. Sklar (1993). "Subsecond modulation of formyl peptide-linked guanine nucleotide-binding proteins by guanosine 5'-O-(3-thio)triphosphate in permeabilized neutrophils." Molec. Pharm. **43**: 734-740.
- Nimchinsky, E. A., P. R. Hof, W. G. M. Janssen, J. H. Morrison and C. Schmauss (1997). "Expression of dopamine D3 receptor dimers and tetramers in brain and in transfected cells." J Biol Chem **272**(46): 29229-37.
- Overton, M. C. and K. J. Blumer (2000). "G-protein-coupled receptors function as oligomers in vivo." Curr Biol **10**(6): 341-4.
- Parent, C. A., B. J. Blacklock, W. M. Froehlich, D. B. Murphy and P. N. Devreotes (1998). "G protein signaling events are activated at the leading edge of chemotactic cells." Cell **95**(1): 81-91.
- Park, Y. W., R. T. Cummings, L. Wu, S. Zheng, P. M. Cameron, A. Woods, D. M. Zaller, A. I. Marcy and J. D. Hermes (1999). "Homogeneous proximity tyrosine kinase assays: scintillation proximity assay versus homogeneous time-resolved fluorescence." Anal Biochem **269**(1): 94-104.

- Penn, R. B., R. A. Panettieri, Jr. and J. L. Benovic (1998). "Mechanisms of acute desensitization of the beta2AR-adenylyl cyclase pathway in human airway smooth muscle." Am J Respir Cell Mol Biol **19**(2): 338-48.
- Pralle, A., P. Keller, E. L. Florin, K. Simons and J. K. Horber (2000). "Sphingolipid-cholesterol rafts diffuse as small entities in the plasma membrane of mammalian cells." J Cell Biol **148**(5): 997-1008.
- Rahmatullah, M. and J. D. Robishaw (1994). "Direct interaction of the alpha and gamma subunits of the G proteins. Purification and analysis by limited proteolysis." J Biol Chem **269**(5): 3574-80.
- Ren, Q., H. Kurose, R. J. Lefkowitz and S. Cotecchia (1993). "Constitutively active mutants of the alpha 2-adrenergic receptor [published erratum appears in J Biol Chem 1994 Jan 14;269(2):1566]." J Biol Chem **268**(22): 16483-7.
- Riccobene, T. (1999). Analysis of G-protein coupled receptor signaling: the relationship between signaling parameters and cellular responses, University of Michigan, Ann Arbor.
- Riccobene, T. A., G. M. Omann and J. J. Linderman (1999). "Modeling activation and desensitization of G-protein coupled receptors - Provides insight into ligand efficacy." Journal of Theoretical Biology **200**(2): 207-222.
- Riccobene, T. A., G. M. Omann and J. J. Linderman (1999). "Modeling activation and desensitization of G-protein coupled receptors provides insight into ligand efficacy [In Process Citation]." J Theor Biol **200**(2): 207-22.
- Rocheville, M., D. C. Lange, U. Kumar, S. C. Patel, R. C. Patel and Y. C. Patel (2000). "Receptors for dopamine and somatostatin: formation of hetero-oligomers with enhanced functional activity." Science **288**(5463): 154-7.
- Rocheville, M., D. C. Lange, U. Kumar, R. Sasi, R. C. Patel and Y. C. Patel (2000). "Subtypes of the somatostatin receptor assemble as functional homo- and heterodimers." J Biol Chem **275**(11): 7862-9.
- Rossier, O., L. Abuin, F. Fanelli, A. Leonardi and S. Cotecchia (1999). "Inverse agonism and neutral antagonism at alpha(1a)- and alpha(1b)-adrenergic receptor subtypes." Mol Pharmacol **56**(5): 858-66.
- Rothman, R. G., Q. Ni and H. Xu (1995). Buprenorphine: A review of the binding literature. Buprenorphine: Combatting drug abuse with a unique opiod. A. Cowan and J. W. Lewis. New York, Wiley-Liss, Inc.: 19-23.
- Roush, W. (1996). "Regulating G protein signaling [news]." Science **271**(5252): 1056-8.

- Rousseau, G., N. Guilbault, A. Da Silva, B. Mouillac, P. Chidiac and M. Bouvier (1997). "Influence of receptor density on the patterns of beta2-adrenoceptor desensitization." European Journal of Pharmacology **326**(1): 75-84.
- Saffman, P. G. and M. Delbruck (1975). "Brownian motion in biological membranes." Proc Natl Acad Sci U S A **72**(8): 3111-3.
- Samama, P., S. Cotecchia, T. Costa and R. J. Lefkowitz (1993). "A mutation-induced activated state of the beta 2-adrenergic receptor. Extending the ternary complex model." J Biol Chem **268**(7): 4625-36.
- Sander, L. M. (2000). "Diffusion-limited aggregation: a kinetic critical phenomenon?" Contemporary Physics **41**(4): 203-218.
- Savageau, M. A. (1998). "Development of fractal kinetic theory for enzyme-catalysed reactions and implications for the design of biochemical pathways." Biosystems **47**(1-2): 9-36.
- Saxton, M. J. (1989). "The spectrin network as a barrier to lateral diffusion in erythrocytes. A percolation analysis." Biophys J **55**(1): 21-8.
- Scaramellini, C. and P. Leff (1998). "A three-state receptor model: predictions of multiple agonist pharmacology for the same receptor type." Ann N Y Acad Sci **861**: 97-103.
- Scheibe, S. D., D. B. Bennett, J. W. Spain, B. L. Roth and C. J. Coscia (1984). "Kinetic evidence for differential agonist binding to bovine hippocampal synaptic membrane opioid receptors." J. Biol. Chem. **259**: 13298-13303.
- Schlessinger, J. and A. Ullrich (1992). "Growth factor signaling by receptor tyrosine kinases." Neuron **9**(3): 383-91.
- Seibold, A., B. Williams, Z. F. Huang, J. Friedman, R. H. Moore, B. J. Knoll and R. B. Clark (2000). "Localization of the sites mediating desensitization of the beta(2)-adrenergic receptor by the GRK pathway." Mol Pharmacol **58**(5): 1162-73.
- Shea, L. and J. J. Linderman (1997). "Mechanistic model of G-protein signal transduction - Determinants of efficacy and effect of precoupled receptors." Biochemical Pharmacology **53**(4): 519-530.
- Shea, L. and J. J. Linderman (1997). "Mechanistic model of G-protein signal transduction. Determinants of efficacy and effect of precoupled receptors." Biochem Pharmacol **53**(4): 519-30.

- Shea, L. D. and J. J. Linderman (1998). "Compartmentalization of receptors and enzymes affects activation for a collision coupling mechanism." J. Theor. Biol. **191**: 249-258.
- Shea, L. D., R. R. Neubig and J. J. Linderman (2000). "Timing is everything - The role of kinetics in G protein activation." Life Sciences **68**(6): 647-658.
- Shea, L. D., G. M. Omann and J. J. Linderman (1997). "Calculation of diffusion-limited kinetics for the reactions in collision coupling and receptor cross-linking." Biophys J **73**(6): 2949-59.
- Shen, K. F. and S. M. Crain (1997). "Ultra-low doses of naltrexone or etorphine increase morphine's antinociceptive potency and attenuate tolerance/dependence in mice." Brain Res **757**(2): 176-90.
- Stadel, J. M., A. DeLean and R. J. Lefkowitz (1980). "A high affinity agonist . beta-adrenergic receptor complex is an intermediate for catecholamine stimulation of adenylate cyclase in turkey and frog erythrocyte membranes." J Biol Chem **255**(4): 1436-41.
- Stickle, D. and R. Barber (1989). "Evidence for the role of epinephrine binding frequency in activation of adenylate cyclase." Mol. Pharm. **36**: 437-445.
- Stickle, D. and R. Barber (1992). "The encounter coupling model for beta-adrenergic receptor/GTP-binding protein interaction in the S49 cell. Calculation of the encounter frequency." Biochem Pharmacol **43**(9): 2015-28.
- Strauer, B. E. (1990). "Beta-blocking agents in heart failure: modern concepts and overview." J Cardiovasc Pharmacol **16 Suppl 5**: S129-32.
- Taylor, C. W. (1990). "The role of G proteins in transmembrane signalling." Biochem J **272**(1): 1-13.
- Thomsen, W. J. and R. R. Neubig (1989). "Rapid kinetics of alpha 2-adrenergic inhibition of adenylate cyclase. Evidence for a distal rate-limiting step." Biochemistry **28**(22): 8778-86.
- Tolkovsky, A. M. (1982). "Etorphine binds to multiple opiate receptors of teh caudate nucleus with equal affinity but with different kinetics." Mol. Pharm. **22**: 648-656.
- Tomura, H., H. Itoh, K. Sho, K. Sato, M. Nagao, M. Ui, Y. Kondo and F. Okajima (1997). "beta gamma Subunits of pertussis toxin-sensitive G proteins mediate A(1) adenosine receptor agonist-induced activation of phospholipase C in collaboration with thyrotropin - A novel stimulatory mechanism through the cross-talk of two types of receptors." Journal of Biological Chemistry **272**(37): 23130-23137.

- Tsao, P. I. and M. von Zastrow (2000). "Type-specific sorting of G protein-coupled receptors after endocytosis." J Biol Chem **275**(15): 11130-40.
- Tucker, C. L., J. F. Gera and P. Uetz (2001). "Towards an understanding of complex protein networks." Trends Cell Biol **11**(3): 102-6.
- Venter, J. C., P. Horne, B. Eddy, R. Greguski and C. M. Fraser (1984). "Alpha 1-adrenergic receptor structure." Mol Pharmacol **26**(2): 196-205.
- Venter, J. C., J. S. Schaber, D. C. U'Prichard and C. M. Fraser (1983). "Molecular size of the human platelet alpha 2-adrenergic receptor as determined by radiation inactivation." Biochem Biophys Res Commun **116**(3): 1070-5.
- Wade, S. M., H. M. Dalman, S. Z. Yang and R. R. Neubig (1994). "Multisite interactions of receptors and G proteins: enhanced potency of dimeric receptor peptides in modifying G protein function." Mol Pharmacol **45**(6): 1191-7.
- Wade, S. M., K. Lan, D. J. Moore and R. R. Neubig (2001). "Inverse agonist activity at the alpha(2A)-adrenergic receptor." Mol Pharmacol **59**(3): 532-42.
- Weiss, A. and J. Schlessinger (1998). "Switching signals on or off by receptor dimerization." Cell **94**(3): 277-80.
- Weiss, J. M., P. H. Morgan, M. W. Lutz and T. P. Kenakin (1996). "The cubic ternary complex receptor-occupancy model I. Model Description." J Theor Biol **178**(2): 151-167.
- Weiss, J. M., P. H. Morgan, M. W. Lutz and T. P. Kenakin (1996). "The cubic ternary complex receptor-occupancy model. III. resurrecting efficacy." J Theor Biol **181**(4): 381-97.
- Woolf, P. J. and J. J. Linderman (2000). From the Static to the Dynamic: 3 Models of Signal Transduction in G-Protein Coupled Receptors. Biomedical Applications of Computer Modeling. A. Christopoulos. New York, CRC Press.
- Yatsui, K., E. L. Becker and R. I. Sha'afi (1992). "Lipopolysaccharide and serum cause the translocation of G-protein to the membrane and prime neutrophils via CD14." Biochem. Biophys. Res. Comm. **183**: 1280-1286.
- Yu, Y., L. Zhang, X. Yin, H. Sun, G. R. Uhl and J. B. Wang (1997). " μ opioid receptor phosphorylation, desensitization, and ligand efficacy." J Biol Chem **272**(46): 28869-74.
- Zeng, F. Y. and J. Wess (1999). "Identification and molecular characterization of m3 muscarinic receptor dimers." J Biol Chem **274**(27): 19487-97.

- Zhang, J., S. S. G. Ferguson, L. S. Barak, S. R. Bodduluri, S. A. Laporte, P. Law and M. G. Caron (1998). "Role for G-protein-coupled receptor kinase in agonist-specific regulation of μ -opioid receptor responsiveness." Neurobiology **95**: 7157-7162.
- Zhong, H., S. M. Wade, P. J. Woolf, J. J. Linderman, M. J. Clark, J. R. Traynor and R. R. Neubig (2001). "A spatial focusing model for G protein signals: RGS protein-mediated kinetic scaffolding." submitted.
- Zuker, C. S. and R. Ranganathan (1999). "The path to specificity [comment]." Science **283**(5402): 650-1.